VŠB – Technical University of Ostrava
Faculty of Electrical Engineering and Computer Science
Department of Applied Mathematics

Numerical solution of partial differential equations using a fictitious domain method

Lukáš Mocek

Ostrava, 2012

Study Programme: Computer Sience, Communication technology and Applied Mathematics (P1807)
Study Branch: Computational and Applied Mathenatics (1103V036)
Supervisor: doc. Ing. Tomáš Kozubek, Ph.D.

First of all I would like to thank my supervisor doc. Ing. Tomáš Kozubek, Ph.D. for his patience, help, support, and leadership during my doctoral studies, also many thanks to Ing. Alexandros Markopoulos, Ph.D. for helping me with the implementation to MatSol library and for many very interesting discussions not only about mathematics. I am very grateful to Ing. Marie Sadowská, Ph.D. for reading the thesis and make corrections. Also, I would like to thank all members of the Department of Applied Mathematics for a possibility to be a part of the team. And last but not least, I thank my parents, my brother, and friends, which supported me for the whole time of my studies, for everything they have done for me.

I would like to dedicate this thesis to my first supervisor of the bachelor thesis Doc. Ing. Nina Častová, CSc. and all my teachers, which have shown me beauty of the mathematics.

This research was supported by the grant of the Ministry of Education of the Czech Republic No. GA CR 103/09/H078.

Abstrakt

Disertační práce se zabývá numerickým řešením eliptických okrajových úloh pro problémy 2D lineární elasticity. Využívá k řešení metodu fiktivních oblastí v kombinaci s efektivními řešiči založených na diskrétní Fourierove transformaci a rozložení oblastí pomocí metody Total-FETI. Zabývá se teoretickým zázemím těchto metod, představuje dané řešiče a demonstruje jejich účinnost na modelových příkladech. Hlavním cílem této práce je rozšíření modifikovaného přístupu metody fiktivních oblastí pro řešení okrajových eliptických úloh pro problémy lineární elasticity a srovnání použití obou řešičů. Tato disertační práce je také základem článků, prezentovaných na domácích a zahraničních konferencích

Klíčová slova: Lineární elasticita, Eliptická okrajová úloha, Metoda fiktivních oblastí, Sedlo-bodový systém, Redukce Schurova doplňku, Metoda nulového prostoru, Ortogonální projektor, Diskrétní Fourierova transformace, Rychlá Fourierova transformace, Total-FETI rozložení oblastí

Abstract

The thesis deals with the numerical solution of elliptic boundary value problems for 2D linear elasticity using the fictitious domain method in combination with the effective solvers based on the discrete Fourier transform or the Total-FETI domain decomposition. We discuss the theoretical background of these methods, introduce resulting solvers, and demonstrate their efficiency on a model benchmark. The main goals of this thesis are the extension of the modified fictitious domain approach for solving elliptic boundary value problems of linear elasticity and the comparison of two above mentioned solvers. The thesis formed the basis of the papers, also presented during several domestic and international conferences.

Keywords: Linear elasticity, Elliptic boundary value problem, Fictitious domain method, Saddle-point system, Schur complement reduction, Null space method, Orthogonal projector, Discrete Fourier transform, Fast Fourier solver, Total-FETI domain decomposition

List of shortcuts and symbols

Ω	–	domain $(0,1) \times (0,1)$ with boundary $\partial\Omega$
Γ_D	–	part of boundary where the Dirichlet boundary condition is prescribed
Γ_N	–	part of boundary where the Neumann boundary condition is prescribed
$\mathbf{K}$, $\mathbf{A}$	–	stiffness matrix
$\mathbf{u}$	–	vector of displacement
$\mathbf{o}$	–	zero vector
$\nabla\mathbf{u}$	–	displacement gradient matrix
$\mathbf{f}$	–	load vector
$Im\mathbf{A}$	–	image of $\mathbf{A}$
$Ker\mathbf{A}$	–	kernel of $\mathbf{A}$
$\mathbf{O}$	–	zero matrix
$\mathbf{I}$	–	identity matrix
$\mathbf{P}$, $\mathbf{Q} = \mathbf{I} - \mathbf{P}$	–	conjugate projectors
Ω_i	–	ith subdomain of Ω
$\boldsymbol{\lambda}$	–	Lagrange multipliers
$\mathbf{B}_G$	–	matrix enforcing the continuity on subdomain interfaces and the Dirichlet boundary conditions
$\mathbb{R}^n$	–	n-dimensional real space
ω	–	real bounded domain with the Lipschitz continuity boundary
$\boldsymbol{\varepsilon}(\mathbf{u})$	–	strain tensor
$\boldsymbol{\sigma}(\mathbf{u})$	–	stress tensor
tr $\mathbf{A}$	–	trace of $\mathbf{A}$
θ, μ	–	the Lamé constants
υ	–	Poisson's ratio
γ, $\partial\omega$	–	smooth boundary of ω
γ_u, γ_p	–	different parts of γ
$\mathbf{p}$	–	density of surface tractions
$\boldsymbol{\nu}$	–	unit outward normal vector
V, Q	–	Hilbert spaces
V', Q'	–	dual spaces to V and Q
$\|.\|_V$, $\|.\|_Q$	–	norms corresponding to V and Q
$\langle , \rangle_{V' \times V}$, $\langle , \rangle_{Q' \times Q}$	–	duality pairing between space and its dual space

V_h, Q_h	–	finite dimensional subspaces of V and Q
$L^2(\Omega)$	–	space of square integrable functions on Ω
$L^2_{loc}(\Omega)$	–	space of locally square integrable functions on Ω
$H^1(\Omega)$	–	space of functions which are square integrable on Ω as well as their first derivatives in the sense of distributions
$H^1_0(\Omega)$	–	subspace of functions from $H^1(\Omega)$ with zero trace on $\partial\Omega$
$H^1_{per}(\Omega)$	–	subspace of functions from $H^1(\Omega)$ with periodic conditions on $\partial\Omega$
$H_0^{1/2}(\omega)$	–	space of traces on $\partial\omega$ of functions from H^1_0
$H_0^{-1/2(\omega)}$	–	dual space to $H_0^{1/2}(\omega)$
R_H	–	rectangulation of Ω
Ξ	–	Lipschitz domain with boundary Γ
δ	–	distance of Γ and γ
$\mathbf{B}_\Gamma$, $\mathbf{B}_{\gamma_u}$	–	the Dirichlet trace matrices
$\mathbf{C}_{\Gamma_p}$	–	the Neumann trace matrix
$\mathbf{u}_h$, $\boldsymbol{\lambda}_H$	–	finite element solutions
$\mathbf{A}^\dagger$	–	general inverse of $\mathbf{A}$
$\mathbf{R}$	–	matrix whose columns form a basis of the kernel of $\mathbf{A}$ or $\mathbf{K}$
$\boldsymbol{\lambda}_{Im}$, $\boldsymbol{\lambda}_{Ker}$	–	particular solutions
$\mathcal{K}_k$	–	kth Krylov subspace
$\mathbf{X}$	–	discrete Fourier transform matrix
d_k	–	kth eigenvalue
FT	–	the Fourier transform
DFT	–	Discrete Fourier Transform
FDM	–	Fictitious Domain Method
FETI	–	Finite Element Tearing and Interconnecting
LE problem	–	linear elasticity problem
b.c.	–	boundary conditions

Contents

List of Tables

List of Figures

1 Introduction

This thesis is motivated by an effort to solve elliptic boundary value problems arising in 2D linear elasticity using the fictitious domain method and the effective solvers based on the discrete Fourier transform or the FETI domain decomposition. Fictitious domain methods represent an efficient tool for the numerical solution of elliptic equations. The key idea of such methods is as follows. A boundary value problem formulated in a domain ω is replaced by a new one defined in a domain Ω having a simple shape (for example a box) and domain ω is embedded into Ω. The new problem in Ω is defined so that its solution restricted to ω matches the solution of the original problem. The domain Ω is called a fictitious domain. The advantage of this approach is that we can use special finite element partitions of Ω so that stiffness matrices have a particular structure which enable us to solve the resulting systems of linear algebraic equations by fast methods.

A possible way to formulate the new problem is based on the use of Lagrange multipliers. The imposed conditions on boundary γ of the original domain ω can be viewed as a constraint. This constraint is enforced by Lagrange multipliers defined on γ. Thus the new formulation in Ω involves two unknowns introduced as the primal variable $\mathbf{u} \in V$ and the corresponding Lagrange multiplier (dual variable) $\boldsymbol{\lambda} \in \Lambda$ enforcing imposed boundary conditions on γ which leads to the singularity of $\mathbf{u}$ concentrated on γ. To improve the convergence rate a modified (smooth) approach was proposed [21]. Its main idea is to move singularity away from γ. Therefore, we introduce a new auxiliary boundary Γ, where the new controls are defined to enforce imposed boundary conditions on γ. The solution to this new formulation still has a singularity in Ω, but now located on Γ instead of γ. Unfortunately, this new formulation and its discretization may have more than one solution in general.

In this thesis, we introduce two fast methods for finding a pair $(\mathbf{u}, \boldsymbol{\lambda}) \in \mathbb{R}^{2n} \times \mathbb{R}^{2m}$ that solves a linear system of algebraic equations resulting from the finite element discretization of fictitious domain formulation of given problem. This system is called the generalized saddle-point system:

$$\left(\begin{array}{c|c} \mathbf{A} & \mathbf{B}_\Gamma^T \\ \hline \mathbf{B}_\gamma & \mathbf{0} \end{array}\right) \left(\begin{array}{c} \mathbf{u} \\ \hline \boldsymbol{\lambda} \end{array}\right) = \left(\begin{array}{c} \mathbf{f} \\ \hline \mathbf{g} \end{array}\right), \tag{1.1}$$

where the $(2n \times 2n)$ diagonal block $\mathbf{A}$ is singular, the $(2m \times 2n)$ off-diagonal blocks $\mathbf{B}_\Gamma$, $\mathbf{B}_\gamma$ are highly sparse, they have full row-ranks and the vectors $\mathbf{f}$ and $\mathbf{g}$ are of order $2n$ and $2m$, respectively. Because of structural partition of domain Ω, the action of a generalized inverse $\mathbf{A}^\dagger$ is "cheap"and the null-space of $\mathbf{A}$ can be easily identified [17].

There are several basic approaches for solving the saddle-point system (1.1). Due to the structure of matrices we focus on the class of methods based on the Schur complement reduction. The main idea is to eliminate the first component $\mathbf{u}$ of the pair $(\mathbf{u}, \boldsymbol{\lambda})$. Because the stiffness matrix $\mathbf{A}$ is singular, $\mathbf{u}$ cannot be completely eliminated from (1.1). Thus the Schur complement reduction leads to another reduced saddle-point system in terms of $\boldsymbol{\lambda}$ and a new unknown $\boldsymbol{\alpha}$, which corresponds to the null-space of $\mathbf{A}$.

As was already mentioned, to find a solution we use the modified fictitious domain method and its formulation of a given problem, and therefore matrices $\mathbf{B}_\Gamma$ and $\mathbf{B}_\gamma$ are

determined by the geometries of Γ and γ, respectively, and they are highly sparse and $\mathbf{B}_\Gamma \neq \mathbf{B}_\gamma$. Since the system (1.1) is non-symmetric, also the reduced system has two different off-diagonal blocks $\mathbf{G}_1$ and $\mathbf{G}_2$. Therefore, two orthogonal projectors on the respective null-spaces of $\mathbf{G}_1$ and $\mathbf{G}_2$ are defined. The resulting system is solved by the projected biorthogonal conjugate gradient method for non-symmetric operators with preconditioning (projBiCGSTAB) [21]. To increase the efficiency of the solving method, we use two types of solvers.

The first solver introduced in this thesis for the solution of systems $\mathbf{Ax} = \mathbf{b}$ with positive semidefinite matrix $\mathbf{A}$ appearing in each iteration is based on the Fourier transform (FT). We use the discrete Fourier transform (DFT) for the spectral decomposition of the stiffness matrix $\mathbf{A}$ and then we can easily evaluate the action of a generalized inverse to $\mathbf{A}$ on a vector by the fast Fourier transform without storing $\mathbf{A}$ [31, 37, 29].

The alternative solver which is also introduced and tested is based on the Total-FETI domain decomposition [7, 39, 40]. The main idea is to decompose the fictitious domain Ω containing the original domain ω into non-overlapping subdomains and find a solution in parallel.

The thesis has two main goals. The extension of the modified smooth fictitious domain approach for solving elliptic boundary value problems to linear elasticity and the comparison of the two above mentioned solvers based on the Discrete Fourier transform and the FETI domain decomposition method, respectively.

The thesis is organized as follows. In Chapter 2, we describe the most important points of theory of the linear elasticity and introduce the formulation of the linear elasticity problem. Chapter 3 presents basics of the fictitious domain method. We mention the theoretical background of the fictitious domain method and introduce the classical and modified fictitious domain formulations of the original linear elasticity problem. In Chapter 4, we explain in detail the use of the method based on the Schur complement reduction in combination with the null-space method to solve a given generalized saddle-point system. Chapter 5 is concerned with the Krylov subspace method that is used to find a solution pair $(\mathbf{u}, \boldsymbol{\lambda})$ and with an algorithmic summarization of the solving procedure of finding a solution. Chapter 6 deals with details of the solver based on the Fourier transform, followed with the numerical experiments. Chapter 7 describes the domain decomposition method in general, and shows details of the use of the Total-FETI domain decomposition method to solve a given linear elasticity problem. Also, we present the numerical results for the proposed solver. Finally, the conclusions of the thesis are summarized in Chapter 8.

2 Linear elasticity

Elasticity is an important mathematical discipline that deals with determination of the stress, strain, and displacement distribution in an elastic solid under load of external forces. We assume the linear and small-deformation theory under the formulation establishes a mathematical model that allows solutions to problems that have interesting applications in many engineering and scientific branches. Civil engineering applications belong to the most important fields of study including contributions to stress and deflection analysis of structures as rods, beams, and plates. The other important applications can be found in geomechanics involving the stresses in materials as rock, concrete, and soil. As next, the linear elasticity is used in mechanical engineering for example to determine the stress fields in crystalline solids, in materials with microstructure and around dislocations. There exists much more applications as in aerospace industry, etc.

The definition of the elastic force-deformation relation was first proposed by Robert Hooke in 1678. However, the major formulation of the mathematical theory of elasticity began to developed later in 19^{th} century. In 1821, Navier presented his study of the general equations of equilibrium, and he was followed by Cauchy who investigated the basic elasticity equations and developed the notation of stress at a point. Belong the other scientists and mathematicians which studied problems of the elasticity and continued in development of the theory are, for example, Poisson, Lamé, Green, Timoshenko, Kolosoff, and others. During the war period the research in elasticity had a great progress and it brought a large amount of analytical solutions to specific problems of engineering interest. In $70s$ and $80s$ of 20^{th} century, numerical methods brought finite and boundary element theories to solve the elasticity problem. Also, during this period the focus of elasticity applications has been moved to anisotropic materials for applications to composites.

The elasticity theory establishes a mathematical model of the deformation problem and this requires mathematical knowledge to understand the formulation and solution procedures. There are various techniques which can be used to solve equations arising in solving of the linear elasticity problems as Fourier methods, variational calculus, integral transforms, finite elements methods, fictitious domain methods, FETI domain decomposition methods, etc. We focus on solving the linear elasticity problems by the fictitious domain method together with the Fourier and FETI based methods. Particular steps of these procedures are introduced and explained in detail in the following chapters.

Let us explain the application of the linear elasticity theory on the behavior of the steel under the effect of forces that stretch the material. In Fig. 2.1, we can see a deformation (stress-strain) curve of steel. It is obvious that the deformation curve of the other materials can be different, but the behavior of the steel is taken as typical. The first part of the curve is linear to the point σ_a - limit of proportionality, after exceeding this point, the strain ε becomes non-linear to the stress σ. The point σ_b is called an elastic limit. Till this point, the deformation of the material is elastic. It means that after releasing the load, the material is returned to its original state. Usually it holds that $\sigma_b \geq \sigma_a$. The next important point is a yield strength σ_c, when the relative strain increases, without

increasing the normal stress (the material becomes longer without bigger strain - creep of the material, the physical properties of the material are changed). The last point σ_d is called a fracture point; when this stress is exceeded, the material ruptures.

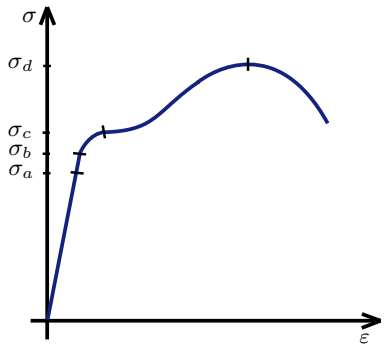

Figure 2.1: Deformation curve

The elastic region is a portion of the curve $\sigma \leq \sigma_b$ where the material returns to its original shape if the load is removed. Theory of linear elasticity deals with the study of elastic deformations. On the other hand, we call the plastic region of that part of curve, $\sigma > \sigma_b$, where some permanent deformation will occur, even if the load is removed. This region is under the study of theory of plasticity.

Before we formulate given linear elasticity problem, we mention some basic concepts of the theory of two-dimensional linear elasticity. Practical situations in three dimensions can be often reduced to two-dimensional cases exploiting the symmetry, etc. Let us consider a two-dimensional elastic body which is represented by a bounded domain $\omega \subset \mathbb{R}^2$ subjected to internal and external forces. Because of these forces, the given body is deformed, which means that a point $\mathbf{x} = (x_1, x_2)$ of the undeformed body becomes a point $\mathbf{y} = (y_1, y_2)$ of the deformed body, where $\mathbf{y}$ can by written as $\mathbf{y} = \mathbf{x} + \mathbf{u}(\mathbf{x})$, with $\mathbf{u} = (u_1, u_2)$ denoting the vector of displacement, see Fig. 2.2.

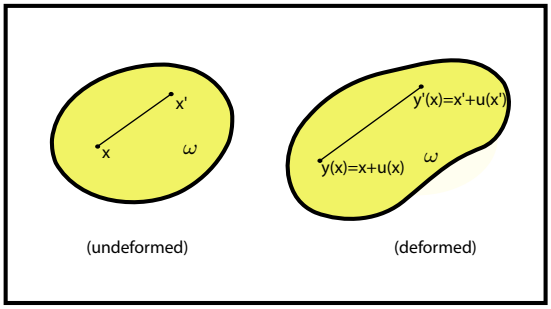

Figure 2.2: Deformation of body ω

As follows, it is necessary to introduce and define basic operators that appear in equilibrium equations of the linear elasticity problem.

The strain which is caused by displacements $\mathbf{u}$ is characterized by the symmetric strain tensor given as

$$\boldsymbol{\varepsilon}(\mathbf{u}) = \frac{1}{2}(\nabla\mathbf{u} + \nabla\mathbf{u}^T),$$

where $\boldsymbol{\varepsilon}$ is the strain tensor, and $\nabla\mathbf{u}$ is the displacement gradient matrix and $(\nabla\mathbf{u})^T$ is its transpose. It follows that if $\mathbf{u} = (u_1, u_2)$, then $\boldsymbol{\varepsilon}(\mathbf{u})$ can be rewritten as

$$\boldsymbol{\varepsilon}(\mathbf{u}) = \left(\begin{array}{c|c} \dfrac{\partial u_1}{\partial x_1} & \dfrac{1}{2}\left(\dfrac{\partial u_1}{\partial x_2} + \dfrac{\partial u_2}{\partial x_1}\right) \\ \hline \dfrac{1}{2}\left(\dfrac{\partial u_1}{\partial x_2} + \dfrac{\partial u_2}{\partial x_1}\right) & \dfrac{\partial u_2}{\partial x_2} \end{array}\right).$$

Similarly, the stresses can be characterized by the symmetric stress tensor $\boldsymbol{\sigma}(\mathbf{u})$. In the equilibrium state the stresses $\boldsymbol{\sigma}(\mathbf{u})$ are related to body forces $\mathbf{f} = (f_1, f_2)$ by the system of equilibrium equations

$$\left.\begin{array}{rcl} \dfrac{\partial \sigma_{11}}{\partial x_1} + \dfrac{\partial \sigma_{12}}{\partial x_2} + f_1 & = & \mathbf{o} \\ \dfrac{\partial \sigma_{21}}{\partial x_1} + \dfrac{\partial \sigma_{22}}{\partial x_2} + f_2 & = & \mathbf{o} \end{array}\right\} \quad \text{in} \quad \omega.$$

In the case of linear elasticity the stress tensor is related to the strain tensor by the linearized Hooke's law for homogeneous isotropic materials, written as:

$$\boldsymbol{\sigma}(\mathbf{u}) = \theta\, tr(\boldsymbol{\varepsilon}(\mathbf{u}))\mathbf{I} + 2\mu\, \boldsymbol{\varepsilon}(\mathbf{u}) \quad \text{in} \quad \omega,$$

where "$tr(\cdot)$"is the trace of matrix (see Definition 2.1), $\mathbf{I} \in \mathbb{R}^{2\times 2}$ is the identity matrix, and $\theta, \mu > 0$ are the Lamé constants defined as follows:

$$\theta = \frac{E\upsilon}{(1+\upsilon)(1-2\upsilon)}, \quad \mu = \frac{E}{2(1+\upsilon)}.$$

Here, $E > 0$ is the Young modulus and $\upsilon \in (0, 1/2)$ is Poisson's ratio.

Definition 2.1. A *trace of the matrix* $\mathbf{A}$ *is defined as*

$$tr(\mathbf{A}) = \sum_{i=1}^{n} a_{ii},$$

where $\mathbf{A} \in \mathbb{R}^{n\times n}$ *and* a_{ij} *is the entry of matrix* $\mathbf{A}$ *in the i-th row and the j-th column.*

The stress tensor can be written as follows:

$$\boldsymbol{\sigma}(\mathbf{u}) = \left(\begin{array}{c|c} (\theta+2\mu)\dfrac{\partial u_1}{\partial x_1} + \theta\dfrac{\partial u_2}{\partial x_2} & \mu\left(\dfrac{\partial u_1}{\partial x_2} + \dfrac{\partial u_2}{\partial x_1}\right) \\ \hline \mu\left(\dfrac{\partial u_1}{\partial x_2} + \dfrac{\partial u_2}{\partial x_1}\right) & \theta\dfrac{\partial u_1}{\partial x_1} + (\theta+2\mu)\dfrac{\partial u_2}{\partial x_2} \end{array}\right).$$

More details about definition and derivation of the concepts arising in the linear elasticity theory can be found in many papers and books, e.g., by authors Nečas and Hlaváček [41] or Saad [43].

2.1 Formulation of a linear elasticity problem

In the previous chapter, we introduced basic linear elasticity concepts together with the equilibrium equation and the most important relations between stress, strain, and external forces which involve the deformation of the given body. According to these observations we can formulate the linear elasticity problem.

We consider elastic body which is represented by a domain $\omega \subset \mathbb{R}^2$ with smooth boundary γ. This boundary is devided into two disjoint parts γ_u and γ_p, where $\gamma = \overline{\gamma_u} \cup \overline{\gamma_p}$, see Fig. 2.3. On these two parts of γ we have prescribed different conditions. The zero displacement is imposed on γ_u while surface tractions of density $\mathbf{p} \in (L^2(\gamma_p))^2$ are prescribed on γ_p. We finally prescribe the interior forces of density $\mathbf{f} \in (L^2(\omega))^2$.

Now we can formulate equilibrium equation together with the Dirichlet and Neumann boundary conditions:

$$\left.\begin{array}{rcll} -\operatorname{div}\boldsymbol{\sigma}(\mathbf{u}) &=& \mathbf{f} \quad \text{in} \quad \omega, \\ \mathbf{u} &=& \mathbf{o} \quad \text{on} \quad \gamma_u, \\ \boldsymbol{\sigma}(\mathbf{u})\boldsymbol{\nu} &=& \mathbf{p} \quad \text{on} \quad \gamma_p, \end{array}\right\} \tag{2.1}$$

where $\boldsymbol{\sigma}(\mathbf{u})$ is the stress tensor, $\boldsymbol{\nu} = (\nu_1, \nu_2)$ is the unit outward normal vector to γ, and $\mathbf{u} = (u_1, u_2)$ is the unknown displacement.

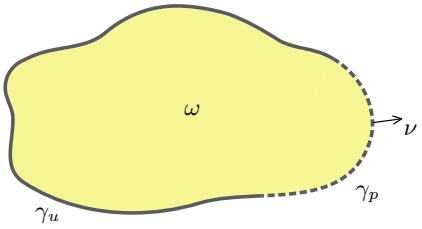

Figure 2.3: Elastic body ω

In equation (2.1) the therm $\operatorname{div}\boldsymbol{\sigma}(\mathbf{u})$ can be written as

$$\operatorname{div}\boldsymbol{\sigma}(\mathbf{u}) = \left(\begin{array}{c|c} (\theta+2\mu)\dfrac{\partial^2(\cdot)}{\partial x_1^2} + \mu\dfrac{\partial^2(\cdot)}{\partial x_2^2} & (\theta+\mu)\dfrac{\partial^2(\cdot)}{\partial x_1 \partial x_2} \\ \hline (\theta+\mu)\dfrac{\partial^2(\cdot)}{\partial x_1 \partial x_2} & \mu\dfrac{\partial^2(\cdot)}{\partial x_1^2} + (\theta+2\mu)\dfrac{\partial^2(\cdot)}{\partial x_2^2} \end{array}\right) \begin{pmatrix} u_1 \\ u_2 \end{pmatrix} \tag{2.2}$$

and density of surface traction $\boldsymbol{\sigma}(\mathbf{u})\boldsymbol{\nu}$ as

$$\boldsymbol{\sigma}(\mathbf{u})\boldsymbol{\nu} = \left(\begin{array}{c|c} \nu_1\left[(\theta+2\mu)\dfrac{\partial(\cdot)}{\partial x_1} + \theta\dfrac{\partial(\cdot)}{\partial x_2}\right] & \nu_2\left[\mu\dfrac{\partial(\cdot)}{\partial x_2} + \mu\dfrac{\partial(\cdot)}{\partial x_1}\right] \\ \hline \nu_1\left[\mu\dfrac{\partial(\cdot)}{\partial x_2} + \mu\dfrac{\partial(\cdot)}{\partial x_1}\right] & \nu_2\left[\theta\dfrac{\partial(\cdot)}{\partial x_1} + (\theta+2\mu)\dfrac{\partial(\cdot)}{\partial x_2}\right] \end{array}\right) \begin{pmatrix} u_1 \\ u_2 \end{pmatrix}. \tag{2.3}$$

Above, we formulated the linear elasticity problem and, in the following chapter, we introduce a method which is used to solve it efficiently. This method is based on the use of a fictitious domain containing the elastic body ω.

3 Fictitious domain method

The fictitious domain method represents an efficient tool for the numerical solution of complicated problems arising in physics and industry. The main reason for its popularity is that it allows us to transform the original problem defined in a domain ω with a possibly complicated geometry to a new one solved in a simple shape domain Ω containing the original domain ω. The advantage of the fictitious domain method (sometimes called also an imbedding method) is that we can use fairly structured meshes in Ω allowing to apply fast effective solvers for the numerical solution of the resulting algebraic system and special preconditioning techniques. There are several ways how to associate the new problem in Ω with the original one defined in ω. For example, we can use the Lagrange multipliers or penalty technique, optimal control approach, etc. In this thesis, we focus on explaining the basics of the fictitious domain method based on Lagrange multipliers (or control variables in non-symmetric variants) to enforce boundary conditions imposed on the boundary of the original domain. At first we introduce a general principle of the fictitious domain method for solving an abstract boundary value problem. Then we apply the method to a simple problem to see the method in more detail and after that we focus our attention on the use of the fictitious domain method for solving a given linear elasticity problem.

Let ω be a bounded domain in $\mathbb{R}^d$, $d = 2, 3$, with the Lipchitz boundary $\partial\omega$. On this domain we define an elliptic boundary value problem

$$\left.\begin{array}{ll} -\mathcal{A}\,u = f & \text{in } \omega, \\ +b.c. & \text{on } \partial\omega, \end{array}\right\} \qquad (P)$$

where $\mathcal{A}$ is an elliptic partial differential operator of the 2nd order, $u \in V(\omega)$ is a solution of (P), and $f \in V'(\omega)$, where $V(\omega)$ is a Hilbert space and $V'(\omega)$ its dual space. It was already mentioned that the main idea of the fictitious domain method is to embed the real domain of our original problem with possibly complicated geometry ω into a new simple shaped domain Ω (for example rectangle or box) called a fictitious domain, see Fig. 3.1. It follows that the original problem (P) is reformulated to a new one defined in the fictitious domain Ω as

$$\left.\begin{array}{ll} -\hat{\mathcal{A}}\,\hat{u} = \hat{f} & \text{in } \Omega, \\ +b.c. & \text{on } \partial\Omega, \end{array}\right\} \qquad (\hat{P})$$

where $\hat{\mathcal{A}}$ is an elliptic partial differential operator of the 2nd order similar to $\mathcal{A}$, $\hat{u} \in V(\Omega)$ is a solution of $(\hat{P})$, and $\hat{f} \in V'(\Omega)$ is a suitable extension of f from the original domain ω to the fictitious domain Ω. This new problem $(\hat{P})$ is chosen so that the solution $\hat{u}$ restricted to the original domain ω is equal to the solution u of the original problem (P).

3.1 Abstract theory of mixed variational formulation for symmetric case

The fictitious domain formulation, which uses Lagrange multipliers to enforce boundary conditions on the original boundary of the domain ω, leads to a mixed variational formulation. Therefore, we introduce an abstract mixed variational formulation and its approximation together with the most important results of existence, uniqueness, and convergence of the solution, for more details see [3].

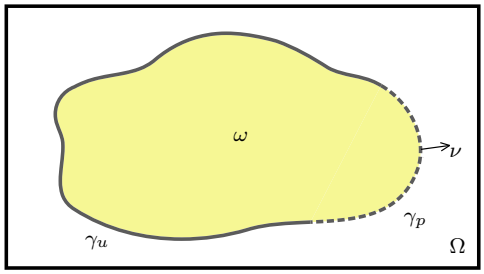

Figure 3.1: Fictitious domain Ω

Let V and Q be Hilbert spaces and $\|.\|_V$, $\|.\|_Q$ be the corresponding norms. Let V' and Q' be their dual spaces and $\langle\,,\rangle_{V'\times V}$ and $\langle\,,\rangle_{Q'\times Q}$ stand for duality pairings between V' and V and Q' and Q, respectively. Also we introduce two bounded bilinear forms $a : V \times V \to \mathbb{R}$ and $b : V \times Q \to \mathbb{R}$, respectively, i.e.:

$$\exists M > 0 : \ |a(u,v)| \leq M\|u\|_V\|v\|_V \quad \forall u, v \in V, \tag{3.1}$$

$$\exists m > 0 : \ |b(v,q)| \leq m\|v\|_V\|q\|_Q \quad \forall (v,q) \in V \times Q, \tag{3.2}$$

and, finally, let $f \in V'$ and $g \in Q'$ be given.

Then the mixed variational formulation reads as follows:

$$\left.\begin{array}{l} \text{Find } (u,\lambda) \in V \times Q \text{ such that} \\ a(u,v) + b(v,\lambda) = \langle f, v\rangle_{V'\times V} \quad \forall v \in V, \\ b(u,q) = \langle g, q\rangle_{Q'\times Q} \quad \forall q \in Q. \end{array}\right\} \qquad (\hat{P}_a)$$

To ensure the existence and uniqueness of the solution (u,λ) of problem $(\hat{P}_a)$ for any $(f,g) \in V' \times Q'$ it is sufficient to satisfy the following assumptions:

$$\exists \alpha > 0 : a(v,v) \geq \alpha\|v\|_V^2 \quad \forall v \in V, \tag{3.3}$$

$$\exists \beta > 0 : \sup_{\substack{v\in V \\ v\neq 0}} \frac{b(v,q)}{\|v\|_V} \geq \beta\|q\|_Q \quad \forall q \in Q. \tag{3.4}$$

Theorem 3.1. *Let conditions (3.1)-(3.4) be satisfied, then $(\hat{P}_a)$ has a unique solution (u,λ) for any $(f,g) \in V' \times Q'$.*

Proof: See [3]. □

The discretization of $(\hat{P}_a)$ is based on the finite element method, where spaces V and Q are replaced by their finite dimensional subspaces V_h and Q_h. We can reformulate problem $(\hat{P}_a)$ as:

$$\left.\begin{array}{l} \text{Find } (u_h,\lambda_h) \in V_h \times Q_h \text{ such that} \\ a(u_h,v_h) + b(v_h,\lambda_h) = \langle f, v_h\rangle_{V'\times V} \quad \forall v_h \in V_h, \\ b(u_h,q_h) = \langle g, q_h\rangle_{Q'\times Q} \quad \forall q_h \in Q_h. \end{array}\right\} \qquad (\hat{P}_a)_h$$

The existence and the uniqueness of the solution $(\hat{u}_h, \lambda_h)$ of problem $(\hat{P}_a)_h$ is guaranteed by the following assumption (the so-called stability condition):

$$[b(v_h, q_h) = 0 \quad \forall v_h \in V_h] \implies q_h = 0. \tag{3.5}$$

To ensure the convergence of the solution of $(\hat{P}_a)_h$ to $(\hat{P}_a)$, $h \to 0+$, we need a stronger assumption as the fulfillment of Ladyzenska-Babuska-Brezzi (LBB)-condition:

$$\exists \beta_0 > 0 : \sup_{\substack{v_h \in V_h \\ v_h \neq 0}} \frac{b(v_h, q_h)}{\|v_h\|_V} \geq \beta_0 \|q_h\|_Q \quad \forall q_h \in Q_h, \, \forall h \to 0+, \tag{3.6}$$

where $\beta_0 > 0$ is independent of h, i.e., the constant β_h from the discrete version of (3.4) is bounded from below by the constant β_0.

Theorem 3.2. *Let conditions (3.1)-(3.4) and (3.6) be satisfied. Also, we assume that systems $\{V_h\}$ and $\{Q_h\}$, $h \to 0+$, are dense in V and Q, respectively. Then the sequence of solutions $\{(u_h, \lambda_h)\}$ of $(\hat{P}_a)_h$ converges to the solution (u, λ) of problem $(\hat{P}_a)$:*

$$\begin{array}{rcll} u_h & \to & u & in\, V, \\ \lambda_h & \to & \lambda & in\, Q, h \to 0+, \end{array}$$

and the following inequality holds:

$$\|u - u_h\|_V + \|\lambda - \lambda_h\|_Q \leq C\{\inf_{v_h \in V_h} \|u - v_h\|_V + \inf_{\varepsilon_h \in Q_h} \|\lambda - \varepsilon_h\|_Q\},$$

where the constant $C > 0$ is independent of h. [27]

For a fixed parameter h, we formulate the following algebraic formulation of problem $(\hat{P}_a)_h$. Let $\{\varphi_i\}_{i=1}^n$ and $\{\psi_j\}_{j=1}^m$, $\dim V_h = n$, $\dim Q_h = m$, be systems of basis functions of spaces V_h and Q_h, respectively. Then $(\hat{P}_a)_h$ leads to the following algebraic system

$$\left(\begin{array}{c|c} \mathbf{A} & \mathbf{B}^T \\ \hline \mathbf{B} & \mathbf{O} \end{array}\right) \left(\begin{array}{c} \mathbf{u} \\ \hline \boldsymbol{\lambda} \end{array}\right) = \left(\begin{array}{c} \mathbf{f} \\ \hline \mathbf{g} \end{array}\right), \tag{3.7}$$

where $\mathbf{u}$ and $\boldsymbol{\lambda}$ are formed by coefficients of functions u_h and λ_h expanded according to the bases $\{\varphi_i\}_{i=1}^n$ and $\{\psi_j\}_{j=1}^m$, respectively. Elements of the matrices $\mathbf{A} \in \mathbb{R}^{n \times n}$ and $\mathbf{B} \in \mathbb{R}^{m \times n}$ are defined as follows:

$$\begin{array}{rcll} a_{ij} & = & a(\varphi_j, \varphi_i), & i, j = 1, \ldots, n, \\ b_{kj} & = & b(\varphi_j, \psi_k), & j = 1, \ldots, n;\ k = 1, \ldots, m. \end{array}$$

Before we focus on solving linear elasticity problems by the fictitious domain method, we use the results from this chapter to introduce a fictitious domain approach for a non-homogeneous Poisson boundary value problem. It is an easier example to explain details of classical (non-smooth) and modified (smooth) fictitious domain approaches which are used later to solve a given linear elasticity problem.

3.2 Poisson boundary value problem and FDM

In this section, we illustrate the use of the fictitious domain method for solving a non-homogenous Poisson problem in 2D. Many derivations was done only for Poisson boundary value problem [1, 3, 15], but can be generalized for problems arising in linear elasticity.

We shall consider a non-homogenous Poisson boundary value problem on a bounded domain $\omega \subset \mathbb{R}^2$ with a Lipschitz continuous boundary γ:

$$\left.\begin{array}{rcl} -\Delta u &=& f \quad \text{in} \quad \omega, \\ u &=& g \quad \text{on} \quad \gamma, \end{array}\right\} \qquad (P(\omega))'$$

where $f \in L^2_{loc}(\mathbb{R}^2)$ and $g \in H^{1/2}(\gamma)$ are given. The weak formulation of $(P(\omega))'$ is given by

$$\left.\begin{array}{l} \text{Find } u \in H^1(\omega) \text{ such that } u = g \text{ on } \gamma \text{ and} \\ \displaystyle\int_\omega \nabla u \cdot \nabla v \,\mathrm{d}\omega = \int_\omega f v \,\mathrm{d}\omega \quad \forall v \in H^1_0(\omega), \end{array}\right\} \qquad (P(\omega))$$

where

$$H^1_0(\omega) = \{v \in H^1(\omega) | v = 0 \text{ on } \partial\omega\}.$$

For solving this weak formulation $(P(\omega))$ we use the fictitious domain method based on Lagrange multipliers defined on the boundary γ to enforce boundary conditions on boundary γ.

Further we denote

$$H^{1/2}(\partial\omega) = \{\varphi \in L^2(\partial\omega) | \exists v \in H^1(\omega) : \varphi = v \text{ on } \partial\omega\}$$

as a space of traces on $\partial\omega$. It is known that $H^{1/2}(\partial\omega)$ is a Banach space equipped with the norm

$$\|\varphi\|_{1/2,\partial\omega} = \inf_{\substack{v \in H^1(\omega) \\ v = \varphi \text{ on } \partial\omega}} \|v\|_{1,\omega}$$

and $H^{-1/2}(\partial\omega)$ is the corresponding dual space. Let Ω be a rectangular fictitious domain into which the original domain ω is embedded, see Fig. 3.2.

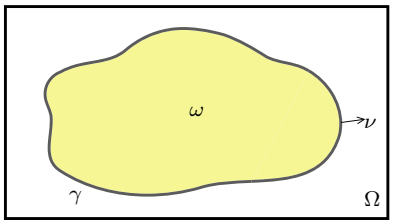

Figure 3.2: FDM

We define a Lagrangian $\mathcal{L} : V \times \Lambda \to \mathbb{R}^1$ as follows:

$$\mathcal{L}(v, \mu) = \frac{1}{2} \int_\Omega |\nabla v|^2 \mathrm{d}\Omega - \int_\Omega \tilde{f} v \,\mathrm{d}\Omega - \langle \mu, v \rangle,$$

where $\tilde{f} \in L^2(\Omega)$ is an extension of f from ω to Ω, the symbol $\langle \cdot, \cdot \rangle$ denotes duality between spaces $\Lambda := H^{-1/2}(\partial\omega)$ and $H^{1/2}(\partial\omega)$, and V is a closed subspace of $H^1(\Omega)$. Typical choices of the space V are: $H^1(\Omega)$, $H_0^1(\Omega)$ or

$$H^1_{per}(\Omega) = \{v \in H^1(\Omega) | v \text{ is periodic on } \partial\Omega\}.$$

In this section, we use $V = H_0^1(\Omega)$, where

$$H_0^1(\Omega) = \{v \in H^1(\Omega) | v = 0 \text{ on } \partial\Omega\}. \tag{3.8}$$

Now we introduce the space Λ of Lagrange multipliers to satisfy the condition that $\hat{u}_{|\omega}$ solves $(P(\omega))$ and, instead of $(P(\omega))$, we consider the following variational problem:

$$\left.\begin{array}{l} \text{Find } (\hat{u}, \lambda) \in V \times \Lambda \text{ such that} \\ \displaystyle\int_\Omega \nabla\hat{u} \cdot \nabla v \,\mathrm{d}\Omega = \int_\Omega \tilde{f} v \,\mathrm{d}\Omega + \langle \lambda, v \rangle \quad \forall v \in V, \\ \langle \mu, \hat{u} \rangle = \langle \mu, g \rangle \quad \forall \mu \in \Lambda. \end{array}\right\} \qquad (P(\Omega))$$

The existence and the uniqueness of the solution to $(P(\Omega))$ is given by Theorem 3.1. with a special choice of data:

$$V = H_0^1(\Omega), \quad \Lambda = H^{-1/2}(\partial\omega), \quad a(u,v) = \int_\Omega \nabla u \cdot \nabla v \,\mathrm{d}\Omega,$$
$$b(v,\lambda) = -\langle \lambda, v \rangle, \quad \langle f, v \rangle_{V' \times V} = \int_\Omega \tilde{f} v \,\mathrm{d}\Omega, \quad v \in V, q \in \Lambda.$$

Problem $(P(\Omega))$ can be interpreted as a deflection of a membrane fixed on a frame given by $\partial\Omega$ and loaded by a force of density $\tilde{f}$. Finally, $\hat{u}$ represents its deflection. Lagrange multipliers play the role of forces concentrated on the boundary $\partial\omega$ enforcing the imposed Dirichlet boundary conditions.

For approximation of variational problem $(P(\Omega))$ we use the mixed finite element method. We replace spaces V and Λ by their finite dimensional subspaces V_h and Λ_H, respectively. Let R_h be a uniform rectangulation of Ω, i.e., Ω is divided into squares with step h. This partition enables us to use efficient solvers to find solution of a given problem. For a given R_h we construct space

$$V_h = \{v_h \in C(\overline{\Omega}) | \quad v_{h|_R} \in Q_1(R) \quad \forall R \in R_h, \quad v_h = 0 \text{ on } \partial\Omega\},$$

i.e., V_h contains all continuous, piecewise bilinear functions vanishing on the boundary $\partial\Omega$. Boundary $\partial\omega$ can be written as $\partial\omega = R_H = \cup_{i=1}^m S_i$, where S_i are parts of boundary $\partial\omega$ not necessarily of the same length, but $3h \le |S_k| \le Lh$, where $L \ge 3$ is fixed and $|S_k|$ denotes the length of S_k. Let $H = \max|S_k|$ and R_H be the corresponding partition of $\partial\omega$. Now we can define the discrete space

$$\Lambda_H = \{\mu_H \in L^2(\partial\omega) | \quad \mu_{H|_S} \in P_0(S) \quad \forall S \in R_H\},$$

i.e., Λ_H is the space of piecewise constant functions on R_H.

The discrete version of $(P(\Omega))$ reads as follows:

$$\left.\begin{array}{l}\text{Find } (\hat{u}_h, \lambda_H) \in V_h \times \Lambda_H \text{ such that} \\ \displaystyle\int_\Omega \nabla \hat{u}_h \cdot \nabla v_h \,\mathrm{d}\Omega = \int_\Omega \tilde{f} v_h \,\mathrm{d}\Omega + \langle \lambda_H, v_h \rangle \quad \forall v_h \in V_h, \\ \langle \mu_H, \hat{u}_h \rangle = \langle \mu_H, g \rangle \quad \forall \mu_H \in \Lambda_H. \end{array}\right\} \qquad (P(\Omega))_h^H$$

To ensure the existence and uniqueness of the solution of $(P(\Omega))_h^H$ we need the stability condition (3.5) in the form

$$[\langle \mu_H, v_h \rangle = 0 \quad \forall v_h \in V_H] \implies \mu_H = 0.$$

This condition is satisfied if the ratio H/h is sufficiently large, for more details see [15].

If $3 \le H/h \le L$, where L is fixed, then the following LBB-condition

$$\sup_{\substack{v_h \in V_h \\ v_h \neq 0}} \frac{\displaystyle\int_{\partial\omega} \mu_H v_h \,\mathrm{d}s}{\|v_h\|_{1,\Omega}} \ge \beta_0 \|\mu_h\|_{-1/2,\partial\omega} \quad \forall \mu_h \in \Lambda_H$$

is also satisfied for any $\beta_0 > 0$ independent of h and H. It is known that the LBB-condition ensures convergence of the solution of problem $(P(\Omega))_h^H$ to the solution of problem $(P(\Omega))$ for $h, H \to 0+$. The following theorem introduces order of the convergence of the sequence $\{(\hat{u}_h, \lambda_H)\}$ to $(\hat{u}, \lambda)$. The proof is shown also in [15].

Theorem 3.3. *Let $3 \le H/h \le L$. Then*

$$\|\hat{u} - \hat{u}_h\|_{1,\Omega} + \|\lambda - \lambda_H\|_{-1/2,\partial\omega} = O(h^{1/2-\epsilon}), \quad h \to 0+$$

for each $\epsilon > 0$, assuming that $\hat{u}_{|\omega} \in H^2(\omega)$ and $\hat{u}_{|\Xi} \in H^2(\Xi)$.

The error estimate mentioned above is not optimal, because the solution $\hat{u}$ is not generally smooth over the whole fictitious domain Ω and therefore we can expect only that $\hat{u} \in H^{3/2-\epsilon}(\Omega)$ for arbitrary small $\epsilon > 0$. It also follows that the sequence $\{\lambda_H\}$ converges to $\lambda = [\frac{\partial \hat{u}}{\partial \nu}]_{\partial\omega}$ (jump of the normal derivative $\frac{\partial \hat{u}}{\partial \nu}$ on $\partial\omega$) only in the norm $H^{-1/2}(\partial\omega)$.

The discrete algebraic form of $(P(\Omega))_h^H$ leads to the algebraic system (3.7), where $\mathbf{A}$ represents the stiffness matrix, $\mathbf{f}$ is a load vector, $\mathbf{g}$ corresponds to the Dirichlet conditions imposed on the boundary $\partial\omega$, and $\mathbf{u}$, $\boldsymbol{\lambda}$ are vectors of nodal values of $\hat{u}_h$ and $-\lambda_H$, respectively.

Elements of matrices $\mathbf{A}$, $\mathbf{B}$ and vectors $\mathbf{f}$ and $\mathbf{g}$ are assembled as follows:

$$a_{ij} = \int_{\Omega} \nabla\varphi_i \cdot \nabla\varphi_j \,\mathrm{d}\Omega,\ i,j = 1,\ldots,n;\ n = \dim V_h,$$

$$b_{kj} = \int_{S_k} \varphi_j \,\mathrm{d}s,\ S_k \in R_H, k = 1,\ldots,m; j = 1,\ldots,n;\ m = \dim \Lambda_H,$$

$$f_j = \int_{\Omega} \tilde{f}\varphi_j \,\mathrm{d}\Omega,\ j = 1,\ldots,n,$$

$$g_k = \int_{S_k} g \,\mathrm{d}s,\ S_k \in R_H,\ k = 1,\ldots,m;\ m = \dim \Lambda_H,$$

where $\{\varphi_i\}_{i=1}^n$ are basis functions of V_h. To solve the above mentioned integrals we can use a technique of numerical integration.

The information about geometry of the real domain ω is contained only in the transformation matrix $\mathbf{B}$ (or in the load vector $\mathbf{f}$), but not in the stiffness matrix $\mathbf{A}$.

Any fictitious domain formulation extends the original problem defined in a domain ω to a new fictitious domain Ω with a simple geometry, which contains ω. We can use structured meshes in Ω ensuring favorable properties of the stiffness matrix represented by $\mathbf{A}$ in (3.7). On the other hand, the method brings some complication. We have to compute and store information concerning the actual geometry, we have more unknowns, also there are problems with local refinements and low regularity. We consider the original boundary conditions as a constraint. In classical approach, a class of fictitious domain methods enforces this constraint by Lagrange multipliers defined on the boundary γ of the original domain ω. Therefore, the fictitious domain solution has a singularity on γ (see Fig. 3.3) that can result in an intrinsic error of the computed solution.

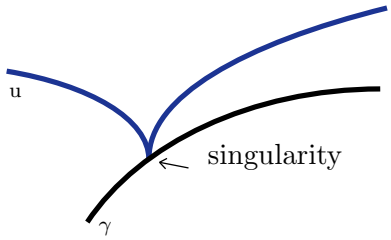

Figure 3.3: Singularity on γ

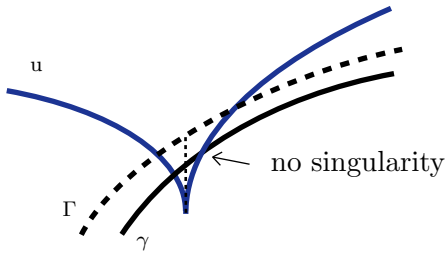

Figure 3.4: No singularity on γ

To remove the above drawback, the authors propose a new approach [21], in which the singularity is moved away from the boundary γ. This modification is based on introduction a new control variable instead of the Lagrange multiplier defined on the other auxiliary boundary Γ located outside of the domain $\overline{\omega}$, see Fig. 3.5. The boundary Γ satisfies the condition $\delta = \mathrm{dist}(\Gamma,\gamma) > 0$. This new control variable enforces the original boundary

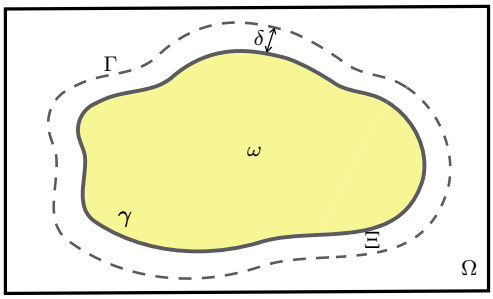

Figure 3.5: Modified FDM

condition on γ. Because the singularity is moved from $\overline{\omega}$, the solution is smoother in ω. See Figs. 3.3 and 3.4.

Let us explain above mentioned modified fictitious domain approach in more details. We shall consider Dirichlet boundary value problem $(P(\omega))'$ together with its weak formulation $(P(\omega))$. Let $\Xi \supset \overline{\omega}$ be another Lipschitz domain with the boundary Γ such that $\delta = \mathrm{dist}(\Gamma, \gamma) > 0$. Finally, $\Omega \supset \overline{\Xi}$ denotes the fictitious domain, see Fig. 3.5. Instead of $(P(\omega))$ we propose to solve an extended problem

$$\left.\begin{array}{l} \text{Find } (\hat{u}, \lambda) \in H_0^1(\Omega) \times H^{-1/2}(\Gamma) \text{ such that} \\ \displaystyle\int_\Omega \nabla\hat{u} \cdot \nabla v \,\mathrm{d}\Omega = \int_\Omega f v \,\mathrm{d}\Omega + \langle \lambda, v\rangle_\Gamma \quad \forall v \in H_0^1(\Omega), \\ \langle \mu, \hat{u}\rangle_\gamma = \langle \mu, g\rangle_\gamma \quad \forall \mu \in H^{-1/2}(\gamma), \end{array}\right\} \qquad (\hat{P}(\Omega))$$

where $\langle\,,\rangle_\Gamma$ and $\langle\,,\rangle_\gamma$ stand for the duality pairings between $H^{-1/2}(\Gamma)$ and $H^{1/2}(\Gamma)$ and $H^{-1/2}(\gamma)$ and $H^{1/2}(\gamma)$, respectively.

If we suppose that problem $(\hat{P}(\Omega))$ has a solution $(\hat{u}, \lambda)$, then we can also see that the solution $(\hat{u}, \lambda)$ satisfies the following partial differential equations:

$$\begin{array}{rcll} -\Delta\hat{u} & = & f & \text{in} \quad \Xi \cup (\Omega\backslash\bar{\Xi}), \\ \hat{u} & = & g & \text{on} \quad \gamma, \\ \hat{u} & = & 0 & \text{on} \quad \partial\Omega, \\ [\frac{\partial\hat{u}}{\partial\nu}]_\Gamma & = & \lambda & \text{on} \quad \Gamma, \end{array}$$

where $[\frac{\partial\hat{u}}{\partial\nu}]_\Gamma$ denotes the jump of the normal derivative $\frac{\partial\hat{u}}{\partial\nu}$ across Γ. We have that $\hat{u}_{|\omega}$ solves the original problem $(P(\omega))$.

Let us compare $(\hat{P}(\Omega))$ with the classical fictitious domain formulation $(P(\Omega))$ with boundary Lagrange multipliers on γ. For this comparison we denote $(\hat{u}, \lambda) := (\hat{w}, \chi)$ in $(P(\Omega))$. The second component χ in $(P(\Omega))$ plays the role of a Lagrange multiplier releasing the constraint $\hat{w} = g$ on γ. On the other hand, λ in $(\hat{P}(\Omega))$ can be viewed as a control variable on Γ forcing $\hat{u}$ to match g on γ. Suppose that Γ and γ are smooth enough so that $\hat{u}_{|\Xi} \in H^2(\Xi)$, $\hat{u}_{|\Omega\setminus\overline{\Xi}} \in H^2(\Omega \setminus \overline{\Xi})$ if $\hat{u}$ solves $(\hat{P}(\Omega))$ and, similarly, $\hat{w}_{|\omega} \in H^2(\omega)$, $\hat{w}_{|\Omega\setminus\overline{\omega}} \in H^2(\Omega \setminus \overline{\omega})$ for $\hat{w}$ solving $(P(\Omega))$. In both cases, however, $\hat{u}$, $\hat{w} \in H^{3/2-\epsilon}(\Omega)$ for

any $\epsilon > 0$ due to a general non-zero jump of $\frac{\partial \hat{u}}{\partial \nu}$ and $\frac{\partial \hat{w}}{\partial \nu}$ across Γ and γ, respectively. Since the singularity of $\hat{u}$ solving $(\hat{P}(\Omega))$ is located on Γ, which has a positive distance from γ, one can expect that the new variant of the fictitious domain approach will increase the convergence rate of approximate solution in ω.

The question under which conditions $(\hat{P}(\Omega))$ has a solution is closely related to the following controllability type problem. We consider for each $\lambda \in H^{-1/2}(\Gamma)$ the following elliptic problem:

$$\left.\begin{array}{l} \text{Find } \hat{u} := \hat{u}(\lambda) \in H_0^1(\Omega) \text{ such that} \\ \displaystyle\int_\Omega \nabla \hat{u} \cdot \nabla v \,\mathrm{d}\Omega = \int_\Omega f v \,\mathrm{d}\Omega + \langle \lambda, v \rangle_\Gamma. \end{array}\right\} \qquad (\hat{P}(\lambda))$$

Since $(\hat{P}(\lambda))$ has a unique solution for every $\lambda \in H^{-1/2}(\Gamma)$, we can define a linear mapping $\Phi : H^{-1/2}(\Gamma) \mapsto H^{1/2}(\gamma)$ by

$$\Phi(\lambda) = \hat{u}(\lambda)_{|\gamma} \quad \forall \lambda \in H^{-1/2}(\Gamma), \tag{3.9}$$

where $\hat{u}(\lambda)$ solves $(\hat{P}(\lambda))$.

Theorem 3.4. *The range $\Phi(H^{-1/2}(\Gamma))$ is dense in $H^{1/2}(\gamma)$.*

Proof: See [21]. □

Thus the problem $(\hat{P}(\Omega))$ has a solution provided that $g \in \Phi(H^{-1/2}(\Gamma))$. In addition, $\hat{u}_{|\omega}$ is uniquely defined and solves $(P(\omega))$. If $g \notin \Phi(H^{-1/2}(\Gamma))$, then for every $\epsilon > 0$ we can find a $\tilde{g} \in \Phi(H^{-1/2}(\Gamma))$ such that

$$\|g - \tilde{g}\|_{1/2,\gamma} \leq \epsilon.$$

Denote by $\hat{w}$ a solution of $(\hat{P}(\Omega))$ with $g := \tilde{g}$. Then there exists a constant $c > 0$ such that

$$\|\hat{u} - \hat{w}\|_{1,\omega} \leq c\|g - \tilde{g}\|_{1/2,\gamma} \leq c\epsilon,$$

i.e., $\hat{w}_{|\omega}$ is a good approximation of the original problem $(P(\omega))'$, too.

In the computations which will be presented later, the space $H_0^1(\Omega)$ will be replaced by $H_{per}^1(\Omega)$, which is the space of periodic functions from $H^1(\Omega)$. Then the approximate controllability result of Theorem 3.4. remains true with the following modifications. Let

$$\Lambda_f(\Gamma) = \{\lambda \in H^{-1/2}(\Gamma) |\, \langle \lambda, 1 \rangle_\Gamma + \int_\Omega f \,\mathrm{d}\Omega = 0\}$$

and

$$H_0^{1/2}(\gamma) = \{\varphi \in H^{1/2}(\gamma) |\, \int_\gamma \varphi \,\mathrm{d}\gamma = 0\}.$$

If $\lambda \in \Lambda_f(\Gamma)$, then (3.13) has a solution $\hat{u}(\lambda)$ determined up to an arbitrary constant. To choose a unique solution we require that $\hat{u}(\lambda)_{|\gamma} \in (H_0^{1/2}(\gamma))^2$. This enables us to consider

the mapping Φ, defined by (3.9) as a mapping from $\Lambda_f(\Gamma)$ into $(H_0^{1/2}(\gamma))^2$. Then using the same approach as in Theorem 3.4. can be shown that $\Phi(\Lambda_f(\Gamma))^2$ is dense in $(H_0^{1/2}(\gamma))^2$ [21].

Let $V_h \subset H_0^1(\Omega)$, $\Lambda_H^\gamma \subset H^{-1/2}(\gamma)$, $\Lambda_H^\Gamma \subset H^{-1/2}(\Gamma)$, $h, H > 0$ be finite dimensional subspaces of the indicated spaces. Let $\dim V_h = n$ and $\dim \Lambda_H^\gamma = \dim \Lambda_H^\Gamma = m$. A discretization of $(\hat{P}(\Omega))$ results in the following problem:

$$\left.\begin{array}{l} \text{Find } (\hat{u}_h, \lambda_H) \in V_h \times \Lambda_H^\Gamma \text{ such that} \\ \displaystyle\int_\Omega \nabla \hat{u}_h \cdot \nabla v_h \,\mathrm{d}\Omega = \int_\Omega f v_h \,\mathrm{d}\Omega + \langle \lambda_H, v_h \rangle_\Gamma \quad \forall v_h \in V_h, \\ \langle \mu_H, \hat{u}_h \rangle_\gamma = \langle \mu_H, g \rangle_\gamma \quad \forall \mu_H \in \Lambda_H^\gamma, \end{array}\right\} \qquad (\hat{P}(\Omega))_h^H$$

where

$$\langle \lambda_H, v_h \rangle_\Gamma := \int_\Gamma \lambda_H v_h \,\mathrm{d}\Gamma$$

and similarly for $\langle\,,\,\rangle_\gamma$.

The discrete algebraic form of $(\hat{P}(\Omega))$ is based on the mixed finite element method and leads to the following generalized algebraic *saddle point* system:

$$\left.\begin{array}{l} \text{Find } (\mathbf{u}, \boldsymbol{\lambda}) \in \mathbb{R}^n \times \mathbb{R}^m \text{ such that} \\ \left(\begin{array}{c|c} \mathbf{A} & \mathbf{B}_\Gamma^T \\ \hline \mathbf{B}_\gamma & \mathbf{O} \end{array}\right)\left(\begin{array}{c} \mathbf{u} \\ \hline \boldsymbol{\lambda} \end{array}\right) = \left(\begin{array}{c} \mathbf{f} \\ \hline \mathbf{g} \end{array}\right), \end{array}\right\} \qquad (3.10)$$

where $\mathbf{A}$ is a $(n \times n)$ stiffness matrix, $\mathbf{B}_\Gamma, \mathbf{B}_\gamma$ are $(m \times n)$ matrices with elements

$$b_{\Gamma,ij} = \int_\Gamma \mu_i^\Gamma \varphi_j \,\mathrm{d}\Gamma, \qquad b_{\gamma,ij} = \int_\gamma \mu_i^\gamma \varphi_j \,\mathrm{d}\gamma, \qquad i = 1, \ldots, m,\ j = 1, \ldots, n,$$

respectively, and the vectors $\mathbf{f} \in \mathbb{R}^n$ and $\mathbf{g} \in \mathbb{R}^m$ are vectors whose components are

$$f_j = \int_\Omega f \varphi_j \,\mathrm{d}\Omega \quad \text{and} \quad g_i = \int_\gamma g \mu_i^\gamma \,\mathrm{d}\gamma, \quad j = 1, \ldots, n,\ i = 1, \ldots, m,$$

respectively. The above mentioned $\{\varphi_j\}_{j=1}^n$, $\{\mu_i^\Gamma\}_{i=1}^m$, and $\{\mu_i^\gamma\}_{i=1}^m$ are basis functions of V_h, Λ_H^Γ, and Λ_h^γ, respectively.

3.3 Linear elasticity problem solved using FDM

In this section, we apply the above described fictitious domain method to solve the linear elasticity problem introduced in the second chapter. To find the solution of a given problem we use the modified fictitious domain approach.

Let us recall the linear elasticity problem (2.1) from the previous chapter. We denote the space

$$V(\omega) = \left\{ \mathbf{v} \in (H^1(\omega))^2 \,|\, \mathbf{v} = \mathbf{o} \text{ on } \gamma_u \right\}.$$

Then the weak formulation of (2.1) reads as follows:

$$\left.\begin{aligned} &\text{Find } \mathbf{u} \in V(\omega) \text{ such that} \\ &a_\omega(\mathbf{u},\mathbf{v}) = \int_\omega \mathbf{f}\cdot\mathbf{v}\,\mathrm{d}\omega + (\mathbf{p},\mathbf{v})_{\gamma_p} \quad \forall \mathbf{v} \in V(\omega), \end{aligned}\right\} \tag{3.11}$$

where

$$a_\omega(\mathbf{u},\mathbf{v}) = \int_\omega \boldsymbol{\sigma}(\mathbf{u}) : \boldsymbol{\varepsilon}(\mathbf{v})\,\mathrm{d}\omega$$

and $(\cdot,\cdot)_{\gamma_p}$ is the scalar product in $(L^2(\gamma_p))^2$. The product $\boldsymbol{\sigma} : \boldsymbol{\varepsilon}$ is prescribed as

$$\boldsymbol{\sigma} : \boldsymbol{\varepsilon} = \sum_{i,j=1}^{n} \boldsymbol{\sigma}_{ij}\boldsymbol{\varepsilon}_{ij}.$$

For solving this weak formulation (3.11) we use the modified fictitious domain method mentioned above. We define the fictitious domain Ω such that $\overline{\omega} \subset \Omega$ and auxiliary boundary Γ surrounding the original domain ω to get a smoother solution of the original problem, see Fig. 3.6.

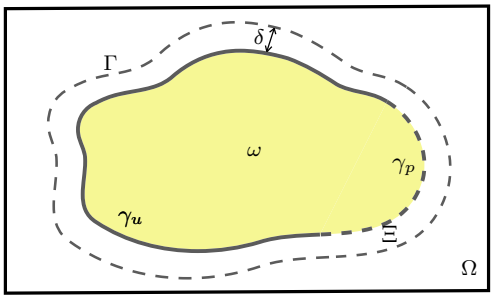

Figure 3.6: Modified FDM for LE problem

Also, we define the space

$$V(\Omega) = (H_0^1(\Omega))^2,$$

where $H_0^1(\Omega)$ is defined by (3.8).

Now we can introduce a modified fictitious domain formulation of the original linear elasticity problem, which is given as:

$$\left.\begin{aligned} &\text{Find } (\hat{\mathbf{u}},\boldsymbol{\lambda}) \in V(\Omega)\times\Lambda(\Gamma) \text{ such that} \\ &a_\Omega(\hat{\mathbf{u}},\mathbf{v}) + \langle \mathbf{v},\boldsymbol{\lambda}\rangle_\Gamma = \int_\Omega \mathbf{f}\cdot\mathbf{v}\,\mathrm{d}\Omega \quad \forall \mathbf{v} \in V(\Omega), \\ &\langle \boldsymbol{\mu}_u, \hat{\mathbf{u}}\rangle_{\gamma_u} = \mathbf{o} \quad \forall \boldsymbol{\mu}_u \in \Lambda(\gamma_u), \\ &\langle \boldsymbol{\mu}_p, \boldsymbol{\sigma}(\hat{\mathbf{u}})\boldsymbol{\nu}\rangle_{\gamma_p} = \langle \boldsymbol{\mu}_p, \mathbf{p}\rangle_{\gamma_p} \quad \forall \boldsymbol{\mu}_p \in \Lambda(\gamma_p), \end{aligned}\right\} \tag{3.12}$$

where $\Lambda(\Gamma) = (H^{-1/2}(\Gamma))^2$, $\Lambda(\gamma_u) = (H^{-1/2}(\gamma_u))^2$, $\Lambda(\gamma_p) = (H^{-1/2}(\gamma_p))^2$ and $\langle\,,\rangle_{\gamma_u}$, and $\langle\,,\rangle_{\gamma_p}$ stand for the duality pairings between $H^{1/2}(\gamma_u)$ and $H^{-1/2}(\gamma_u)$ and $H^{1/2}(\gamma_p)$ and

$H^{-1/2}(\gamma_p)$, respectively. Finally, $a_\Omega : V(\Omega) \times V(\Omega) \to \mathbb{R}$ and $\langle \mathbf{v}, \boldsymbol{\lambda} \rangle_\Gamma : V(\Omega) \times \Lambda(\Gamma) \to \mathbb{R}$ are two bounded bilinear forms. Here, the second component $\boldsymbol{\lambda}$ can be viewed as a control variable working on Γ to enforce the boundary conditions imposed on the original boundary.

If we suppose that problem (3.12) has a solution $(\hat{\mathbf{u}}, \boldsymbol{\lambda})$, then we can also see that the solution $(\hat{\mathbf{u}}, \boldsymbol{\lambda})$ satisfies the following problem and boundary conditions

$$\begin{aligned} -\operatorname{div} \boldsymbol{\sigma}(\hat{\mathbf{u}}) &= \mathbf{f} \quad \text{in} \quad \Xi \cup (\Omega \backslash \bar{\Xi}), \\ \hat{\mathbf{u}} &= \mathbf{o} \quad \text{on} \quad \gamma_u, \\ \boldsymbol{\sigma}(\hat{\mathbf{u}})\boldsymbol{\nu} &= \mathbf{p} \quad \text{on} \quad \gamma_p, \\ \hat{\mathbf{u}} &= \mathbf{o} \quad \text{on} \quad \partial\Omega, \\ [\boldsymbol{\sigma}(\hat{\mathbf{u}})\boldsymbol{\nu}]_\Gamma &= \boldsymbol{\lambda} \quad \text{on} \quad \Gamma, \end{aligned}$$

where $[\,]_\Gamma$ denotes the jump across Γ. We realize that $\hat{\mathbf{u}}_{|\omega}$ solves the original problem (2.1).

Let us consider for each $\boldsymbol{\lambda} \in (H^{-1/2}(\Gamma))^2$ the elliptic problem

$$\left.\begin{aligned} &\text{Find } \hat{\mathbf{u}}(\boldsymbol{\lambda}) \in (H_0^1(\Omega))^2 \text{ such that} \\ &a_\Omega(\hat{\mathbf{u}}, \mathbf{v}) + \langle \mathbf{v}, \boldsymbol{\lambda} \rangle_\Gamma = \int_\Omega \mathbf{f} \cdot \mathbf{v} \, \mathrm{d}\Omega \quad \forall \mathbf{v} \in V(\Omega). \end{aligned}\right\} \tag{3.13}$$

Then the conditions for the solution of (3.12) are related to problem (3.13). Since this problem has a unique solution for every $\boldsymbol{\lambda} \in (H^{-1/2}(\Gamma))^2$, we can define a linear mapping $\Phi : (H^{-1/2}(\Gamma))^2 \mapsto (H^{1/2}(\gamma))^2$ by

$$\Phi(\boldsymbol{\lambda}) = \hat{\mathbf{u}}(\boldsymbol{\lambda})_{|\gamma} \quad \forall \boldsymbol{\lambda} \in (H^{-1/2}(\Gamma))^2,$$

where $\hat{\mathbf{u}}(\boldsymbol{\lambda})$ solves (3.13) and get the equivalent controlability result as in Theorem 3.4.

Let $V_h \subset (H_0^1(\Omega))^2$, $\Lambda_H^{\gamma_u} \subset (H^{-1/2}(\gamma_u))^2$, $\Lambda_H^{\gamma_p} \subset (H^{-1/2}(\gamma_p))^2$, $\Lambda_H^\Gamma \subset (H^{-1/2}(\Gamma))^2$, $h, H > 0$ be finite dimensional subspaces of the indicated spaces. Let $\dim \Lambda_H^{\gamma_u} = 2m_u$, $\dim \Lambda_H^{\gamma_p} = 2m_p$, and $\dim \Lambda_H^\Gamma = 2m$, where

$$m_u + m_p = m.$$

When we have finite dimensional subspaces, we can discretize variational problem (3.12) and reformulate it into the following one:

$$\left.\begin{aligned} &\text{Find } (\hat{\mathbf{u}}_h, \boldsymbol{\lambda}_H) \in V_h \times \Lambda_H^\Gamma \text{ such that} \\ &a_\Omega(\hat{\mathbf{u}}_h, \mathbf{v}_h) + \langle \boldsymbol{\lambda}_H, \mathbf{v}_h \rangle_\Gamma = \int_\Omega \mathbf{f} \cdot \mathbf{v}_h \, \mathrm{d}\Omega \quad \forall \mathbf{v}_h \in V_h, \\ &\langle \boldsymbol{\mu}_u^H, \hat{\mathbf{u}}_h \rangle_{\gamma_u} = \mathbf{o} \quad \forall \boldsymbol{\mu}_u^H \in \Lambda_H^{\gamma_u}, \\ &\langle \boldsymbol{\mu}_p^H, \boldsymbol{\sigma}(\hat{\mathbf{u}}_h)\boldsymbol{\nu} \rangle_{\gamma_p} = \langle \boldsymbol{\mu}_p^H, \mathbf{p} \rangle_{\gamma_p} \quad \forall \boldsymbol{\mu}_p^H \in \Lambda_H^{\gamma_p}, \end{aligned}\right\} \tag{3.14}$$

where

$$\langle \boldsymbol{\lambda}_H, \mathbf{v}_h \rangle_\Gamma = \int_\Gamma \boldsymbol{\lambda}_H \cdot \mathbf{v}_h \, \mathrm{d}\Gamma,$$

and similarly for $\langle\,,\rangle_{\gamma_u}$ and $\langle\,,\rangle_{\gamma_p}$.

The theoretical results (existence, uniqueness) are equivalent to the results of the previous section.

The discrete algebraic form of (3.14) is based on the mixed finite element method and leads to the following generalized algebraic *saddle point* system:

$$\left.\begin{array}{c}\text{Find } (\mathbf{u},\boldsymbol{\lambda})\in\mathbb{R}^{2n}\times\mathbb{R}^{2m} \text{ such that}\\ \left(\begin{array}{c|c}\mathbf{A} & \mathbf{B}_\Gamma^T\\ \hline \mathbf{B}_{\gamma_u} & \mathbf{O}\\ \mathbf{C}_{\gamma_p} & \mathbf{O}\end{array}\right)\left(\begin{array}{c}\mathbf{u}\\ \hline \boldsymbol{\lambda}\end{array}\right)=\left(\begin{array}{c}\mathbf{f}\\ \hline \mathbf{o}\\ \mathbf{p}\end{array}\right),\end{array}\right\} \tag{3.15}$$

where $\mathbf{A}\in\mathbb{R}^{2n\times 2n}$ is a stiffness matrix, $\mathbf{B}_\Gamma\in\mathbb{R}^{2m\times 2n}$ and $\mathbf{B}_{\gamma_u}\in\mathbb{R}^{2m_u\times 2n}$ are the Dirichlet trace matrices on Γ and γ_u, respectively, with elements

$$b_{\Gamma,ij}=\int_\Gamma \mu_i^\Gamma\varphi_j\,\mathrm{d}\Gamma,\qquad b_{\gamma_u,kj}=\int_{\gamma_u}\mu_k^{\gamma_u}\varphi_j\,\mathrm{d}\gamma,\quad i=1,\dots,2m,\ j=1,\dots,2n,\ k=1,\dots,2m_u.$$

The matrix $\mathbf{C}_{\gamma_p}\in\mathbb{R}^{2m_p\times 2n}$ is the Neumann trace matrix (i.e. $\mathbf{C}_{\gamma_p}\mathbf{u}$ represents the trace of $\boldsymbol{\sigma}(\mathbf{u})\boldsymbol{\nu}$ on γ_p) (see (2.3)) defined as

$$\mathbf{C}_{\gamma_p}=\left(\begin{array}{c|c}\mathbf{C}_{11} & \mathbf{C}_{12}\\ \hline \mathbf{C}_{21} & \mathbf{C}_{22}\end{array}\right),$$

where

$$\mathbf{C}_{11}(i,j)=\int_{S_i}\mu_i^{\gamma_p}\nu_1\left[(\theta+2\mu)\frac{\partial(\varphi_j)}{\partial x_1}+\theta\frac{\partial(\varphi_j)}{\partial x_2}\right]\mathrm{d}s,\quad \operatorname{supp}\varphi_j\cap S_i\neq\emptyset,$$

where S_i are parts of boundary $\partial\omega$. Similarly we define $\mathbf{C}_{12}(i,j)$, $\mathbf{C}_{21}(i,j)$, $\mathbf{C}_{22}(i,j)$ according to the block structure in (2.3).

The vectors $\mathbf{f}=\left(\mathbf{f}_1^T,\mathbf{f}_2^T\right)^T\in\mathbb{R}^{2n}$ and $\mathbf{p}=\left(\mathbf{p}_1^T,\mathbf{p}_2^T\right)^T\in R^{2m_p}$ are assembled by

$$f_{1j}=\int_\Omega f_1\varphi_j\,\mathrm{d}\Omega,\quad f_{2j}=\int_\Omega f_2\varphi_j\,\mathrm{d}\Omega,\quad j=1,\dots,n,$$

and

$$p_{1l}=\int_{\gamma_p}p_1\mu_l^{\gamma_p}\,\mathrm{d}\gamma,\quad p_{2l}=\int_{\gamma_p}p_2\mu_l^{\gamma_p}\,\mathrm{d}\gamma\quad l=1,\dots,m_p,$$

respectively. The above $\{\varphi_j\}_{j=1}^n$, $\{\mu_i^\Gamma\}_{i=1}^m$, $\{\mu_k^{\gamma_u}\}_{k=1}^{m_u}$, and $\{\mu_l^{\gamma_p}\}_{l=1}^{m_p}$ are componentwise basis functions of V_h, Λ_H^Γ, $\Lambda_H^{\gamma_u}$, and $\Lambda_H^{\gamma_p}$, respectively.

The saddle point system is also called equilibrium equations or especially in the optimization literature "KKT system", from the Karush-Kuhn-Tucker constraint qualification.

For solving non-symmetric algebraic saddle-point system (3.15) we use the algorithm based on combination of the projected Schur complement method together with the null-space method. We show more details in the following chapter.

4 The Schur complement reduction and the null-space method

Before we start to explain details of the solving procedure based on the Schur complement reduction and the null-space method, we simplify notation used in (3.15) as

$$\left(\begin{array}{c|c} \mathbf{A} & \mathbf{B}_\Gamma^T \\ \hline \mathbf{B}_\gamma & \mathbf{O} \end{array}\right) \left(\begin{array}{c} \mathbf{u} \\ \hline \boldsymbol{\lambda} \end{array}\right) = \left(\begin{array}{c} \mathbf{f} \\ \hline \mathbf{g} \end{array}\right), \tag{4.1}$$

where the stiffness matrix $\mathbf{A} \in \mathbb{R}^{2n\times 2n}$ is singular, matrices $\mathbf{B}_\Gamma \in \mathbb{R}^{2m\times 2n}$ and $\mathbf{B}_\gamma = (\mathbf{B}_{\gamma_u}^T, \mathbf{C}_{\gamma_p}^T)^T \in \mathbb{R}^{2m\times 2n}$ are determined by the geometries of Γ and γ, respectively, and by the imposed boundary conditions, they have full row-ranks and also they are highly sparse. Morever, $\mathbf{f} \in \mathbb{R}^{2n}$ and $\mathbf{g} = (\mathbf{o}^T, \mathbf{p}^T)^T \in \mathbb{R}^{2m}$. Since $\mathbf{B}_\Gamma \neq \mathbf{B}_\gamma$, system (4.1) is non-symmetric, with n large and m much smaller than n with the defect $l = 2n - rank\,\mathbf{A}$, much smaller than m.

Remark 4.1. Let the matrix $\mathbf{A}$ be square. If there is a matrix $\mathbf{B}$ satisfying

$$\mathbf{AB} = \mathbf{BA} = \mathbf{I},$$

where $\mathbf{I}$ is an identity matrix, then the matrix $\mathbf{B}$ is the inverse matrix to $\mathbf{A}$ and can be written as $\mathbf{B} = \mathbf{A}^{-1}$. If this inversion exists, then the matrix $\mathbf{A}$ is *non-singular*. In the opposite case, the matrix $\mathbf{A}$ is called *singular*.

We can solve algebraic system (4.1) with several approaches, but due to the structure of our matrices, we focus on solving methods based on the Schur complement reduction. The main idea of these methods is an elimination of the first component $\mathbf{u}$ of the solution pair $(\mathbf{u}, \boldsymbol{\lambda})$. If the stiffness matrix $\mathbf{A}$ is non-singular, the elimination leads to a reduced system for the second unknown $\boldsymbol{\lambda}$, as

$$\mathbf{B}_\gamma \mathbf{A}^{-1} \mathbf{B}_\Gamma^T \boldsymbol{\lambda} = \mathbf{B}_\gamma \mathbf{A}^{-1} \mathbf{f} - \mathbf{g}, \tag{4.2}$$

where $\mathcal{S} = -\mathbf{B}_\gamma \mathbf{A}^{-1} \mathbf{B}_\Gamma^T$ is the Schur complement to $\mathbf{A}$. After we compute $\boldsymbol{\lambda}$ by (4.2), we obtain $\mathbf{u}$ from

$$\mathbf{Au} = \mathbf{f} - \mathbf{B}_\Gamma^T \boldsymbol{\lambda},$$

so

$$\mathbf{u} = \mathbf{A}^{-1}(\mathbf{f} - \mathbf{B}_\Gamma^T \boldsymbol{\lambda}).$$

When $\mathbf{A}$ is singular, the first component $\mathbf{u}$ from (4.1) cannot be completely eliminated. To solve this problem, we use the *projected* Schur complement method presented in [21]. It combines the Schur complement reduction with the null-space method implemented by orthogonal projectors. It follows that the Schur complement reduction leads to another algebraic system with two unknowns: the first unknown $\boldsymbol{\lambda}$ from the previous saddle point system and a new unknown $\boldsymbol{\alpha}$, which corresponds to the null-space of $\mathbf{A}$.

Remark 4.2. Let us recall the definition of the null-space (kernel) and the range-space (image) of an $(m_c \times n_c)$ matrix $\mathbf{C}$ on the space $V \subset \mathbb{R}^{n_c}$:

$$\begin{aligned} Ker(\mathbf{C}|V) &:= \{\mathbf{v} \in V : \mathbf{C}\mathbf{v} = \mathbf{o}\}, \\ Im(\mathbf{C}|V) &:= \{\boldsymbol{\mu} \in \mathbb{R}^{m_c} : \boldsymbol{\mu} = \mathbf{C}\mathbf{v}, \mathbf{v} \in V\}. \end{aligned}$$

Let us also mention that $Ker(\mathbf{C}^T)$ is the orthogonal complement of $Im(\mathbf{C})$ in $\mathbb{R}^{m_c}$, especially, if $\mathbf{v} \perp Ker(\mathbf{C}^T)$, there is a vector $\mathbf{w} \in \mathbb{R}^{n_c}$ such that $\mathbf{v} = \mathbf{C}\mathbf{w}$.

We suppose that the saddle-point system (4.1) has a unique solution that is guaranteed by the following necessary and sufficient conditions [21]:

$$Ker(\mathbf{B}_\Gamma^T) = \{\mathbf{o}\}, \tag{4.3}$$

$$Ker(\mathbf{A}) \cap Ker(\mathbf{B}_\gamma) = \{\mathbf{o}\}, \tag{4.4}$$

$$Ker(\mathbf{A}|Ker(\mathbf{B}_\gamma)) \cap Ker(\mathbf{B}_\Gamma^T) = \{\mathbf{o}\}. \tag{4.5}$$

As next, we denote

$$l = 2n - rank\,\mathbf{A} = \dim Ker(\mathbf{A}),$$

as a defect of $\mathbf{A}$, $1 \leq l \ll m$ in our case. Thus we define $(2n \times l)$ matrix $\mathbf{R}$ whose columns span the null-space $Ker(\mathbf{A})$ of $\mathbf{A}$, i.e.

$$\mathbf{A}\mathbf{R} = \mathbf{O}.$$

Definition 4.1. *Let matrix $\mathbf{A} \in \mathbb{R}^{m_A \times n_A}$ be given. Then $\mathbf{A}^\dagger$ is a general inverse to $\mathbf{A}$, iff*

$$\mathbf{A} = \mathbf{A}\mathbf{A}^\dagger\mathbf{A}.$$

It follows that the generalized Schur complement of $\mathbf{A}$ in (4.1) is defined by

$$\mathcal{S} := \begin{pmatrix} -\mathbf{B}_\gamma\mathbf{A}^\dagger\mathbf{B}_\Gamma^T & \mathbf{B}_\gamma\mathbf{R} \\ \mathbf{R}^T\mathbf{B}_\Gamma^T & \mathbf{O} \end{pmatrix}.$$

Theorem 4.1. *The Schur complement $\mathcal{S}$ is invertible iff conditions (4.3) - (4.5) are satisfied.*

Proof: See [21]. □

Remark 4.3. Any symmetric positive semi-definite matrix $\mathbf{A} \in \mathbb{R}^{m_A \times n_A}$ can be factorized into a product $\mathbf{L}\mathbf{D}\mathbf{L}^T$ with a non-singular lower triangular matrix $\mathbf{L}$ and a diagonal matrix $\mathbf{D} = \mathrm{diag}(d_1, \ldots, d_{n_A})$. Let us define $\mathbf{D}^\dagger = \mathrm{diag}(d_1^\dagger, \ldots, d_{n_A}^\dagger)$, where $d_i^\dagger = 1/d_i$ if $d_i \neq 0$ and $d_i^\dagger = 0$ if $d_i = 0$, $i = 1, \ldots, n_A$. It can be verified that $\mathbf{A}^\dagger = (\mathbf{L}^T)^{-1}\mathbf{D}^\dagger(\mathbf{L})^{-1}$ is symmetric positive semi-definite and satisfies

$$\mathbf{A} = \mathbf{A}\mathbf{A}^\dagger\mathbf{A}.$$

Other very efficient strategies of computing generalized inverses were published in [4, 30].

Now we can formulate a new algebraic system with unknowns $(\boldsymbol{\lambda}, \boldsymbol{\alpha})$. It follows that the second unknown $\boldsymbol{\lambda}$ of system (4.1) is the first unknown of the linear system

$$\begin{pmatrix} \mathbf{B}_\gamma \mathbf{A}^\dagger \mathbf{B}_\Gamma^T & -\mathbf{B}_\gamma \mathbf{R} \\ -\mathbf{R}^T \mathbf{B}_\Gamma^T & \mathbf{O} \end{pmatrix} \begin{pmatrix} \boldsymbol{\lambda} \\ \boldsymbol{\alpha} \end{pmatrix} = \begin{pmatrix} \mathbf{B}_\gamma \mathbf{A}^\dagger \mathbf{f} - \mathbf{g} \\ -\mathbf{R}^T \mathbf{f} \end{pmatrix}$$

and the first unknown $\mathbf{u}$ of algebraic system (4.1) is given by

$$\mathbf{u} = \mathbf{A}^\dagger (\mathbf{f} - \mathbf{B}_\Gamma^T \boldsymbol{\lambda}) + \mathbf{R}\boldsymbol{\alpha}. \tag{4.6}$$

We simplify our notation and get

$$\begin{pmatrix} \mathbf{F} & \mathbf{G}_1^T \\ \mathbf{G}_2 & \mathbf{O} \end{pmatrix} \begin{pmatrix} \boldsymbol{\lambda} \\ \boldsymbol{\alpha} \end{pmatrix} = \begin{pmatrix} \mathbf{d} \\ \mathbf{e} \end{pmatrix}, \tag{4.7}$$

where

$$\begin{array}{llll} \mathbf{F} := \mathbf{B}_\gamma \mathbf{A}^\dagger \mathbf{B}_\Gamma^T, & \mathbf{G}_1 := -\mathbf{R}^T \mathbf{B}_\gamma^T, & \mathbf{G}_2 := -\mathbf{R}^T \mathbf{B}_\Gamma^T, & \\ \mathbf{d} := \mathbf{B}_\gamma \mathbf{A}^\dagger \mathbf{f} - \mathbf{g} & \mathbf{e} := -\mathbf{R}^T \mathbf{f}. & & \end{array}$$

When we compare sizes of algebraic systems (4.1) and (4.7), we see that the size of the first system is much larger than the size of the second one. Algebraic system (4.7) can be solved again by the Schur complement reduction or more efficiently by the null-space method using orthogonal projectors. We can construct these projectors from non-diagonal blocks $\mathbf{G}_1$ and $\mathbf{G}_2$. More precisely, we define two orthogonal projectors onto the null-spaces of $\mathbf{G}_1$ and $\mathbf{G}_2$.

Before we explain the use of these projectors, we briefly mention the definition of the orthogonal projector onto particular space.

Remark 4.4. Let $\mathbf{G} \in \mathbb{R}^{m_G \times n_G}$, $m_G < n_G$, be a matrix with full row-rank. The linear operator

$$\mathbf{P} : \mathbb{R}^{n_G} \to Ker(\mathbf{G})$$

is an orthogonal projector onto $Ker(\mathbf{G})$ if it satisfies these two conditions:

$$\begin{array}{ll} (i) & \mathbf{P}\mathbf{x} = \mathbf{x} \quad \forall \mathbf{x} \in Ker(\mathbf{G}), \\ (ii) & (\mathbf{x} - \mathbf{P}\mathbf{x}, \mathbf{y}) = \mathbf{o} \quad \forall \mathbf{x} \in \mathbb{R}^{n_G} \ \forall \mathbf{y} \in Ker(\mathbf{G}). \end{array}$$

The geometrical interpretation of these two conditions are illustrated in Figure (4.1):

We can identify the orthogonal projector with the matrix

$$\mathbf{P} := \mathbf{I} - \mathbf{G}^T (\mathbf{G}\mathbf{G}^T)^{-1} \mathbf{G} \tag{4.8}$$

and simply verify that

$$\mathbf{G}\mathbf{P} = \mathbf{O} \quad \mathbf{P}\mathbf{G}^T = \mathbf{O} \quad \text{and} \quad Ker(\mathbf{P}) = Im(\mathbf{G}^T) \ .$$

Let us denote by $\mathbf{P}_1$ and $\mathbf{P}_2$ the orthogonal projectors associated with the matrices $\mathbf{G}_1$ and $\mathbf{G}_2$, respectively.

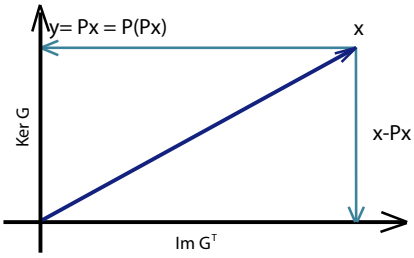

Figure 4.1: Projection

The first projector splits the saddle-point algebraic structure of the reduced system, the second projector decomposes the unknown $\boldsymbol{\lambda} \in \mathbb{R}^{2m}$ into two components $\boldsymbol{\lambda}_{Im}$ and $\boldsymbol{\lambda}_{Ker}$ as

$$\boldsymbol{\lambda} := \boldsymbol{\lambda}_{Im} + \boldsymbol{\lambda}_{Ker},$$

where $\boldsymbol{\lambda}_{Im}$ belongs to the range-space of $\mathbf{G}_2^T$ ($\boldsymbol{\lambda}_{Im} \in Im(\mathbf{G}_2^T)$) and $\boldsymbol{\lambda}_{Ker}$ belongs to the null-space of $\mathbf{G}_2$ ($\boldsymbol{\lambda}_{Ker} \in Ker(\mathbf{G}_2)$). Then $\boldsymbol{\lambda}$ is the first component of the solution to the algebraic system (4.7) iff

$$\boldsymbol{\lambda}_{Im} = \mathbf{G}_2^T(\mathbf{G}_2\mathbf{G}_2^T)^{-1}\mathbf{e} \tag{4.9}$$

and $\boldsymbol{\lambda}_{Ker}$ satisfies the following equation:

$$\mathbf{P}_1\mathbf{F}\boldsymbol{\lambda}_{Ker} = \mathbf{P}_1(\mathbf{d} - \mathbf{F}\boldsymbol{\lambda}_{Im}). \tag{4.10}$$

The component $\boldsymbol{\lambda}_{Ker}$ can be computed by a projected Krylov subspace method for non-symmetric operators. Therefore we use the projected BiCGSTAB algorithm derived from the non-projected one [48]. We introduce this method in more detail in the following chapter.

Finally, the second component of algebraic system (4.7) is given by

$$\boldsymbol{\alpha} = (\mathbf{G}_1\mathbf{G}_1^T)^{-1}\mathbf{G}_1(\mathbf{d} - \mathbf{F}\boldsymbol{\lambda}). \tag{4.11}$$

Example 4.1. Let us find the solution pair $(\hat{\mathbf{u}}, \hat{\boldsymbol{\lambda}})$ of the following generalized algebraic saddle-point system 4.1 with the following data:

$$\left(\begin{array}{c|c} \mathbf{A} & \mathbf{B}_\Gamma^T \\ \hline \mathbf{B}_\gamma & \mathbf{O} \end{array}\right) = \left(\begin{array}{ccc|cc} 1 & 0 & 0 & 0 & 0 \\ 0 & 0 & 0 & 1 & 0 \\ 0 & 0 & 1 & 2 & 1 \\ \hline 0 & 1 & 2 & 0 & 0 \\ 0 & 1 & 1 & 0 & 0 \end{array}\right), \quad \mathbf{f} = \begin{pmatrix} 2 \\ 2 \\ 1 \end{pmatrix}, \text{ and } \quad \mathbf{g} = \begin{pmatrix} 4 \\ 1 \end{pmatrix}.$$

We can verify that (4.3) - (4.5) hold, i.e. the system matrix is invertible and

$$\mathbf{A}^\dagger = \mathbf{A}$$

is the generalized inverse satisfying $\mathbf{A} = \mathbf{A}\mathbf{A}^{\dagger}\mathbf{A}$. Finally, the matrix $\mathbf{R}$ whose columns span the kernel of $\mathbf{A}$ can be read as

$$\mathbf{R} = \begin{pmatrix} 0 \\ 1 \\ 0 \end{pmatrix}.$$

Now we apply the Schur complement reduction and get the reduced system (4.7) with

$$\begin{pmatrix} \mathbf{F} & \mathbf{G}_1^T \\ \mathbf{G}_2 & \mathbf{O} \end{pmatrix} = \left(\begin{array}{cc|c} 4 & 2 & -1 \\ 2 & 1 & -1 \\ \hline -1 & 0 & 0 \end{array}\right) \quad \text{and} \quad \begin{pmatrix} \mathbf{d} \\ \mathbf{e} \end{pmatrix} = \left(\begin{array}{c} -2 \\ 0 \\ \hline -2 \end{array}\right).$$

The orthogonal projectors $\mathbf{P}_1$ and $\mathbf{P}_2$ onto

$$\begin{array}{rcl} Ker(\mathbf{G}_1) & = & \{(\lambda_1, \lambda_2)^T \in \mathbb{R}^2 : \lambda_1 + \lambda_2 = 0\}, \\ Ker(\mathbf{G}_2) & = & \{(\lambda_1, \lambda_2)^T \in \mathbb{R}^2 : \lambda_1 = 0\} \end{array}$$

are given by their definition in (4.8) as follows:

$$\mathbf{P}_1 = \begin{pmatrix} 1/2 & -1/2 \\ -1/2 & 1/2 \end{pmatrix} \quad \text{and} \quad \mathbf{P}_2 = \begin{pmatrix} 0 & 0 \\ 0 & 1 \end{pmatrix},$$

respectively. Using expression (4.9), we obtain the result for $\boldsymbol{\lambda}_{Im}$ as

$$\hat{\boldsymbol{\lambda}}_{Im} = \begin{pmatrix} -1 \\ 0 \end{pmatrix} (1)^{-1}(-2) = \begin{pmatrix} 2 \\ 0 \end{pmatrix}.$$

As

$$\mathbf{P}_1\mathbf{F} = \begin{pmatrix} 1 & 1/2 \\ -1 & -1/2 \end{pmatrix} \quad \text{and} \quad \mathbf{P}_1(\mathbf{d} - \mathbf{F}\hat{\boldsymbol{\lambda}}_{Im}) = \begin{pmatrix} -3 \\ 3 \end{pmatrix},$$

we see that equation (4.10) reads as

$$\begin{array}{rcl} \lambda_1 + 1/2\lambda_2 & = & -3, \\ -\lambda_1 - 1/2\lambda_2 & = & 3, \end{array} \tag{4.12}$$

where

$$\hat{\boldsymbol{\lambda}}_{Ker} = \begin{pmatrix} \lambda_1 \\ \lambda_2 \end{pmatrix}.$$

Since $\hat{\boldsymbol{\lambda}}_{Ker} \in Ker(\mathbf{G}_2)$, we get $\lambda_1 = 0$ so that (4.12) implies $\lambda_2 = -6$ and

$$\hat{\boldsymbol{\lambda}} = \hat{\boldsymbol{\lambda}}_{Ker} + \hat{\boldsymbol{\lambda}}_{Im} = \begin{pmatrix} 2 \\ -6 \end{pmatrix}.$$

Then according to (4.11) we can enumerate

$$\boldsymbol{\alpha} = (2)^{-1}(-1, -1)\left(\begin{pmatrix} -2 \\ 0 \end{pmatrix} - \begin{pmatrix} 2 \\ 2 \end{pmatrix}\right) = -2$$

and, finally, the formula (4.6) gives the first unknown of the solution pair

$$\hat{\mathbf{u}} = \begin{pmatrix} 2 \\ -2 \\ 3 \end{pmatrix}.$$

In this chapter, we explained details of the methods based on the combination of the Schur complement reduction and null-space method implemented by orthogonal projectors. In the next chapter, we use these methods and combine them with an efficient solver for computing $\boldsymbol{\lambda}_{Ker}$ from (4.10).

At first, before we bring technical details of solving procedures to find a pair $(\mathbf{u}, \boldsymbol{\lambda})$, let us introduce the main principle of the Krylov subspace method for solving saddle point systems.

5 Krylov subspace method

In this section, we introduce the Krylov subspace method for solving saddle point systems. At first we describe the main principles and properties of the basic use of this method for the unpreconditioned and non-singular saddle point systems and in the following sections, we describe the general ideas of the Krylov subspace method for singular saddle-point system and its generalized variant with non-symmetric operators.

5.1 The basics of the Krylov subspace method

Let us have the linear system

$$\mathbf{A}\mathbf{x} = \mathbf{b},$$

where the matrix $\mathbf{A} \in \mathbb{R}^{n_A \times n_A}$ is square and positive definite.

Suppose that $\mathbf{x}_0$ is an initial iteration for the solution $\mathbf{x}$ of this system and next we define an initial residual $\mathbf{r}_0 = \mathbf{b} - \mathbf{A}\mathbf{x}_0$. The Krylov subspace method belongs to iterative methods and the kth iterate $\mathbf{x}_k$ satisfies

$$\mathbf{x}_k \in \mathbf{x}_0 + \mathcal{K}_k(\mathbf{A}, \mathbf{r}_0), \quad k = 1, 2, \ldots, \tag{5.1}$$

where

$$\mathcal{K}_k(\mathbf{A}, \mathbf{r}_0) := \mathrm{Span}\{\mathbf{r}_0, \mathbf{A}\mathbf{r}_0, \ldots, \mathbf{A}^{k-1}\mathbf{r}_0\} \tag{5.2}$$

denotes the kth Krylov subspace generated by $\mathbf{A}$ and $\mathbf{r}_0$.

Definition 5.1. A *vector space called a linear span is a set*

$$Span\{\mathbf{v}_1, \ldots, \mathbf{v}_k\} = \{\mathbf{v} \in \mathbb{R}^n : \mathbf{v} = \alpha_1\mathbf{v}_1 + \cdots + \alpha_k\mathbf{v}_k,\ \alpha_i \in \mathbb{R},\ \forall i\},$$

where vectors $\mathbf{v}_1, \ldots, \mathbf{v}_k \in \mathbb{R}^n$ *are given.*

It follows that k constraints are needed to make $\mathbf{x}_k$ unique. We can achieve this by the requirement that the kth residual $\mathbf{r}_k = \mathbf{b} - \mathbf{A}\mathbf{x}_k$ is orthogonal to a k-dimensional space $\mathcal{C}_k$ called constraints space, i.e.,

$$\mathbf{r}_k = \mathbf{b} - \mathbf{A}\mathbf{x}_k \in \mathbf{r}_0 + \mathbf{A}\mathcal{K}_k(\mathbf{A}, \mathbf{r}_0), \quad \mathbf{r}_k \perp \mathcal{C}_k. \tag{5.3}$$

The previous relations show, that the Krylov subspace method is a general type of the projection process which can be found in many areas of mathematics. The interpretation of Krylov subspace method as projection processes has been described by Saad in [44]. By the knowledge of the properties of the system matrix $\mathbf{A}$ we can possibly determine constraint spaces $\mathcal{C}_k$ and it leads to uniquely defined iterates $\mathbf{x}_k$, $k = 1, 2, \ldots$, where k is the dimension of the Krylov subspace. Examples for such spaces are given in the following theorem.

Theorem 5.1. *Suppose that the Krylov subspace $\mathcal{K}_k(\mathbf{A}, \mathbf{r}_0)$ has the dimension k. If*
(1) A is symmetric positive definite and $\mathcal{C}_k = \mathcal{K}_k(\mathbf{A}, \mathbf{r}_0)$, or
(2) A is non-singular and $\mathcal{C}_k = \mathbf{A}\mathcal{K}_k(\mathbf{A}, \mathbf{r}_0)$,
then there exists a uniquely defined iterate $\mathbf{x}_k$ of the form (5.1), for which the residual $\mathbf{r}_k = \mathbf{b} - \mathbf{A}\mathbf{x}_k$ satisfies (5.3).

Proof: See [44]. □

The theorem mentioned above represents mathematical characterizations of the projection properties of well known Krylov subspace methods. The item (1) characterizes the conjugate gradient (CG) method for symmetric positive definite matrices. Implementations of the projection process characterized by the item (2) are the minimal residual (MINRES) method for non-singular symmetric (possibly indefinite) matrices, and the generalized minimal residual (GMRES) method for general non-singular matrices.

Numerous other choices of constraint spaces for constructing Krylov subspace methods exist. In the case of a non-symmetric matrix $\mathbf{A}$, one may choose $\mathcal{C}_k = \mathcal{K}_k(\mathbf{A}^T, \mathbf{r}_0)$ which represents a generalization of the projection process characterized in the item (1). Specific implementations based on this choice include the method of Lanczos and the biconjugate gradient (BiCG) method. However, for a general non-symmetric matrix $\mathbf{A}$ the process based on $\mathcal{C}_k = \mathcal{K}_k(\mathbf{A}^T, \mathbf{r}_0)$ is not well defined since it may happen that no iterate $\mathbf{x}_k$ satisfying (5.1)-(5.2) and (5.3) exists. In an implementation such as (BiCG) it leads to a breakdown. Such instabilities are often overcome by the stabilized BiCG (BiCGSTAB) method which combines the BiCG projection principle with an additional minimization step in order to stabilize the convergence behavior, for more details see [31].

5.2 Krylov subspace method for symmetric operator

Let us recall the algebraic system (4.1), where $\mathbf{A}$ is singular and we denote

$$\mathbf{B} := \mathbf{B}_\gamma = \mathbf{B}_\Gamma.$$

Here we summarize the procedure for solving a given saddle-point system with singular matrix $\mathbf{A}$. To compute the solution pair $(\mathbf{u}, \boldsymbol{\lambda})$ we use a projected Schur complement method for symmetric operators, described as follows:

Algorithm: Projected Schur Complement Method (symmetric case)

1. Assemble $\mathbf{G} := -\mathbf{R}^T\mathbf{B}^T$, $\mathbf{d} := \mathbf{B}\mathbf{A}^\dagger\mathbf{f} - \mathbf{g}$, $\mathbf{e} := -\mathbf{R}^T\mathbf{f}$.
2. Assemble $\mathbf{H} := (\mathbf{G}\mathbf{G}^T)^{-1}$.
3. Assemble $\boldsymbol{\lambda}_{Im} := \mathbf{G}^T\mathbf{H}\mathbf{e}$.
4. Assemble $\tilde{\mathbf{d}} := \mathbf{P}(\mathbf{d} - \mathbf{F}\boldsymbol{\lambda}_{Im})$.
5. Solve the equation $\mathbf{P}\mathbf{F}\boldsymbol{\lambda}_{Ker} = \tilde{\mathbf{d}}$ on $Ker(\mathbf{G})$.
6. Assemble $\boldsymbol{\lambda} := \boldsymbol{\lambda}_{Ker} + \boldsymbol{\lambda}_{Im}$.
7. Assemble $\boldsymbol{\alpha} := \mathbf{H}\mathbf{G}(\mathbf{d} - \mathbf{F}\boldsymbol{\lambda})$.
8. Assemble $\mathbf{u} := \mathbf{A}^\dagger(\mathbf{f} - \mathbf{B}^T\boldsymbol{\lambda}) + \mathbf{R}\boldsymbol{\alpha}$.

Matrices $\mathbf{F}$, $\mathbf{P}$ are of the order $(2m \times 2m)$. They are not stored, since only their matrix-vector products are needed:

$$\mathbf{Fv} := \mathbf{B}(\mathbf{A}^{\dagger}(\mathbf{Bv})) \quad \text{and} \quad \mathbf{Pv} := \mathbf{v} - \mathbf{G}(\mathbf{H}(\mathbf{G}^T\mathbf{v})).$$

To solve the equation and find a particular solution $\boldsymbol{\lambda}_{Ker}$ in Step 5, we introduce a projected conjugate gradient method with preconditioning (PCGP). We want to solve $\boldsymbol{\lambda}_{Ker}$ by solving the system

$$\mathbf{PF}\boldsymbol{\lambda}_{Ker} = \tilde{\mathbf{d}} \quad \text{on} \quad Ker(\mathbf{G}) \tag{5.4}$$

with the cheap lumped preconditioner $\overline{\mathbf{F}^{-1}}$ to $\mathbf{F}$ (see [10]).

Remark 5.1. For an orthonormal matrix $\mathbf{B}$ we get

$$\overline{\mathbf{F}^{-1}} = \mathbf{BAB}^T.$$

Now, we introduce the PCGP algorithm for solving problem (5.4).

Algorithm: PCGP $[\varepsilon, \mathbf{F}, \mathbf{P}, \tilde{\mathbf{d}}] \rightarrow \boldsymbol{\lambda}_{Ker}$
Initialize: Let $\mathbf{r}^0 = \tilde{\mathbf{d}}$, $\boldsymbol{\lambda}^0_{Ker} = \mathbf{o}$
Iterate: $k = 1, 2, \ldots,$ until convergence
While $\|\mathbf{r}^k\| > \varepsilon$

Project $\mathbf{w}_{k-1} = \mathbf{P}\mathbf{r}_{k-1}$.
Precondition $\mathbf{z}_{k-1} = \overline{\mathbf{F}^{-1}}\mathbf{w}_{k-1}$.
Project $\mathbf{y}_{k-1} = \mathbf{P}\mathbf{z}_{k-1}$.
$\beta_k = (\mathbf{y}_{k-1})^T\mathbf{w}_{k-1}/(\mathbf{y}_{k-2})^T\mathbf{w}_{k-2}, \quad (\beta_1 = 0).$
$\mathbf{p}_k = \mathbf{y}_{k-1} + \beta_k\mathbf{p}_{k-1}, \quad (p_1 = y_0).$
$\alpha_k = (\mathbf{y}_{k-1})^T\mathbf{w}_{k-1}/(\mathbf{p}_k)^T\mathbf{F}\mathbf{p}_k,$
$\boldsymbol{\lambda}^k_{Ker} = \boldsymbol{\lambda}^{k-1}_{Ker} + \boldsymbol{\alpha}_k\mathbf{p}_k,$
$\mathbf{r}_k = \mathbf{r}_{k-1} - \alpha_k\mathbf{F}\mathbf{p}_k,$

End while
Return: $\boldsymbol{\lambda}_{Ker} := \boldsymbol{\lambda}^k_{Ker}$.

The solving algorithms introduced above for symmetric case summarize the procedure to find the solution pair $(\hat{\mathbf{u}}, \hat{\boldsymbol{\lambda}})$ of the saddle-point system (7.3) which can be seen later in Chapter 7.

5.3 Krylov subspace method for non-symmetric operator

Let us bring more technical details of the procedure for non-symmetric operators. Before we see the whole algorithm for solving this given algebraic problem, let us describe some particular numerical procedures, which are used in this algorithm.

Let us recall the saddle-point system (4.1), where $\mathbf{A}$ is singular matrix and

$$\mathbf{B}_\gamma \neq \mathbf{B}_\Gamma.$$

Thus, we get a generalized (non-symmetric) saddle-point system and in the following part we introduce algorithms to find the solution of this system. These procedures are based on the already mentioned methods described in Chapter 4. At first, we can formulate the algorithm for the method based on the Schur complement reduction as follows.

Algorithm: Projected Schur Complement Method (non-symmetric case)

1. Assemble $\mathbf{G}_1 := -\mathbf{R}^T\mathbf{B}_\gamma^T$,$\mathbf{G}_2 := -\mathbf{R}^T\mathbf{B}_\Gamma^T$, $\mathbf{d} := \mathbf{B}_2\mathbf{A}^\dagger\mathbf{f} - \mathbf{g}$, $\mathbf{e} := -\mathbf{R}^T\mathbf{f}$.
2. Assemble $\mathbf{H}_1 := (\mathbf{G}_1\mathbf{G}_1^T)^{-1}$ and $\mathbf{H}_2 := (\mathbf{G}_2\mathbf{G}_2^T)^{-1}$.
3. Assemble $\boldsymbol{\lambda}_{Im} := \mathbf{G}_2^T\mathbf{H}_2\mathbf{e}$.
4. Assemble $\tilde{\mathbf{d}} := \mathbf{P}_1(\mathbf{d} - \mathbf{F}\boldsymbol{\lambda}_{Im})$.
5. Solve the equation $\mathbf{P}_1\mathbf{F}\boldsymbol{\lambda}_{Ker} = \tilde{\mathbf{d}}$ on $Ker(\mathbf{G}_2)$.
6. Assemble $\boldsymbol{\lambda} := \boldsymbol{\lambda}_{Ker} + \boldsymbol{\lambda}_{Im}$.
7. Assemble $\boldsymbol{\alpha} := \mathbf{H}_1\mathbf{G}_1(\mathbf{d} - \mathbf{F}\boldsymbol{\lambda})$.
8. Assemble $\mathbf{u} := \mathbf{A}^\dagger(\mathbf{f} - \mathbf{B}_\Gamma^T\boldsymbol{\lambda}) + \mathbf{R}\boldsymbol{\alpha}$.

The most important step of this algorithm is Step 5. It finds a particular solution $\boldsymbol{\lambda}_{Ker}$ of the solution $\boldsymbol{\lambda}$:

$$\mathbf{P}_1\mathbf{F}\boldsymbol{\lambda}_{Ker} = \tilde{\mathbf{d}} \quad \text{on} \quad Ker(\mathbf{G}_2). \tag{5.5}$$

It was already mentioned that, this solution can be efficiently found by a projected Krylov subspace method for non-symmetric operators.

It is easy to see that the matrix $\mathbf{P}_1\mathbf{F}$ is of the order $(2m \times 2m)$, but we solved this problem on $Ker(\mathbf{G}_2)$, and therefore we need only a restriction to the $(2m-l)$ dimensional subspace $Ker(\mathbf{G}_2)$. Before the algorithm for the Krylov method (ProjBiCGSTAB) is shown, it is important to mention that if the solution of (5.5) belongs to the subspace $Ker(\mathbf{G}_2)$, also the iterations $\boldsymbol{\lambda}_{Ker}^k$ of ProjBiCGSTAB algorithm belongs to this subspace. This can be achieved by choosing the first iterate $\boldsymbol{\lambda}_{Ker}^0$ in $Ker(\mathbf{G}_2)$ and by projecting each ProjBiCGSTAB directions $\mathbf{p}^k$ and $\mathbf{s}^k$ onto $Ker(\mathbf{G}_2)$, this can be written as

$$\boldsymbol{\lambda}_{Ker}^{k+1} = \boldsymbol{\lambda}_{Ker}^k + \boldsymbol{\alpha}_k\mathbf{P}_2\mathbf{p}^k + \boldsymbol{\omega}_k\mathbf{P}_2\mathbf{s}^k.$$

Let us introduce the ProjBiCGSTAB algorithm for solving problem (5.5).

Algorithm: ProjBiCGSTAB[$\varepsilon, \mathbf{F}, \mathbf{P}_1, \mathbf{P}_2, \tilde{\mathbf{d}}$] $\rightarrow \boldsymbol{\lambda}_{Ker}$

Initialize: Let $\boldsymbol{\lambda}_{Ker}^0 \in Ker(\mathbf{G}_2)$ be given, $\mathbf{r}^0 := \mathbf{P}_2\mathbf{F}^T(\tilde{\mathbf{d}} - \mathbf{P}_1\mathbf{F}\mathbf{P}_2\boldsymbol{\lambda}_{Ker}^0)$, $\mathbf{p}^0 := \mathbf{r}^0$, $\tilde{\mathbf{r}}^0$ arbitrary, $k := 0$.

While $\|\mathbf{r}^k\| > \varepsilon$

$\tilde{\mathbf{p}}^k := \mathbf{P}_2\mathbf{F}^T\mathbf{P}_1\mathbf{F}\mathbf{p}^k$

$\alpha_k := (\mathbf{r}^k)^T\tilde{\mathbf{r}}^0/(\tilde{\mathbf{p}}^k)^T\tilde{\mathbf{r}}^0$

$\mathbf{s}^k := \mathbf{r}^k - \alpha_k\tilde{\mathbf{p}}^k,$

$\tilde{\mathbf{s}}^k := \mathbf{P}_2\mathbf{F}^T\mathbf{P}_1\mathbf{F}\mathbf{s}^k$

$\omega_k := (\tilde{\mathbf{s}}^k)^T\mathbf{s}^k/(\tilde{\mathbf{s}}^k)^T\tilde{\mathbf{s}}^k$

$\boldsymbol{\lambda}_{Ker}^{k+1} := \boldsymbol{\lambda}_{Ker}^k + \alpha_k\mathbf{p}^k + \omega_k\mathbf{s}^k$

$\mathbf{r}^{k+1} := \mathbf{s}^k - \omega_k\tilde{\mathbf{s}}^k$

$\beta_{k+1} := (\alpha_k/\omega_k)(\mathbf{r}^{k+1})^T\tilde{\mathbf{r}}^0/(\mathbf{r}^k)^T\tilde{\mathbf{r}}^0$

$\mathbf{p}^{k+1} := \mathbf{r}^{k+1} + \beta_{k+1}(\mathbf{p}^k - \omega_k\tilde{\mathbf{p}}^k)$

$k := k + 1$

end.

Return: $\boldsymbol{\lambda}_{Ker} := \boldsymbol{\lambda}_{Ker}^k$.

Because of the small order of the matrices $\mathbf{G}_1$ and $\mathbf{G}_2$ which is $(l \times 2m)$, it is easy to store these matrices also with the $(l \times l)$ matrices $\mathbf{H}_1 := (\mathbf{G}_1\mathbf{G}_1^T)^{-1}$ and $\mathbf{H}_2 := (\mathbf{G}_2\mathbf{G}_2^T)^{-1}$, respectively. On the other hand, the matrices $\mathbf{F}$, $\mathbf{P}_1$, and $\mathbf{P}_2$ are of the order $(2m \times 2m)$, and therefore, they are not stored because only their matrix-vector products are needed. This holds since the actions on arbitrary vector $\mathbf{v}$ can be solved in the order indicated using parentheses on the right-hand side as

$$\mathbf{F}\mathbf{v} := \mathbf{B}_\gamma(\mathbf{A}^\dagger(\mathbf{B}_\Gamma\mathbf{v})) \quad \text{and} \quad \mathbf{P}_k\mathbf{v} := \mathbf{v} - \mathbf{G}_k(\mathbf{H}_k(\mathbf{G}_k^T\mathbf{v})), \quad k = 1, 2.$$

The matrices $\mathbf{B}_\Gamma$ and $\mathbf{B}_\gamma$ are sparse, so the actions of these matrices are cheap. Finally, the matrices $\mathbf{A}^\dagger$ and $\mathbf{R}$ are easily computed, because the stiffness matrix $\mathbf{A}$ is the matrix corresponding to the fictitious domain with a simple geometry and a regular mesh.

Remark 5.2. The algorithm ProjBiCGSTAB differs from the algorithm BiCGSTAB (not-projected) only in the initialization step and in the occurence of the operators $\mathbf{P}_1$ and $\mathbf{P}_2$, and $\mathbf{F}^T$ before $\mathbf{F}$.

We introduced the method for solving the generalized saddle-point systems. It can be used to find a solution pair $(\mathbf{u}, \boldsymbol{\lambda})$ of the saddle-point system (4.1), which arises from the smooth fictitious domain formulation and the finite element discretization of the problem (3.11). In the following two chapters, we introduce two efficient procedures for numerical computation of the action by $\mathbf{A}^\dagger$ on a vector. Chapter 6 introduces a linear solver based on the discrete Fourier transform and Chapter 7 explains the use of the alternative domain decomposition method solver.

6 Solver for the linear elasticity problem based on FT

In this part we introduce and explain details of a solver based on the Fourier transform (FT) which is used to improve process of finding a solution of a given linear elasticity problem. This solver is based on the use of the discrete Fourier transform for the spectral decomposition of the stiffness matrix and the efficient evaluation of matrix-vector products arising in the solving procedure of the method based on the Schur complement reduction described in Chapters 4 and 5.

Let us recall the linear elasticity problem (2.1). We solve this problem using the modified (smooth) fictitious domain method by using its fictitious domain formulation (3.12), where the space $V(\Omega) = (H_0^1(\Omega))^2$ is replaced by

$$V(\Omega) = (H^1_{per}(\Omega))^2,$$

$$H^1_{per}(\Omega) = \{v \in H^1(\Omega) | v \text{ is periodic on } \partial\Omega\}.$$

For this choice of the space, the stiffness matrix $\mathbf{A}$ is singular, but, on the other hand, the advantage is in the fact that it has a block circulant structure which allows to use a highly efficient solver based on the discrete Fourier transform (DFT). We can use DFT for the spectral decomposition of the stiffness matrix $\mathbf{A}$ and after that we can easily evaluate matrix-vector products by the fast Fourier transform without storing $\mathbf{A}$ and $\mathbf{A}^\dagger$. This is a big advantage against other competitive solvers, because the order of the stiffness matrix is usually large.

Before we explain the principles mentioned above, we focus, at first, on basics of the circulant matrix and its relation to the Fourier transform.

6.1 Circulants and the Fourier transform

Matrices called circulants belong to the class of Toeplitz matrices. A Toeplitz matrix is an $(n \times n)$ matrix $\mathbf{T}_n = [t_{kj}]$, $k, j = 0, \ldots, n-1$, where $t_{k,j} = t_{k-j}$, i.e., a matrix of the form

$$\mathbf{T}_n = \begin{bmatrix} t_0 & t_{-1} & t_{-2} & \cdots & t_{-(n-1)} \\ t_1 & t_0 & t_{-1} & & \\ t_2 & t_1 & t_0 & & \\ \vdots & & & \ddots & \vdots \\ t_{n-1} & & & \cdots & t_0 \end{bmatrix}.$$

Such matrices arise in many problems in mathematics and applied science, e.g., in time series analysis, spline approximation, solution of certain partial differential equations, and many others. These problems lead to the solution of linear systems having circulant coefficient matrices.

Let us define a circulant matrix as follows:

Definition 6.1. *A square $(n \times n)$ matrix $\mathbf{C} = (c_{ij})$ is called a circulant matrix if $c_{ij} = c_{i+1,j+1}$, and the subscripts are taken modulo n. Thus a circulant matrix can be written*

as

$$\mathbf{C} = \begin{bmatrix} c_0 & c_1 & c_2 & \cdots & c_{n-1} \\ c_{n-1} & c_0 & c_1 & \cdots & c_{n-2} \\ c_{n-2} & c_{n-1} & c_0 & \cdots & c_{n-3} \\ \vdots & \vdots & \vdots & \ddots & \vdots \\ c_1 & c_2 & c_3 & \cdots & c_0 \end{bmatrix},$$

i.e., each column is a shift of the first column.

It is clear that $\mathbf{C}$ contains at most n distinct elements and therefore it is often denoted by

$$\mathbf{C} = circ(c_0, c_1, \ldots, c_{n-1}).$$

Properties of circulant matrices can be very useful for solving large linear systems of equations. Let us mention two properties which are important for efficient implementation of the matrix-vector product needed in solving procedure:

- The orthonormal eigenvectors of all $(n \times n)$ circulant matrices are the columns of the Fourier matrix.
- The eigenvalues are the corresponding roots of the primitive nth root of unity with the elements of the matrices as its coefficients.

These properties make it simple to achieve the invertibility of the matrix, and to solve circulant linear systems. Furthermore, the fast Fourier transform can be used to calculate eigenvalues and to solve given linear systems using SVD decomposition.

It is well known [5] that if $\mathbf{C}$ is a circulant matrix, then it can be decomposed as

$$\mathbf{C} = \mathbf{X}^{-1} diag(d_1, d_2, \ldots, d_n)\mathbf{X}, \tag{6.1}$$

where $\mathbf{X}$ is an $(n \times n)$ matrix called a DFT matrix with (i,j)-element $(\omega^{(i-1)(j-1)})$, $i, j = 1, \ldots, n$, $\mathbf{X}^{-1}$ is a matrix of the eigenvectors of the matrix $\mathbf{C}$,

$$d_k = \sum_{l=0}^{n-1} c_l (\omega^{k-1})^l, \quad k = 1, \ldots, n,$$

are the eigenvalues of $\mathbf{C}$, and $\omega = e^{-i2\pi/n}$ is the primitive nth root of unity, see Fig. 6.1.

Remark 6.1. We denote $diag(d_1, d_2, \ldots, d_n)$ for an $(n \times n)$ diagonal matrix with diagonal elements $d_1, d_2, \ldots, d_n$.

Remark 6.2. Eigenvalues of any circulant can be obtained by the DFT of its first column while, eigenvectors are the columns of the inverse to the DFT matrix.

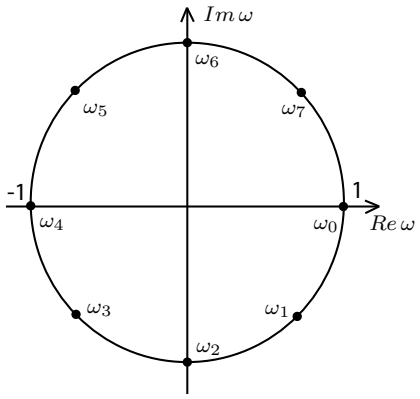

Figure 6.1: Roots of unity (n=8)

Let us also mention that the DFT of the vector $\mathbf{v}$ is given as:

$$\tilde{\mathbf{v}} = \mathbf{X}\mathbf{v},$$

and because $\mathbf{X}$ is symmetric and fulfils $\mathbf{X}\overline{\mathbf{X}}^T = n\mathbf{I}$, with $\overline{\mathbf{X}}$ being the complex conjugate, then the inverse Fourier transform of the vector $\mathbf{v}$ is defined as

$$\mathbf{v} = \frac{1}{n}\overline{\mathbf{X}}\tilde{\mathbf{v}},$$

if $\mathbf{v}$ has real entries.

If $\mathbf{C}$ is nonsingular, then the inverse of $\mathbf{C}$ is also a circulant matrix and from (6.1) it is given by:

$$\mathbf{C}^{-1} = \mathbf{X}^{-1} diag(d_1^{-1}, d_2^{-1}, \ldots, d_n^{-1})\mathbf{X}. \tag{6.2}$$

In case the matrix $\mathbf{C}$ is singular, some of the eigenvalues of $\mathbf{C}$ are zero and the inverse of $\mathbf{C}$ does not exist. However, there exists a unique matrix called the Moore-Penrose generalized inverse of $\mathbf{C}$ denoted by $\mathbf{C}^\dagger$, which is given by

$$\mathbf{C}^\dagger = \mathbf{X}^{-1} diag(d_1^\dagger, d_2^\dagger, \ldots, d_n^\dagger)\mathbf{X}, \tag{6.3}$$

where

$$d_k^\dagger = \begin{cases} 0, & \text{if } d_k = 0, \\ d_k^{-1}, & \text{if } d_k \neq 0, \end{cases} \quad k = 1, 2, \ldots, n.$$

We described several important properties of a circulant matrix, for more details about circulants, see [5]. We also mentioned relation of circulants to the Fourier transform necessary to use a solver based on the FT. Now let us get back to the fictitious domain formulation of the linear elasticity problem and to see the solving procedure.

6.2 Solving procedure based on the use of the Fourier transform

Let us recall that we solve a given linear elasticity problem in the fictitious domain Ω. On the edges of $\Omega = (0, L_x) \times (0, L_y)$ we consider equidistant partitions into n_x and n_y segments with stepsizes $h_x = L_x/n_x$ and $h_y = L_y/n_y$, respectively. It follows that the domain Ω is partitioned into $n := n_x n_y$ rectangles.

On this rectangulation, we introduce a finite element subspace

$$V_h \subset V(\Omega) := (H^1_{per}(\Omega))^2,$$

which is formed by piecewise bilinear periodic functions. After the discretization of the fictitious domain formulation (3.12) we get the algebraic saddle-point system (3.15), where its diagonal block $\mathbf{A} \in \mathbb{R}^{2n \times 2n}$ is circulant and singular due to the imposed periodic boundary conditions.

Let us now focus on the stiffness matrix $\mathbf{A}$. Since the finite element subspace V_h is represented by the tensor product functions, the stiffness matrix $\mathbf{A}$ can be rewritten by the Kronecker product as

$$\mathbf{A} = \left(\begin{array}{c|c} (\theta + 2\mu)\mathbf{A}_x \otimes \mathbf{M}_y + \mu \mathbf{M}_x \otimes \mathbf{A}_y & (\theta + \mu)\mathbf{B}_x \otimes \mathbf{B}_y \\ \hline (\theta + \mu)\mathbf{B}_x \otimes \mathbf{B}_y & \mu \mathbf{A}_x \otimes \mathbf{M}_y + (\theta + 2\mu)\mathbf{M}_x \otimes \mathbf{A}_y \end{array} \right), \tag{6.4}$$

where symbol $\otimes$ stands for the Kronecker tensor product, θ, μ are the Lamé constants, and $\mathbf{A}_k$, $\mathbf{M}_k$, $\mathbf{B}_k \in \mathbb{R}^{n_k \times n_k}$, $k = x, y$, are circulant due to the use of the periodic boundary condition on $\partial\Omega$, with the first columns

$$\begin{aligned} \mathbf{a}_k &= \frac{1}{h_k}(2, -1, 0, \ldots, 0, -1)^T \in \mathbb{R}^{n_k}, \quad k = x, y, \\ \mathbf{m}_k &= \frac{h_k}{6}(4, 1, 0, \ldots, 0, 1)^T \in \mathbb{R}^{n_k}, \quad k = x, y, \\ \mathbf{b}_k &= \frac{1}{2}(0, -1, 0, \ldots, 0, 1)^T \in \mathbb{R}^{n_k}, \quad k = x, y, \end{aligned}$$

respectively.

Definition 6.2. *Let $\mathbf{A} \in \mathbb{R}^{m \times n}$, $\mathbf{C} \in \mathbb{R}^{p \times q}$. Then the Kronecker product (or tensor product) of $\mathbf{A}$ and $\mathbf{B}$ is defined as the matrix*

$$\mathbf{A} \otimes \mathbf{B} = \begin{bmatrix} a_{11}\mathbf{B} & \cdots & a_{1n}\mathbf{B} \\ \vdots & \ddots & \vdots \\ a_{m1}\mathbf{B} & \cdots & a_{mn}\mathbf{B} \end{bmatrix} \in \mathbb{R}^{mp \times nq}.$$

Example 6.1. Let $\mathbf{A} = \begin{bmatrix} 3 & 2 & 1 \\ 1 & 2 & 3 \end{bmatrix}$ and $\mathbf{B} = \begin{bmatrix} 2 & 2 \\ 1 & 3 \end{bmatrix}$. Then

$$\mathbf{A} \otimes \mathbf{B} = \begin{bmatrix} 3\mathbf{B} & 2\mathbf{B} & \mathbf{B} \\ \mathbf{B} & 2\mathbf{B} & 3\mathbf{B} \end{bmatrix} = \begin{bmatrix} 6 & 6 & 4 & 4 & 2 & 2 \\ 3 & 9 & 2 & 6 & 1 & 3 \\ 2 & 2 & 4 & 4 & 6 & 6 \\ 1 & 3 & 2 & 6 & 3 & 9 \end{bmatrix}.$$

Let us mention some properties of the Kronecker product needed for the decomposition of the stiffness matrix $\mathbf{A}$ in the following theorem.

Theorem 6.1. (*Properties of the Kronecker product)*
Let $\mathbf{A} \in \mathbb{R}^{m\times n}$, $\mathbf{B} \in \mathbb{R}^{r\times s}$, $\mathbf{C} \in \mathbb{R}^{n\times p}$, *and* $\mathbf{D} \in \mathbb{R}^{s\times t}$. *Then the following propositions hold:*

1. $(\mathbf{A}\otimes\mathbf{B})(\mathbf{C}\otimes\mathbf{D}) = \mathbf{AC}\otimes\mathbf{BD} \in \mathbb{R}^{(mr\times pt)}$.
2. *For all* $\mathbf{A}$ *and* $\mathbf{B}$, $(\mathbf{A}\otimes\mathbf{B})^T = \mathbf{A}^T\otimes\mathbf{B}^T$.
3. $\mathbf{A}\otimes\mathbf{B} \neq \mathbf{B}\otimes\mathbf{A}$,
4. *If* $\mathbf{A} \in \mathbb{R}^{n\times n}$ *and* $\mathbf{B} \in \mathbb{R}^{m\times m}$ *are symmetric, then* $\mathbf{A}\otimes\mathbf{B}$ *is symmetric.*
5. *If* $\mathbf{A}$ *and* $\mathbf{B}$ *are non-singular, then* $(\mathbf{A}\otimes\mathbf{B})^{-1} = \mathbf{A}^{-1}\otimes\mathbf{B}^{-1}$.
6. *Let* $\mathbf{A} \in \mathbb{R}^{m\times n}$ *have a singular value decomposition* $\mathbf{U}_A\mathbf{\Sigma}_A\mathbf{V}_A^T$ *and let* $\mathbf{B} \in \mathbb{R}^{p\times q}$ *have a singular value decomposition* $\mathbf{U}_B\mathbf{\Sigma}_B\mathbf{V}_B^T$. *Then*

$$(\mathbf{U}_A\otimes\mathbf{U}_B)(\mathbf{\Sigma}_A\otimes\mathbf{\Sigma}_B)(\mathbf{V}_A^T\otimes\mathbf{V}_B^T)$$

   yields a singular value decomposition of $\mathbf{A}\otimes\mathbf{B}$ *(after a simple reordering of the diagonal elements of* $\mathbf{\Sigma}_A\otimes\mathbf{\Sigma}_B$ *and the corresponding right and left singular vectors).*

7. *Let* $\mathbf{A} \in \mathbb{R}^{n\times n}$ *have eigenvalues* τ_i, $i = 1,\dots,n$, *and let* $\mathbf{B} \in \mathbb{R}^{m\times m}$ *have eigenvalues* μ_j, $j = 1,\dots,m$. *Then the* mn *eigenvalues of* $\mathbf{A}\otimes\mathbf{B}$ *are*

$$\tau_1\mu_1,\dots,\tau_1\mu_m,\tau_2\mu_1,\dots,\tau_2\mu_m,\dots,\tau_n\mu_m.$$

   Moreover if $\mathbf{x}_1,\dots,\mathbf{x}_p$ *are linearly independent right eigenvectors of* $\mathbf{A}$ *corresponding to* $\tau_1,\dots,\tau_p$ $(p \le n)$ *and* $\mathbf{y}_1,\dots,\mathbf{y}_q$ *are linearly independent right eigenvectors of* $\mathbf{B}$ *corresponding to* $\mu_1,\dots,\mu_q$ $(q \le m)$, *then* $\mathbf{x}_i\otimes\mathbf{y}_j \in \mathbb{R}^{mn}$ *are linearly independent right eigenvectors of* $(\mathbf{A}\otimes\mathbf{B})$ *corresponding to* $\tau_i\mu_j$, $i = 1,\dots,p$, $j = 1,\dots,q$.

Proof: See [33]. □

Let us define the matrix of the discrete Fourier transform as

$$\mathbf{X} = (\omega^{(k-1)(l-1)})_{k,l=1}^{n}, \quad \omega = e^{-i2\pi/n}.$$

According to observations (6.1) from Section 6.1, we can rewrite the components of the stiffness matrix $\mathbf{A}$ defined by (6.4) as

$$\mathbf{A}_k = \mathbf{X}_k^{-1}\mathbf{D}_{A_k}\mathbf{X}_k, \quad \mathbf{M}_k = \mathbf{X}_k^{-1}\mathbf{D}_{M_k}\mathbf{X}_k, \quad \mathbf{B}_k = \mathbf{X}_k^{-1}\mathbf{D}_{B_k}\mathbf{X}_k, \quad k = x, y,$$

where $\mathbf{D}_{A_k}$, $\mathbf{D}_{M_k}$, $\mathbf{D}_{B_k}$, $k = x, y$ are the corresponding diagonal matrices of eigenvalues and $\mathbf{X}_k$, $k = x, y$, are DFT matrices. Substituting these expressions into (6.4) and using the properties of the Kronecker tensor product, we obtain

$$\mathbf{A} = \left(\begin{array}{c|c} \mathbf{X}^{-1} & \mathbf{O} \\ \hline \mathbf{O} & \mathbf{X}^{-1} \end{array}\right) \left(\begin{array}{c|c} \mathbf{D}_{11} & \mathbf{D}_{12} \\ \hline \mathbf{D}_{21} & \mathbf{D}_{22} \end{array}\right) \left(\begin{array}{c|c} \mathbf{X} & \mathbf{O} \\ \hline \mathbf{O} & \mathbf{X} \end{array}\right), \tag{6.5}$$

where

$$\begin{aligned} \mathbf{X} &= \mathbf{X}_x \otimes \mathbf{X}_y, \\ \mathbf{D}_{11} &= (\theta + 2\mu)\mathbf{D}_{A_x} \otimes \mathbf{D}_{M_y} + \mu \mathbf{D}_{M_x} \otimes \mathbf{D}_{A_y}, \\ \mathbf{D}_{22} &= \mu \mathbf{D}_{A_x} \otimes \mathbf{D}_{M_y} + (\theta + 2\mu)\mathbf{D}_{M_x} \otimes \mathbf{D}_{A_y}, \\ \mathbf{D}_{12} &= (\theta + \mu)\mathbf{D}_{B_x} \otimes \mathbf{D}_{B_y}, \\ \mathbf{D}_{21} &= \mathbf{D}_{12}, \end{aligned}$$

and θ, μ are the Lamé constants.

Let us denote by $\mathbf{D}$ the second matrix on the right hand-side of (6.5). We can rewrite $\mathbf{D}$ by the following factorization:

$$\mathbf{D} = \left(\begin{array}{c|c} \mathbf{I} & \mathbf{O} \\ \hline \mathbf{D}_{21}\mathbf{D}_{11}^{\dagger} & \mathbf{I} \end{array}\right) \left(\begin{array}{c|c} \mathbf{D}_{11} & \mathbf{O} \\ \hline \mathbf{O} & \mathbf{D}_{22} - \mathbf{D}_{21}D_{11}^{\dagger}\mathbf{D}_{12} \end{array}\right) \left(\begin{array}{c|c} \mathbf{I} & \mathbf{D}_{11}^{\dagger}\mathbf{D}_{12} \\ \hline \mathbf{O} & \mathbf{I} \end{array}\right), \tag{6.6}$$

where $\mathbf{D}_{11}^{\dagger} = \mathrm{diag}(d_1^{\dagger}, \cdots, d_n^{\dagger})$ with

$$d_k^{\dagger} = \begin{cases} 0, & \text{if } d_k = 0, \\ d_k^{-1}, & \text{if } d_k \neq 0, \end{cases} \quad k = 1, 2, \ldots, n.$$

According to relation (6.3) we can obtain generalized inverse $\mathbf{A}^{\dagger}$ by replacing $\mathbf{D}$ by $\mathbf{D}^{\dagger}$ in (6.5). We denote

$$\mathbf{D}_{22m} := \mathbf{D}_{22} - \mathbf{D}_{21}\mathbf{D}_{11}^{\dagger}\mathbf{D}_{12},$$

so that

$$\mathbf{D}^{\dagger} = \left(\begin{array}{c|c} \mathbf{I} & \mathbf{D}_{11}^{\dagger}\mathbf{D}_{12} \\ \hline \mathbf{O} & \mathbf{I} \end{array}\right)^{-1} \left(\begin{array}{c|c} \mathbf{D}_{11}^{\dagger} & \mathbf{O} \\ \hline \mathbf{O} & \mathbf{D}_{22m}^{\dagger} \end{array}\right) \left(\begin{array}{c|c} \mathbf{I} & \mathbf{O} \\ \hline \mathbf{D}_{21}\mathbf{D}_{11}^{\dagger} & \mathbf{I} \end{array}\right)^{-1}, \tag{6.7}$$

and,finally, we get the Moore-Penrose generalized inverse of the stiffness matrix $\mathbf{A}$ as

$$\mathbf{A}^{\dagger} = \left(\begin{array}{c|c} \mathbf{X}^{-1} & \mathbf{O} \\ \hline \mathbf{O} & \mathbf{X}^{-1} \end{array}\right) \mathbf{D}^{\dagger} \left(\begin{array}{c|c} \mathbf{X} & \mathbf{O} \\ \hline \mathbf{O} & \mathbf{X} \end{array}\right), \tag{6.8}$$

where $\mathbf{D}^{\dagger}$ is given by (6.7) and $\mathbf{X} = \mathbf{X}_x \otimes \mathbf{X}_y$ is the matrix of two dimensional FT.

We explained the SVD decomposition of the stiffness matrix $\mathbf{A}$ according to properties of the Kronecker tensor product and by the use of the Fourier transform. Also, we introduced a technique to find the Moore-Penrose generalized inverse of the stiffness matrix

A. Let us now apply this knowledge to a matrix-vector multiplication appearing in each iteration of PCGP and in reconstruction formula (4.6). Using (6.7) and (6.8) we can write the product $\mathbf{A}^{\dagger}\mathbf{y}$, where $\mathbf{A} \in \mathbb{R}^{2n\times 2n}$ and $\mathbf{y} = (\mathbf{y}_1^T, \mathbf{y}_2^T)^T \in \mathbb{R}^{2n}$ as follows:

- Step 1.
$$\begin{pmatrix} \tilde{\mathbf{y}}_1 \\ \tilde{\mathbf{y}}_2 \end{pmatrix} = \left(\begin{array}{c|c} \mathbf{X}_x \otimes \mathbf{X}_y & \mathbf{O} \\ \hline \mathbf{O} & \mathbf{X}_x \otimes \mathbf{X}_y \end{array}\right) \begin{pmatrix} \mathbf{y}_1 \\ \mathbf{y}_2 \end{pmatrix},$$

- Step 2.
$$\left(\begin{array}{c|c} \mathbf{I} & \mathbf{O} \\ \hline \mathbf{D}_{21}\mathbf{D}_{11}^{\dagger} & \mathbf{I} \end{array}\right) \begin{pmatrix} \mathbf{x}_1 \\ \mathbf{x}_2 \end{pmatrix} = \begin{pmatrix} \tilde{\mathbf{y}}_1 \\ \tilde{\mathbf{y}}_2 \end{pmatrix}$$
$$\Downarrow$$
$$\left.\begin{array}{rcl} \mathbf{x}_1 & = & \tilde{\mathbf{y}}_1 \\ \mathbf{D}_{21}\mathbf{D}_{11}^{\dagger}\mathbf{x}_1 + \mathbf{x}_2 & = & \tilde{\mathbf{y}}_2 \end{array}\right\} \Rightarrow \begin{array}{rcl} \mathbf{x}_1 & = & \tilde{\mathbf{y}}_1 \\ \mathbf{x}_2 & = & \tilde{\mathbf{y}}_2 - \mathbf{D}_{21}\mathbf{D}_{11}^{\dagger}\tilde{\mathbf{y}}_1, \end{array}$$

- Step 3.
$$\begin{pmatrix} \overline{\mathbf{x}}_1 \\ \overline{\mathbf{x}}_2 \end{pmatrix} = \left(\begin{array}{c|c} \mathbf{D}_{11}^{\dagger} & \mathbf{O} \\ \hline \mathbf{O} & \mathbf{D}_{22m}^{\dagger} \end{array}\right) \begin{pmatrix} \mathbf{x}_1 \\ \mathbf{x}_2 \end{pmatrix}$$
$$\Downarrow$$
$$\begin{array}{rcl} \overline{\mathbf{x}}_1 & = & \mathbf{D}_{11}^{\dagger}\mathbf{x}_1 \\ \overline{\mathbf{x}}_2 & = & \mathbf{D}_{22m}^{\dagger}\mathbf{x}_2, \end{array}$$

- Step 4.
$$\left(\begin{array}{c|c} \mathbf{I} & \mathbf{D}_{11}^{\dagger}\mathbf{D}_{12} \\ \hline \mathbf{O} & \mathbf{I} \end{array}\right) \begin{pmatrix} \overline{\mathbf{y}}_1 \\ \overline{\mathbf{y}}_2 \end{pmatrix} = \begin{pmatrix} \overline{\mathbf{x}}_1 \\ \overline{\mathbf{x}}_2 \end{pmatrix}$$
$$\Downarrow$$
$$\left.\begin{array}{rcl} \overline{\mathbf{y}}_1 + \mathbf{D}_{11}^{\dagger}\mathbf{D}_{12}\overline{\mathbf{y}}_2 & = & \overline{\mathbf{x}}_1 \\ \overline{\mathbf{y}}_2 & = & \overline{\mathbf{x}}_2 \end{array}\right\} \Rightarrow \begin{array}{rcl} \overline{\mathbf{y}}_1 & = & \overline{\mathbf{x}}_1 - \mathbf{D}_{11}^{\dagger}\mathbf{D}_{12}\overline{\mathbf{x}}_2 \\ \overline{\mathbf{y}}_2 & = & \overline{\mathbf{x}}_2, \end{array}$$

- Step 5.
$$\left(\begin{array}{c|c} \mathbf{X}_x^{-1} \otimes \mathbf{X}_y^{-1} & \mathbf{O} \\ \hline \mathbf{O} & \mathbf{X}_x^{-1} \otimes \mathbf{X}_y^{-1} \end{array}\right) \begin{pmatrix} \overline{\mathbf{y}}_1 \\ \overline{\mathbf{y}}_2 \end{pmatrix} = \mathbf{A}^{\dagger}\mathbf{y}.$$

It was already mentioned, and we can also see from the multiplying procedure described above that the matrix-vector multiplication of the generalized inverse of the stiffness matrix $\mathbf{A}$ with the vector $\mathbf{y}$ can be easily evaluated without storing $\mathbf{A}$. Moreover, actions of $\mathbf{X}$ and $\mathbf{X}^{-1}$ on a vector maybe implemented efficiently using FFT (fast Fourier transform) and IFFT (inverse fast Fourier transform) methods. Therefore, we replace the space $H_0^1(\Omega)$ by the space $H_{per}^1(\Omega)$ in order to use the properties of circulant matrices and Fourier transform.

In the following section we introduce numerical experiments based on the use of the Fourier transform for solving linear elasticity problems.

6.3 Numerical experiments

In this section we demonstrate the performance of the described solving procedure based on the use of the discrete Fourier transform. In each experiment, we introduce an elastic body described by the original domain ω and loaded with a force $\mathbf{f}$, together with the Dirichlet and Neumann conditions imposed on its boundary.

The fictitious domain Ω is defined as a square domain $\Omega = (0,1) \times (0,1)$, see Fig. 6.2 and it is the same for all presented examples.

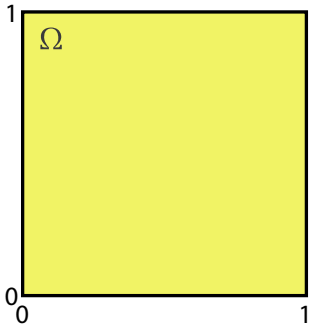

Figure 6.2: Fictitious domain

As next, we show results of the experiments for various distance between original boundary γ and auxiliary boundary Γ, defined as

$$\delta = \mathrm{dist}(\Gamma, \gamma) > 0,$$

and also we enumerate relative errors of approximate solution $\hat{\mathbf{u}}_h$ to exact solution $\hat{\mathbf{u}}$ in these norms:

$$E_{rel,(L_2(\omega))^2} = \frac{\|\hat{\mathbf{u}}_h - \hat{\mathbf{u}}\|_{(L_2(\omega))^2}}{\|\hat{\mathbf{u}}\|_{(L_2(\omega))^2}}, \quad \|\mathbf{u}\|_{(L_2(\omega))^2} = \sqrt{\sum_{i=1}^{2} \int_\omega |u_i|^2 \, \mathrm{d}\omega},$$

$$E_{rel,(L_2(\gamma))^2} = \frac{\|\hat{\mathbf{u}}_h - \hat{\mathbf{u}}\|_{(L_2(\gamma))^2}}{\|\hat{\mathbf{u}}\|_{(L_2(\gamma))^2}}, \quad \|\mathbf{u}\|_{(L_2(\gamma))^2} = \sqrt{\sum_{i=1}^{2} \int_\gamma |u_i|^2 \, \mathrm{d}\gamma},$$

and

$$E_{rel,(H^1(\omega))^2} = \frac{\|\hat{\mathbf{u}}_h - \hat{\mathbf{u}}\|_{(H^1(\omega))^2}}{\|\hat{\mathbf{u}}\|_{(H^1(\omega))^2}}, \quad \|\mathbf{u}\|_{(H^1(\omega))^2} = \sqrt{\|\mathbf{u}\|^2_{(L_2(\omega))^2} + \|\nabla \mathbf{u}\|^2_{(L_2(\omega))^2}}.$$

The ratio between the discretization H of the boundary γ and the step of the discretization h of the fictitious domain is chosen experimentally [21] as

$$H/h = |log_2(h)|.$$

Tables of the computational results contain the dicsretization step h, number of primal and dual variables $(\hat{\mathbf{u}}_h, \boldsymbol{\lambda}_H)$, number of the matrix-vector multiplications in the BICGStab algorithm, computational time, and relative errors of approximate solution $\hat{\mathbf{u}}_h$ to exact solution $\mathbf{u}$.

6.3.1 Example 1

Let us consider an elastic body which is represented by the domain $\omega \subset \mathbb{R}^2$ with a smooth boundary γ_u. We formulate the equilibrium equation together with the Dirichlet boundary conditions:

$$\left.\begin{array}{rcl} -\mathrm{div}\,\boldsymbol{\sigma}(\mathbf{u}) &=& \mathbf{f} \quad \text{in} \quad \omega, \\ \mathbf{u} &=& \mathbf{c} \quad \text{on} \quad \gamma_u. \end{array}\right\} \tag{6.9}$$

The domain ω is defined as the interior of the circle:

$$\omega = \{(x, y) \in \mathbb{R}^2 | (x - 0.5)^2 + (y - 0.5)^2 < 0.25^2\},$$

which is embedded into the fictitious domain Ω, see Fig. 6.3. The right-hand sides of (6.9) are $\mathbf{f} = -div\,\boldsymbol{\sigma}(\hat{\mathbf{u}})$ and $\mathbf{c} = \hat{\mathbf{u}}|_{\gamma_u}$, where $\hat{\mathbf{u}}(x, y) = (0.1xy, 0.1xy)$, $(x, y) \in \mathbb{R}^2$. The auxiliary boundary Γ is constructed by shifting γ_u by the step $\delta = 5h$ in the direction of outward normal vector $\boldsymbol{\nu}$.

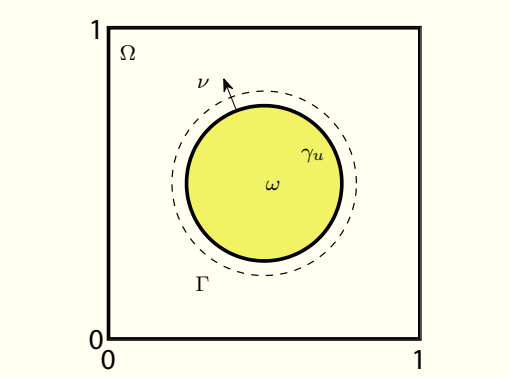

Figure 6.3: Ex.1. Geometry

Fig. 6.4 shows the original and deformed geometry of the domain ω and Table 1 contains results for the different discretization steps of a given example.

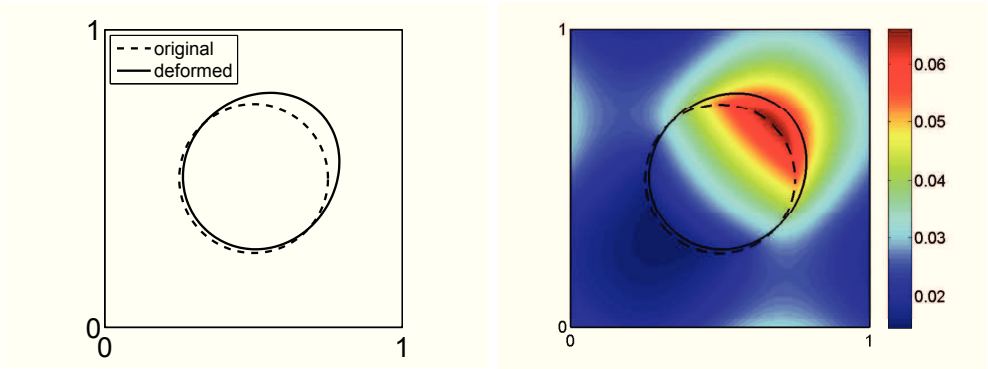

Figure 6.4: Ex.1. Original and deformed geometry and total displacement

Table 1: Ex.1. Computational results

h	1/64	1/128	1/256	1/512	1/1024
Primal var.	8,450	33,282	132,098	526,338	1,050,625
Dual var.	32	56	100	180	320
Matrix mult.	9	13	42	73	122
Time[s]	0.078	2.543	11.84	40.01	312.8
$E_{rel,(L_2(\omega))^2}$	8.7913e-04	1.9516e-04	8.7012e-05	3.0108e-05	1.5813e-05
$E_{rel,(H^1(\omega))^2}$	1.0165e+00	4.8339e-01	3.2264e-01	1.8981e-01	1.3759e-01
$E_{rel,(L_2(\gamma_u))^2}$	2.2568e-03	5.6009e-04	3.7781e-04	1.6286e-04	1.1352e-04

6.3.2 Example 2

In Example 2, we consider the same problem as in Ex.1 but with mixed boundary conditions.

Let us formulate the equilibrium equation together with the Dirichlet and Neumann boundary conditions (see Fig.6.5) as:

$$\left.\begin{array}{rcll} -\mathrm{div}\,\boldsymbol{\sigma}(\mathbf{u}) & = & \mathbf{f} \quad \text{in} & \omega, \\ \mathbf{u} & = & \mathbf{c} \quad \text{on} & \gamma_u, \\ \boldsymbol{\sigma}(\mathbf{u})\boldsymbol{\nu} & = & \mathbf{p} \quad \text{on} & \gamma_p. \end{array}\right\} \tag{6.10}$$

The right-hand sides of (6.10) are $\mathbf{f} = -div\,\boldsymbol{\sigma}(\hat{\mathbf{u}})$, $\mathbf{c} = \hat{\mathbf{u}}|_{\gamma_u}$, and $\mathbf{p} = \boldsymbol{\sigma}(\hat{\mathbf{u}})\boldsymbol{\nu}$, where $\hat{\mathbf{u}}(x,y) = (0.1xy, 0.1xy)$, $(x,y) \in \mathbb{R}^2$. The auxiliary boundary Γ is constructed by shifting γ by the step $\delta = 5h$ in the direction of outward normal vector $\boldsymbol{\nu}$.

Figure 6.6 shows the original and deformed geometry and total displacement and in Table 2 we can see the computational results.

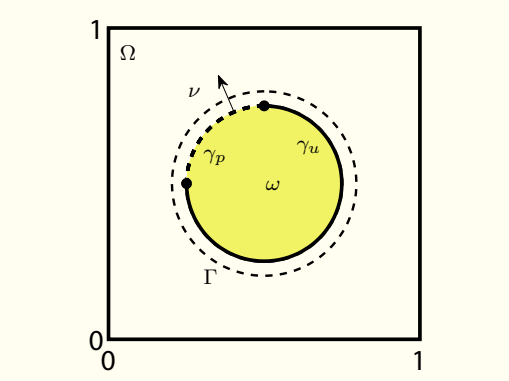

Figure 6.5: Ex.2. Geometry

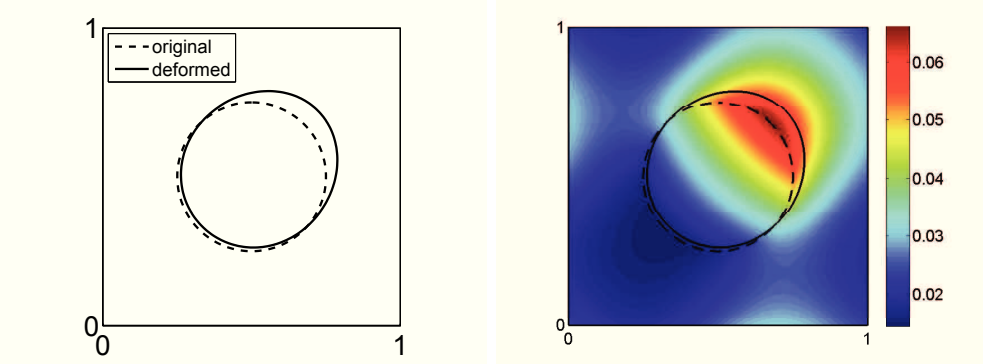

Figure 6.6: Ex.2. Original and deformed geometry and total displacement

Table 2: Ex.2. Computational results

h	1/64	1/128	1/256	1/512	1/1024
Primal var.	8,450	33,282	132,098	526,338	1,050,625
Dual var.	32	60	100	180	320
Matrix mult.	24	30	80	168	356
Time[s]	0.1248	4.789	21.73	82.62	913.8
$E_{rel,(L_2(\omega))^2}$	9.9599e-04	4.5353e-04	2.4301e-04	6.4444e-05	3.1381e-05
$E_{rel,(H^1(\omega))^2}$	1.0922e+00	7.2585e-01	5.3878e-01	2.7776e-01	1.9201e-01
$E_{rel,(L_2(\gamma))^2}$	2.2201e-03	1.2456e-03	8.3455e-04	3.0992e-04	1.7065e-04

6.3.3 Example 3

Let us consider an elastic body which is represented by the domain $\omega \subset \mathbb{R}^2$ defined as the interior of the ellipse

$$\omega = \left\{ (x,y) \in \mathbb{R}^2 | \frac{(x-0.5)^2}{0.3^2} + \frac{(y-0.5)^2}{0.2^2} < 1 \right\},$$

with a smooth boundary γ_u, which is embedded into the fictitious domain Ω, see Fig. 6.7.

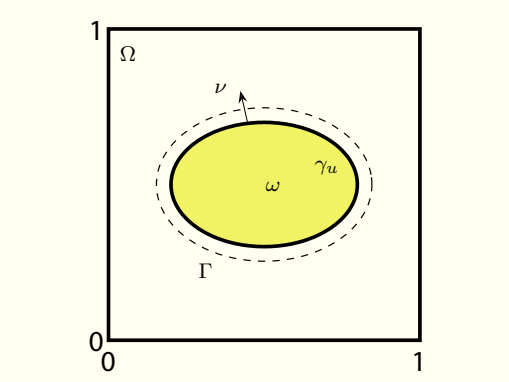

Figure 6.7: Ex.3. Geometry

We formulate the equilibrium equation together with the Dirichlet boundary condition:

$$\left.\begin{aligned} -\mathrm{div}\,\boldsymbol{\sigma}(\mathbf{u}) &= \mathbf{f} \quad \text{in} \quad \omega, \\ \mathbf{u} &= \mathbf{c} \quad \text{on} \quad \gamma_u. \end{aligned}\right\} \tag{6.11}$$

The right-hand sides of (6.11) are $\mathbf{f} = -div\,\boldsymbol{\sigma}(\hat{\mathbf{u}})$ and $\mathbf{c} = \hat{\mathbf{u}}|_{\gamma_u}$, where $\hat{\mathbf{u}}(x,y) = (0.03(2x-3y)^3, -0.5(x-y)^4)$, $(x,y) \in \mathbb{R}^2$. The auxiliary boundary Γ is constructed by shifting γ_u by the step $\delta = 5h$ in the direction of outward normal vector $\boldsymbol{\nu}$.

In Fig. 6.8, we can see the original and deformed geometry and total displacement and Table 3 shows the computational results.

Table 3: Ex.3. Computational results

h	1/64	1/128	1/256	1/512	1/1024
Primal var.	8,450	33,282	132,098	526,338	1,050,625
Dual var.	32	60	100	180	324
Matrix mult.	9	21	41	63	158
Time[s]	0.0936	5.148	10.62	34.06	402.2
$E_{rel,(L_2(\omega))^2}$	6.3106e-02	1.6483e-02	9.8150e-03	2.7415e-03	9.9682e-04
$E_{rel,(H^1(\omega))^2}$	1.5559e+01	7.9646e+00	6.1490e+00	3.2491e+00	1.9598e+00
$E_{rel,(L_2(\gamma))^2}$	7.6116e-02	2.6757e-02	1.8868e-02	7.0919e-03	3.4092e-03

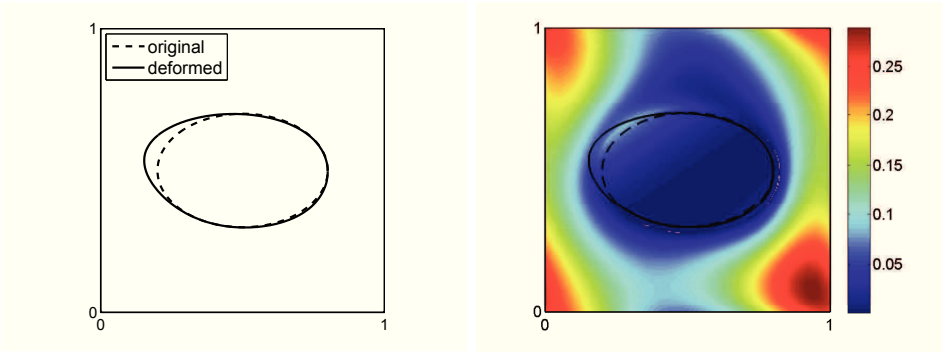

Figure 6.8: Ex.3. Original and deformed geometry and total displacement

6.3.4 Example 4

In this example, we consider the same elastic body as in the previous example, but the boundary is divided into two disjoint parts γ_u and γ_p, where $\gamma = \overline{\gamma_u} \cup \overline{\gamma_p}$ (see Fig. 6.9). On these two parts of γ, different conditions are prescribed.

Let us formulate the equilibrium equation together with the Dirichlet and Neumann boundary conditions:

$$\left.\begin{array}{rcl} -\mathrm{div}\,\boldsymbol{\sigma}(\mathbf{u}) &=& \mathbf{f} \quad \text{in} \quad \omega, \\ \mathbf{u} &=& \mathbf{c} \quad \text{on} \quad \gamma_u, \\ \boldsymbol{\sigma}(\mathbf{u})\boldsymbol{\nu} &=& \mathbf{p} \quad \text{on} \quad \gamma_p. \end{array}\right\} \tag{6.12}$$

The right-hand sides of (6.12) are $\mathbf{f} = -div\,\boldsymbol{\sigma}(\hat{\mathbf{u}})$, $\mathbf{c} = \hat{\mathbf{u}}|_{\gamma_u}$, and $\mathbf{p} = \boldsymbol{\sigma}(\hat{\mathbf{u}})\boldsymbol{\nu}$, where $\hat{\mathbf{u}}(x,y) = (0.02\log(x+y+1), 0.4xy)$, $(x,y) \in \mathbb{R}^2$. The auxiliary boundary Γ is constructed by shifting γ by the step $\delta = 4h$ in the direction of outward normal vector $\boldsymbol{\nu}$.

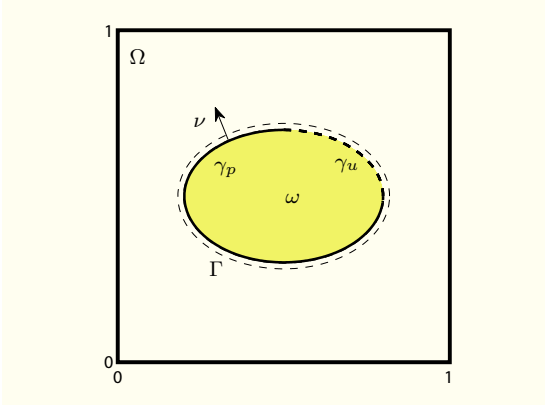

Figure 6.9: Ex.4. Geometry

Figure 6.10 shows the original and deformed geometry and total displacement and Table 4 shows the computational results.

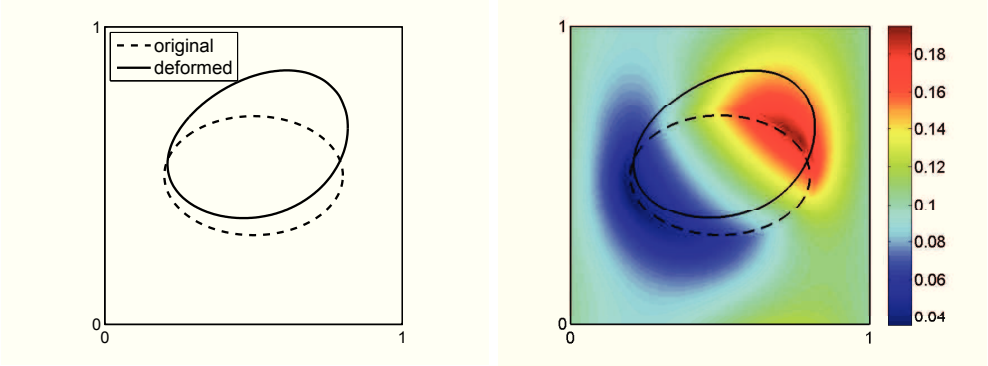

Figure 6.10: Ex.4. Original and deformed geometry and total displacement

Table 4: Ex.4. Computational results

h	1/64	1/128	1/256	1/512	1/1024
Primal var.	8,450	33,282	132,098	526,338	1,050,625
Dual var.	32	60	100	180	324
Matrix mult.	17	30	66	98	246
Time[s]	0.1404	4.805	14.35	51.98	622.9
$E_{rel,(L_2(\omega))^2}$	4.2496e-03	2.7012e-03	9.6872e-04	1.0466e-03	8.0074e-04
$E_{rel,(H^1(\omega))^2}$	7.3764e+00	5.9345e+00	3.5690e+00	3.7219e+00	3.2534e+00
$E_{rel,(L_2(\gamma))^2}$	1.0249e-02	7.2589e-03	2.3406e-03	1.4774e-03	9.9793e-04

6.3.5 Example 5

Let us consider an elastic body which is represented by the domain $\omega \subset \mathbb{R}^2$ with a smooth boundary γ_u.

Let us formulate the equilibrium equation together with the Dirichlet boundary condition:

$$\left.\begin{array}{rcl} -\mathrm{div}\,\boldsymbol{\sigma}(\mathbf{u}) &=& \mathbf{f} \quad \text{in} \quad \omega, \\ \mathbf{u} &=& \mathbf{c} \quad \text{on} \quad \gamma_u. \end{array}\right\} \tag{6.13}$$

The domain ω is defined as the interior of the Cassini oval

$$\omega = \{(x,y) \in \mathbb{R}^2 | (x+x_c)^2 + (y+y_c)^2 - 2a^2(x+x_c)^2 - (y+y_c)^2 + a^4 = b^4\},$$

where $x_c = 0.5$, $y_c = 0.5$, $a = 0.22$, $b = 0.255$, which is embedded into the fictitious domain Ω, see Fig. 6.11. The right-hand sides of (6.13) are $\mathbf{f} = -div\,\boldsymbol{\sigma}(\hat{\mathbf{u}})$ and $\mathbf{c} = \hat{\mathbf{u}}|_{\gamma_u}$, where $\hat{\mathbf{u}}(x,y) = (-0.2\log(x+y+1), -0.3xy)$, $(x,y) \in \mathbb{R}^2$. The auxiliary boundary Γ is

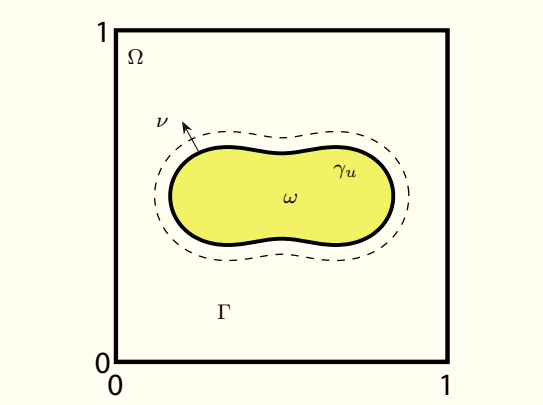

Figure 6.11: Ex.5. Geometry

constructed by shifting γ_u by the step $\delta = 4h$ in the direction of outward normal vector $\boldsymbol{\nu}$.

In Fig. 6.12 we can see the original and deformed geometry and total displacement and Table 5 shows the computational results of a given solution.

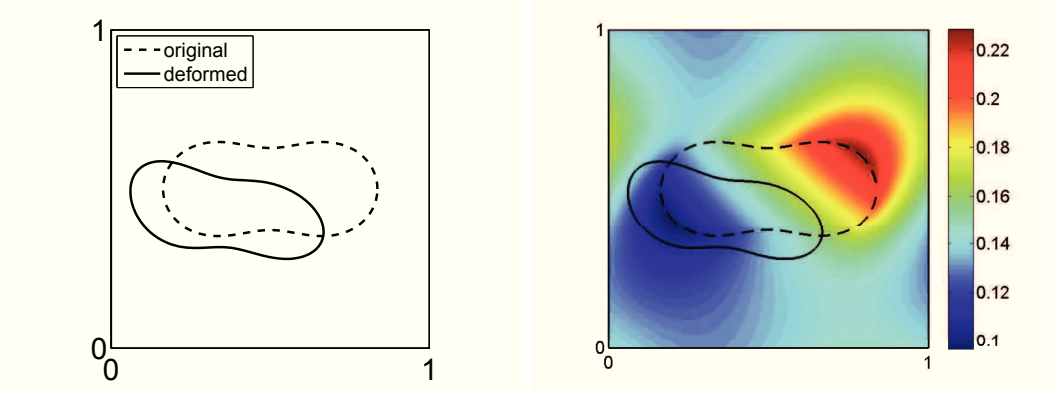

Figure 6.12: Ex.5. Original and deformed geometry and total displacement

Table 5: Ex.5. Computational results

h	1/64	1/128	1/256	1/512	1/1024
Primal var.	8,450	33,282	132,098	526,338	1,050,625
Dual var.	36	60	108	192	344
Matrix mult.	13	29	46	278	216
Time[s]	0.078	6.287	15.05	38.47	552.6
$E_{rel,(L_2(\omega))^2}$	9.0313e-04	1.5937e-04	9.2554e-05	3.4716e-05	1.0538e-05
$E_{rel,(H^1(\omega))^2}$	3.8499e-01	1.6361e-01	1.1914e-01	7.3503e-02	4.1151e-02
$E_{rel,(L_2(\gamma))^2}$	2.3118e-03	5.1638e-04	3.7379e-04	1.7391e-04	7.4454e-05

6.3.6 Example 6

In the last example, we consider the same problem as in the previous example but with mixed boundary conditions. The auxiliary boundary Γ is constructed by shifting γ by the

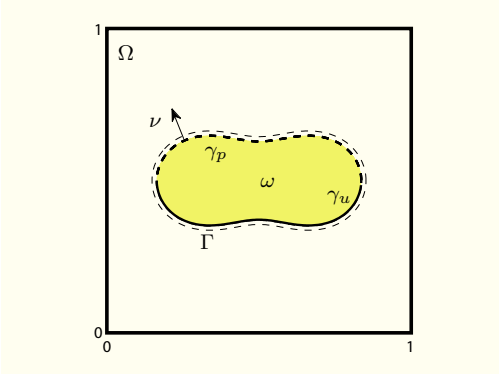

Figure 6.13: Ex.6. Geometry

step $\delta = 4h$ in the direction of outward normal vector $\boldsymbol{\nu}$. Fig. 6.14 shows the original and deformed geometry and total displacement and Table 6 shows the computational results of a given solution.

Table 6: Ex.6. Computational results

h	1/64	1/128	1/256	1/512	1/1024
Primal var.	8,450	33,282	132,098	526,338	1,050,625
Dual var.	32	64	104	194	344
Matrix mult.	21	48	97	253	359
Time[s]	0.1404	9.89	25.15	132.4	916.2
$E_{rel,(L_2(\omega))^2}$	2.4046e-03	5.7935e-04	1.7958e-04	1.0133e-04	7.7296e-05
$E_{rel,(H^1(\omega))^2}$	1.1002e+00	5.2510e-01	3.0850e-01	2.4812e-01	2.1800e-01
$E_{rel,(L_2(\gamma))^2}$	4.8620e-03	1.5074e-03	4.2777e-04	1.8361e-04	1.1258e-04

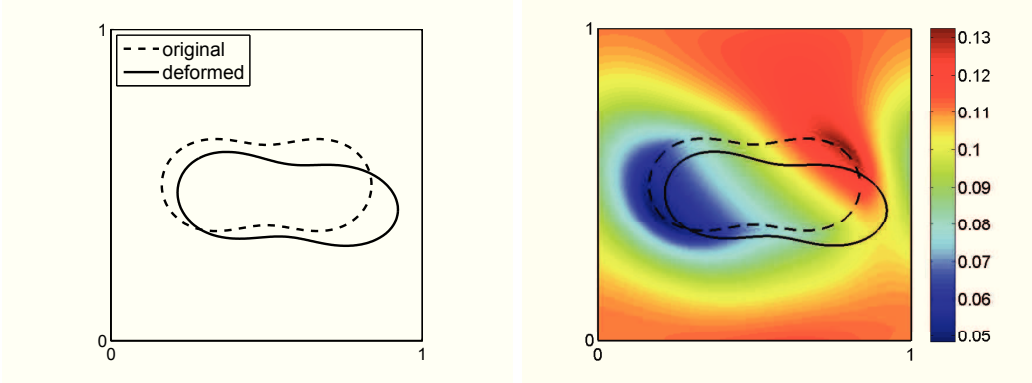

Figure 6.14: Ex.6. Original and deformed geometry and total displacement

6.4 Conclusions to examples

In previous section we introduced various examples of solving the linear elasticity problems based on the use of the Fourier transform solver. We solved problems for a different real domains ω in combination with the pure Dirichlet or mixed boundary conditions. In figures we can see original and deformed geometry of the real domain ω, together with the total displacement. The tables show the numerical results for δ and different discretization steps. With the increasing discretization step the number of iterations and matrix multiplication increase, but the relative errors decrease.

In Fig. (6.15) and (6.16) we can see the sensitivity of solution for Example 1 and Example 2, on the choice of distance δ, between real and auxiliary boundary. We compare the number of iterations and relative error $E_{rel,(L_2(\omega))^2}$.

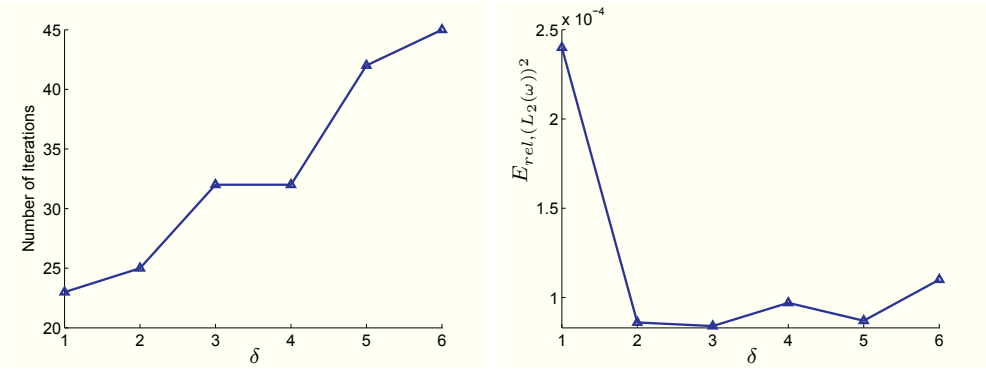

Figure 6.15: Ex.1. Sensitivity of the solution on δ

We can see increasing of number of iterations with increasing distance between real and auxiliary boundary. On the opposite side, there is a decreasing trend of the relative

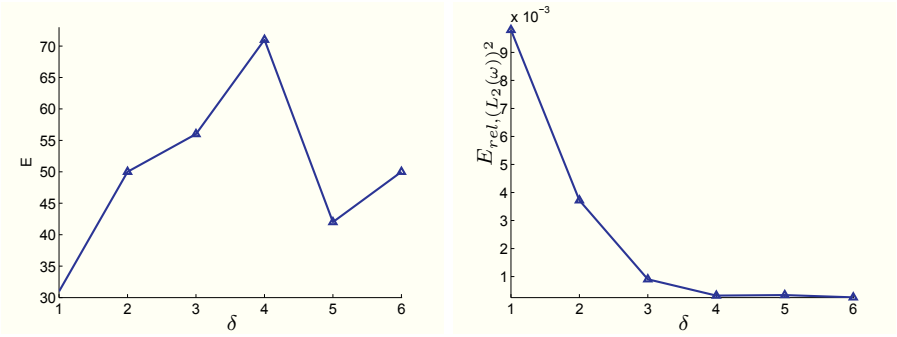

Figure 6.16: Ex.2. Sensitivity of the solution on δ

error $E_{rel,(L_2(\omega))^2}$. Thus we choose the distance δ optimally according to the number of iterations and the expected relative error.

7 Solver for the linear elasticity problems based on the domain decomposition

This chapter deals with a numerical solution of the linear elasticity problems obtained by using the method based on the domain decomposition techniques. The finite element method for partial differential equations results in extremely large sparse linear systems. The solution of sparse systems of linear equations is an important but time consuming step in computational mechanics simulations.

Techniques for solving linear systems can be divided into two groups - direct and iterative. Each has its power and drawbacks. Direct methods are robust and reliable, with a predictable CPU time. However, they require a global data structure that grows rapidly with the problem size. Further, direct solvers are not scalable to massively parallel systems with thousand of processors. Iterative methods, on the other hand, usually scale well with increasing number of processors, but they are not yet as reliable and robust as direct solvers. In particular, iterative solvers perform poorly on problems common in computational mechanics simulations, which include characteristics such as material softening and damage, material anisotropy, etc.

Domain decomposition algorithms are developed to take advantage of a new generation of parallel computers for solving these systems. The domain is decomposed into overlapping or non-overlapping subdomains (see Figs. 7.1 and 7.2). For a discussion of the relationship between the overlapping and non-overlapping schemes, see, e.g., [2].

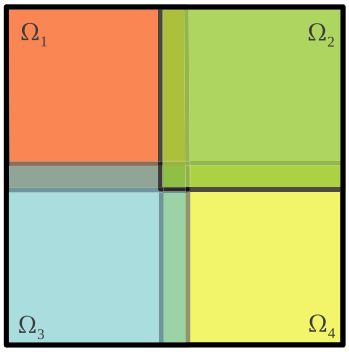

Figure 7.1: Partitioning into four overlapping subdomains

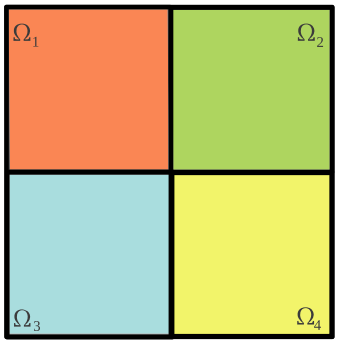

Figure 7.2: Partitioning into four non-overlapping subdomains

In the last three decades, extensive research efforts have been devoted to the development of efficient solution methods for finite element simulations and have led to the development of several high performance solvers. Domain Decomposition Methods (DDM) constitute today an important category of methods for the solution of a variety of problems in Computational Mechanics. Their performance in both serial and parallel computer environments is demonstrated in the last decade.

In Structural Mechanics, the most popular DDM can be divided in two major categories, the Primal and Dual Substructuring Methods [14]. In the early 90s, an important

dual DDM, the Finite Element Tearing and Inter-connecting (FETI) domain decomposition method was introduced by Farhat and Roux [12]. Since their introduction, FETI and several variant methods have gained a high performance and today are considered as highly efficient Domain Decomposition Methods. Furthermore, an important family of primal DDM are considered to be the Balancing Domain Decomposition (BDD) methods, introduced by Mandel [34].

7.1 The FETI-1 domain decomposition

The FETI decomposition method belongs among a class of methods that are referred to as non-overlapping domain decomposition methods in the numerical analysis literature [46], and as conjugate-gradient-based methods in the structural analysis community [11]. The FETI became to be one of the most powerful method for parallel solution of ill-conditioned systems of linear equations arising is structural mechanics problems and very popular domain decomposition method in the computational mechanics community.

Let us show the details of the FETI-1 method on the example of a cantilever beam which is represented by domain Ω with the boundary Γ, see Fig. 7.3.

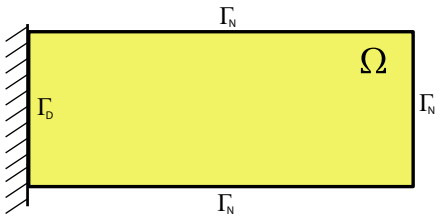

Figure 7.3: Cantilever beam

We assume that the boundary is divided into two disjoint parts Γ_N and Γ_D, $\Gamma = \overline{\Gamma}_N \cup \overline{\Gamma}_D$ and the Neumann condition (representing the surface tractions) is imposed on Γ_N and the Dirichlet boundary condition imposed on Γ_D represents the prescribed displacements.

The main idea of this method is decomposing the large problem defined on the computational domain into smaller non-overlapping subdomains, see Fig. 7.4. The intersubdomain continuity is then enforced by Lagrange multipliers across the interface defined by the subdomain boundaries.

The finite element tearing process which was described above may cause some floating subdomains Ω_f which are characterized by singular subdomain stiffness matrices $\mathbf{K}_f$, where the Neumann boundary conditions are prescribed.

The condition number of its interface problem grows asymptotically [42] only as

$$\kappa = O\left(1 + \log^2\left(\frac{H_m}{h}\right)\right),$$

where h denotes the mesh size (and therefore is an indirect measure of the problem size), and H_m denotes the substructure size (and therefore is an indirect measure of the number

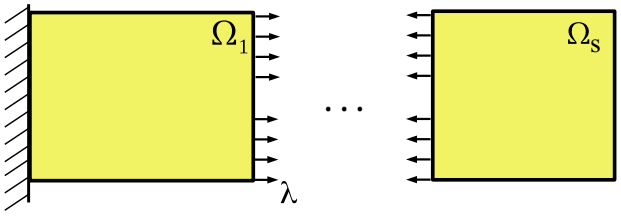

Figure 7.4: FETI-1 decomposition of cantilever beam

of substructures). This condition number estimate establishes the numerical scalability of the FETI method with respect to both the problem size and the number of substructures - that is, its ability to solve larger problems using a large number of substructures in almost constant number of iterations. The parallel scalability of the FETI method - that is, its suitability for massively parallel computing - has also been demonstrated on a large massively parallel processors for several realistic structural and structural dynamic problems, e.g., [13]. Because of these numerical and parallel scalability properties, the FETI method has attracted the attention of both the academic community and finite element practitioners. In particulary, it has been recognized by many finite element production code developers as a robust and powerful iterative solver on sequential as well as massively parallel computers.

The complexity of the FETI method depends on the order of the partial differential equation underlying the discrete problem to be solved, and can be characterized by the complexity of the associated "coarse problem". The latter problem is a relatively small size auxiliary problem that is generated by the FETI method in order to propagate the error globally during the PCG iterations, which accelerate the convergence. For second-order elastostatic and elastodynamic problems, the coarse problem is constructed using the substructure rigid body modes only, and the corresponding computational overhead is relatively insignificant up to a thousand of cores.

Since the time of the introduction of the FETI methods in early 90's, some variants, as A-FETI [42], FETI-2 [9], FETI-DP [8], have been studied extensively. The method FETI-2 was proposed for faster solution of plate and shell problems. The difference between FETI-1 and FETI-DP is that FETI-DP enforces the continuity of the displacements at the corners on primal level so that the stiffness matrices of the subdomains of the FETI-DP method are invertible, for more details about these modifications and examples, see its references.

For solving a given linear elasticity problem we focus on the variant of the FETI method called Total-FETI, which is introduced by Dostál, Horák, Kučera [7], where also Dirichlet conditions are enforced by Lagrange multipliers. Before we use this method for solving problem (2.1), we describe the Total-FETI method and its differences from FETI-1.

7.2 The Total-FETI domain decomposition

The basic idea of the Total-FETI [7] method is to simplify the inversion of the subdomain stiffness matrices by using the Lagrange multipliers not only for gluing of the subdomains along the auxiliary interfaces, but also for the implementation of the Dirichlet boundary conditions. In this case, the kernel-space is as large as possible, since all diagonal blocks of $\mathbf{K}$ are subdomain stiffness matrices to the original PDEs with pure homogeneous Neumann boundary conditions. The advantage is that the null-space basis is known à-priori and may be easily assembled.

We apply the FETI domain decomposition technique to domain Ω and decompose Ω into s subdomains so that $\overline{\Omega} = \overline{\Omega}_1 \cup \cdots \cup \overline{\Omega}_s$ and $\Omega_i \cap \Omega_j = \emptyset$, where $i \neq j$, $i, j = 1, \ldots, s$ as in Fig. 7.4.

The finite element discretization of $\overline{\Omega} = \overline{\Omega}_1 \cup \cdots \cup \overline{\Omega}_s$ results in the discretized quadratic programming problem

$$\min_{\mathbf{u}} \frac{1}{2}\mathbf{u}^T\mathbf{K}\mathbf{u} - \mathbf{u}^T\mathbf{f} \quad \text{subject to} \quad \mathbf{B}\mathbf{u} = \mathbf{c}, \tag{7.1}$$

where $\mathbf{K} = \mathrm{diag}(\mathbf{K}_1, \ldots, \mathbf{K}_s)$ denotes a symmetric positive semidefinite block diagonal stiffness matrix of order $2n$, $\mathbf{B} = \mathrm{diag}(\mathbf{B}_1, \ldots, \mathbf{B}_s)$ denotes a $(2m \times 2n)$ full rank constraint matrix, $\mathbf{u} = (\mathbf{u}_1, \ldots, \mathbf{u}_s)^T$ denotes a displacement vector of the size $2n$, $\mathbf{f} = (\mathbf{f}_1, \ldots, \mathbf{f}_2)^T \in \mathbb{R}^{2n}$ is a load vector, and $\mathbf{c} \in \mathbb{R}^{2m}$ is a constraint vector.

The FETI-1 method assumes that the boundary subdomain Ω_1 inherits the Dirichlet conditions from the original problem, see Figure 7.4, so that the defect of the stiffness matrices $\mathbf{K}_p$ may be different from zero corresponding to the boundary subdomain with sufficient Dirichlet data to the maximum corresponding to the interior floating domains. Let us mention that for 2D linear elasticity, this maximum of the defect of all $\mathbf{K}_p$ is three, which corresponds to the number of independent rigid body motions.

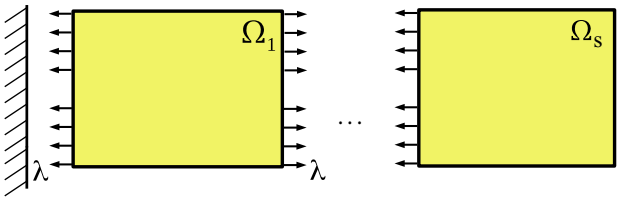

Figure 7.5: Total-FETI decomposition of cantilever beam

On the other hand, the Total-FETI method keeps all subdomain stiffness matrices $\mathbf{K}_s$ floating, without prescribed displacements and the information about prescribed displacement is added into the matrix of constraints $\mathbf{B}$. The prescribed displacement will be enforced by Lagrange multipliers which may be interpreted as forces, see Fig. 7.5.

The diagonal blocks $\mathbf{K}_p$ that correspond to subdomains Ω_p are positive semidefinite and sparse with known kernels. The matrix $\mathbf{B}$ with the rows $\mathbf{b}_i$ and the vector $\mathbf{c}$ with the entries $\mathbf{c}_i$ enforce the continuity of the displacements across the auxiliary boundaries and also the prescribed displacements on the part of the boundary where the Dirichlet boundary conditions are imposed. The continuity requires that

$$\mathbf{b}_i\mathbf{u} = \mathbf{c}_i = \mathbf{o},$$

where $\mathbf{b}_i$ are vectors of the order n with zero entries except $\{-1, 0, 1\}$ at appropriate positions.

Problem (7.1) is a linear quadratic problem, which can be hardly numerically computed, because the stiffness matrix $\mathbf{K}$ is usually ill-conditioned, very large, and singular. To eliminate this drawback we use its dual formulation (see, e.g., [6]).

We introduce a Lagrangian associated with problem (7.1) as

$$L(\mathbf{u}, \boldsymbol{\lambda}) = \frac{1}{2}\mathbf{u}^T\mathbf{K}\mathbf{u} - \mathbf{u}^T\mathbf{f} + \boldsymbol{\lambda}^T(\mathbf{B}\mathbf{u} - \mathbf{c}).$$

It is well known [6] that the problem (7.1) is equivalent to the saddle point problem

$$L(\hat{\mathbf{u}}, \hat{\boldsymbol{\lambda}}) = \sup_{\boldsymbol{\lambda}} \inf_{\mathbf{u}} L(\mathbf{u}, \boldsymbol{\lambda}), \tag{7.2}$$

which leads to the problem to find a solution $(\hat{\mathbf{u}}, \hat{\boldsymbol{\lambda}}) \in \mathbb{R}^{2n} \times \mathbb{R}^{2m}$ of the saddle-point system

$$\begin{pmatrix} \mathbf{K} & \mathbf{B}^T \\ \mathbf{B} & \mathbf{O} \end{pmatrix} \begin{pmatrix} \mathbf{u} \\ \boldsymbol{\lambda} \end{pmatrix} = \begin{pmatrix} \mathbf{f} \\ \mathbf{c} \end{pmatrix}. \tag{7.3}$$

The remaining procedure is exactly the same as in PSCM described in Sections 4 and 5.

Remark 7.1. Let us note that the kernels $\mathbf{R}_p$ of the local stiffness matrices $\mathbf{K}_p$ are known and assembled directly. If the subdomain Ω_p, $p = 1, \dots s$, of a 2D linear elasticity problem is discretized by means of n_p nodes with the coordinates (x_i, y_i), $i = 1, \dots, n_p$, then

$$\mathbf{R}_p^T = [(\mathbf{R}_p^1)^T, \dots, (\mathbf{R}_p^{n_p})^T]^T,$$

where

$$\mathbf{R}_p^i = \begin{pmatrix} 1 & 0 & -y_i \\ 0 & 1 & x_i \end{pmatrix}, \quad i = 1, \dots, n_p.$$

Then we can assemble the block-diagonal matrix $\mathbf{R}$, representing the kernel basis of $\mathbf{K}$ as

$$\mathbf{R} = \begin{pmatrix} \mathbf{R}_1 & \cdots & \mathbf{O} \\ \vdots & \ddots & \vdots \\ \mathbf{O} & \cdots & \mathbf{R}_s \end{pmatrix}.$$

7.3 Total-FETI domain decomposition and FD method for linear elasticity

In the previous section, we described ideas of the Total-FETI method on a basic example. Now we apply this knowledge to the problem of linear elasticity solved using the fictitious domain method based on the modified (smooth) approach.

Let us consider the generalized saddle-point system

$$\begin{pmatrix} \mathbf{K} & \mathbf{B}_\Gamma^T \\ \mathbf{B}_\gamma & 0 \end{pmatrix} \begin{pmatrix} \mathbf{u} \\ \boldsymbol{\lambda} \end{pmatrix} = \begin{pmatrix} \mathbf{f} \\ \mathbf{g} \end{pmatrix}, \tag{7.4}$$

where $\boldsymbol{K} \in \mathbb{R}^{2n\times 2n}$ is the stiffness matrix, $\mathbf{B}_\gamma = (\mathbf{B}_{\gamma_u}^T, \mathbf{C}_{\gamma_p}^T)^T \in \mathbb{R}^{2m\times 2n}$, $\mathbf{f} \in \mathbb{R}^{2n}$, and $\mathbf{g} = (\mathbf{o}^T, \mathbf{p}^T)^T \in \mathbb{R}^{2m}$, resulting from the discretization of the FD formulation to the linear elasticity problem.

If we decompose a given domain Ω into s subdomains Ω^p, $p = 1, \ldots, s$, see Fig. 7.6, then

$$\mathbf{K} = \mathrm{diag}(\mathbf{K}_1, ..., \mathbf{K}_s).$$

The diagonal blocks $\mathbf{K}_p$ that correspond to the subdomains Ω^p are positive semidefinite sparse stiffness matrices with a-priori known kernels and

$$\mathbf{f} = (\mathbf{f}_1, ..., \mathbf{f}_s) \in \mathbb{R}^{2n}.$$

We introduce a $(2M \times 2n)$ full rank gluing matrix $\mathbf{B}_G$ and the corresponding vector $\mathbf{c}_G$

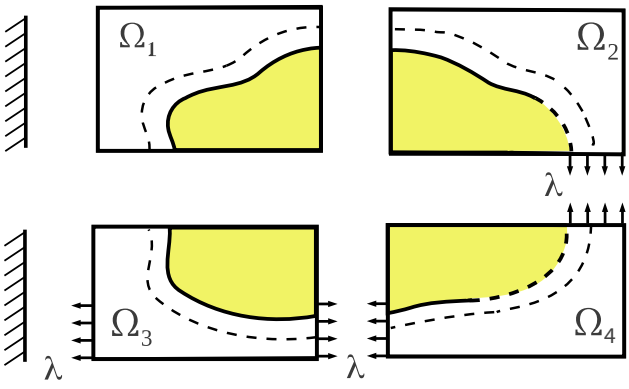

Figure 7.6: Total-FETI decomposition of the fictitious domain Ω

of order $2M$. Using the notation $m := M + m$,

$$\mathbf{B}_\gamma := (\mathbf{B}_G^T, \mathbf{B}_\gamma^T)^T \in \mathbb{R}^{2m\times 2n}, \quad \mathbf{B}_\Gamma := (\mathbf{B}_G^T, \mathbf{B}_\Gamma^T)^T \in \mathbb{R}^{2m\times 2n},$$

and

$$\mathbf{g} := (\mathbf{c}_G^T, \mathbf{g}^T)^T \in \mathbb{R}^{2m}$$

we get again a problem of the same type as (7.4), which is solved by the method explained in Chapter 4 that is based on the Schur complement reduction in combination with the null-space method, which are algorithmically summarized in Chapter 5.

In the following section, we introduce numerical examples to illustrate the performance of Total-FETI decomposition method in combination with the smooth fictitious domain method for solution of a given linear elasticity problem.

7.4 Numerical experiments

In what follows, we illustrate the use of the Total-FETI domain decomposition method for solving the linear elasticity problems. For numerical experiments we define unit square fictitious domain Ω and introduce its Total-FETI domain decomposition, see Fig. 7.7. Here we can see the size of subdomains H_m and the decomposition parameter h.

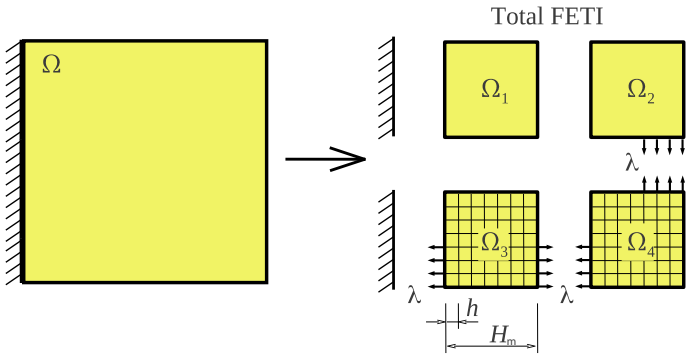

Figure 7.7: Domain decomposition of Ω

Figures of our computed results are shown for the decomposition into 25 square subdomains of size $H_m = 1/5$ with the discretization parameter $h = 1/160$. The results for each example are reported in tables which contain the number of subdomains s, discretization step h, numbers of primal and control variables, number of matrix-vector multiplications in the BICGStab algorithm, computational time, and relative errors $E_{rel,(L_2(\omega))^2}$, $E_{rel,(H^1(\omega))^2}$, $E_{rel,(L_2(\gamma))^2}$ defined in Section 6.3. The experiments are solved in parallel by cluster TERI with 24 cores [47].

7.4.1 Example 1

Let us consider an elastic body which is represented by the domain $\omega \subset \mathbb{R}^2$ with a smooth boundary γ_u. We formulate equilibrium equation together with the Dirichlet boundary conditions:

$$\left.\begin{array}{rcl} -\mathrm{div}\,\boldsymbol{\sigma}(\mathbf{u}) &=& \mathbf{f} \quad \text{in} \quad \omega, \\ \mathbf{u} &=& \mathbf{c} \quad \text{on} \quad \gamma_u. \end{array}\right\} \tag{7.5}$$

The domain ω is defined as the interior of the circle

$$\omega = \{(x, y) \in \mathbb{R}^2 | (x - 0.5)^2 + (y - 0.5)^2 < 0.25^2\},$$

which is embedded into the fictitious domain Ω, see Fig. 7.8. The right-hand sides of (7.5) are $\mathbf{f} = -div\,\boldsymbol{\sigma}(\hat{\mathbf{u}})$ and $\mathbf{c} = \hat{\mathbf{u}}|_{\gamma_u}$, where $\hat{\mathbf{u}}(x, y) = (0.1xy, 0.1xy)$, $(x, y) \in \mathbb{R}^2$. The auxiliary boundary Γ is constructed by shifting γ_u by the step $\delta = 5h$ in the direction of outward normal vector $\boldsymbol{\nu}$.

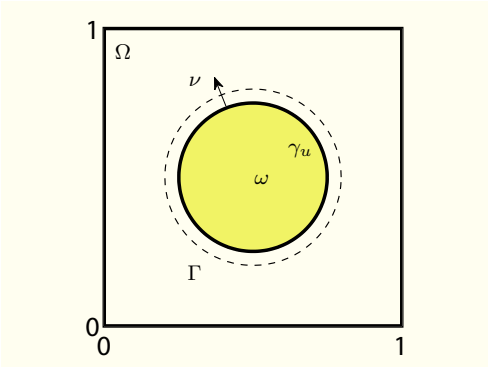

Figure 7.8: Ex.1. Geometry

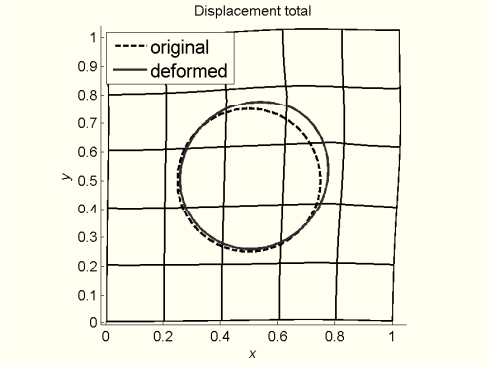

Figure 7.9: Ex.1. Original and deformed geometry

Fig. 7.9 shows the original and deformed geometry and Fig. 7.10 shows the total displacement and stress in the fictious domain Ω. Table 7 shows the computational results for the distance $\delta = 5h$ of the original and the auxiliary boundary.

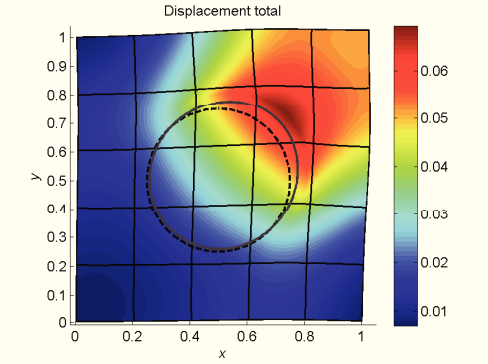

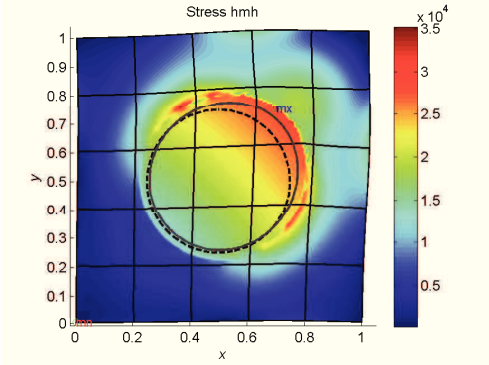

Figure 7.10: Ex.1. Total displacement and von Mises stress

Table 7: Ex.1. Computational results

s	64	144	196	256
h	1/256	1/384	1/448	1/512
Primal var.	139,393	313,632	426,888	557,568
Control var.	7,394	17,322	23,846	31,410
Matrix mult.	142	149	157	212
Time[s]	34	79	84	173
$E_{rel,(L_2(\omega))^2}$	9.1377e-05	8.2487e-05	4.3265e-05	4.0752e-05
$E_{rel,(H^1(\omega))^2}$	3.3057e-01	3.1335e-01	2.2759e-01	2.2076e-01
$E_{rel,(L_2(\gamma_u))^2}$	3.4621e-04	3.5915e-04	2.0544e-04	2.0157e-04

7.4.2 Example 2

In example 2 we consider an elastic body which is represented by the domain $\omega \subset \mathbb{R}^2$ with a smooth boundary γ. This boundary is divided into two disjoint parts γ_u and γ_p, where $\gamma = \overline{\gamma_u} \cup \overline{\gamma_p}$. On these two parts of γ, different conditions are prescribed.

Let us formulate the equilibrium equation together with the Dirichlet and Neumann boundary conditions as:

$$\left.\begin{array}{rcll} -\mathrm{div}\,\boldsymbol{\sigma}(\mathbf{u}) &=& \mathbf{f} \quad \text{in} \quad \omega, \\ \mathbf{u} &=& \mathbf{c} \quad \text{on} \quad \gamma_u, \\ \boldsymbol{\sigma}(\mathbf{u})\boldsymbol{\nu} &=& \mathbf{p} \quad \text{on} \quad \gamma_p. \end{array}\right\} \tag{7.6}$$

The domain ω is defined as the interior of the circle

$$\omega = \{(x,y) \in \mathbb{R}^2 | (x-0.5)^2 + (y-0.5)^2 < 0.25^2\},$$

which is embedded into the fictitious domain Ω, see Fig. 7.11. The righthand sides of (7.6) are $\mathbf{f} = -div\,\boldsymbol{\sigma}(\hat{\mathbf{u}})$, $\mathbf{c} = \hat{\mathbf{u}}|_{\gamma_u}$, and $\mathbf{p} = \boldsymbol{\sigma}(\hat{\mathbf{u}})\boldsymbol{\nu}$, where $\hat{\mathbf{u}}(x,y) = (0.1xy, 0.1xy)$, $(x,y) \in \mathbb{R}^2$. The auxiliary boundary Γ is constructed by shifting γ by the step δ in the direction of outward normal vector $\boldsymbol{\nu}$.

Fig. 7.12 shows the original and deformed geometry. In Fig. 7.13 we show the total displacement and stress. In Table 8, there are the computational results for the distance $\delta = 5h$ of the original and the auxiliary boundary.

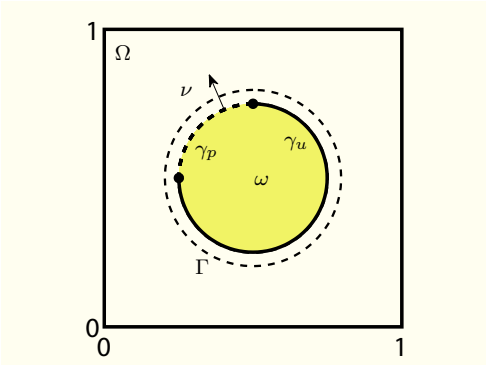

Figure 7.11: Ex.2. Geometry

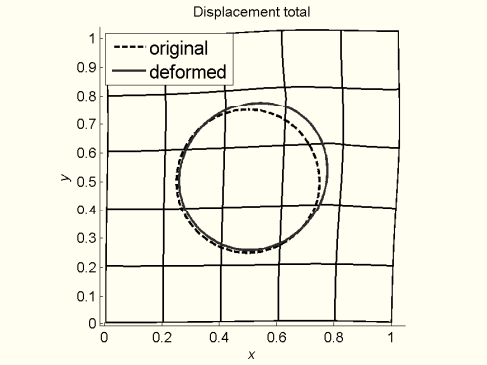

Figure 7.12: Ex.2. Original and deformed geometry

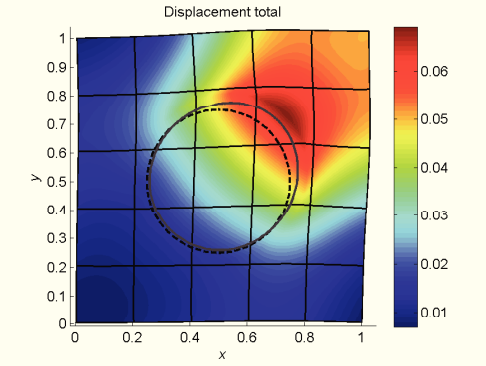

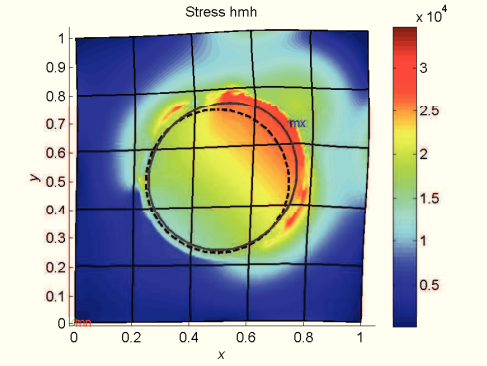

Figure 7.13: Ex.2. Total displacement and von Mises stress

Table 8: Ex.2. Computational results

s	64	144	196	256
h	1/256	1/384	1/448	1/512
Primal var.	139,393	313,632	426,888	557,568
Control var.	7,394	17,320	23,844	31,410
Matrix mult.	242	331	381	376
Time[s]	59	180	204	310
$E_{rel,(L_2(\omega))^2}$	6.3602e-03	4.6746e-03	4.1804e-03	3.0301e-03
$E_{rel,(H^1(\omega))^2}$	2.7396e+00	2.2864e+00	2.1455e+00	1.8487e+00
$E_{rel,(L_2(\gamma))^2}$	7.7359e-03	6.0334e-03	5.2300e-03	4.0011e-03

7.4.3 Example 3

Let us consider an elastic body which is represented by the domain $\omega \subset \mathbb{R}^2$, defined as the interior of the ellipse

$$\omega = \left\{ (x,y) \in \mathbb{R}^2 | \frac{(x-0.5)^2}{0.3} + \frac{(y-0.5)^2}{0.2} < 1 \right\},$$

with a smooth boundary γ_u, which is embedded into the fictitious domain Ω, see Fig. 7.14.

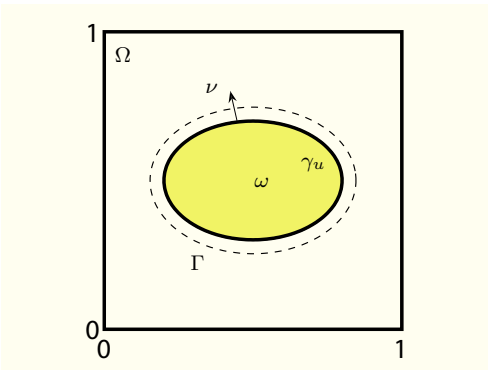

Figure 7.14: Ex.3. Geometry

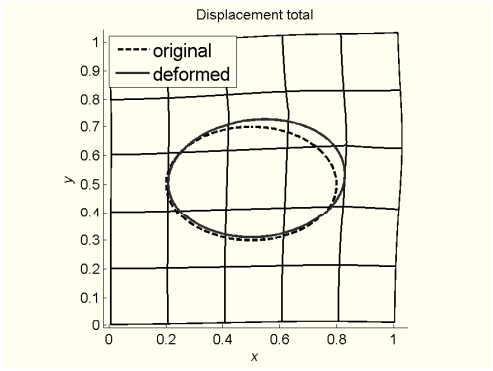

Figure 7.15: Ex.3. Original and deformed geometry

We formulate the equilibrium equation together with the Dirichlet boundary condition:

$$\left.\begin{aligned} -\mathrm{div}\,\boldsymbol{\sigma}(\mathbf{u}) &= \mathbf{f} \quad \text{in} \quad \omega, \\ \mathbf{u} &= \mathbf{c} \quad \text{on} \quad \gamma_u. \end{aligned}\right\} \tag{7.7}$$

The right-hand sides of (7.7) are $\mathbf{f} = -div\,\boldsymbol{\sigma}(\hat{\mathbf{u}})$ and $\mathbf{c} = \hat{\mathbf{u}}|_{\gamma_u}$, where $\hat{\mathbf{u}}(x,y) = (0.1xy, 0.1xy)$, $(x,y) \in \mathbb{R}^2$. The auxiliary boundary Γ is constructed by shifting γ_u by the step δ in the direction of outward normal vector $\boldsymbol{\nu}$.

In Fig. 7.15, we can see the original and deformed geometry and in Fig. 7.16 there are the total displacement and stress. Table 9 shows the computational results for the distance $\delta = 5h$ of the original and the auxiliary boundary.

7.4.4 Example 4

In Example 4, we consider an elastic body which is represented by the domain $\omega \subset \mathbb{R}^2$ with a smooth boundary γ. This boundary is divided into two disjoint parts γ_u and γ_p, where $\gamma = \overline{\gamma_u} \cup \overline{\gamma_p}$. On these two parts of γ, we prescribe different conditions.

Let us formulate the equilibrium equation together with the Dirichlet and Neumann boundary conditions:

$$\left.\begin{aligned} -\mathrm{div}\,\boldsymbol{\sigma}(\mathbf{u}) &= \mathbf{f} \quad \text{in} \quad \omega, \\ \mathbf{u} &= \mathbf{c} \quad \text{on} \quad \gamma_u, \\ \boldsymbol{\sigma}(\mathbf{u})\boldsymbol{\nu} &= \mathbf{p} \quad \text{on} \quad \gamma_p. \end{aligned}\right\} \tag{7.8}$$

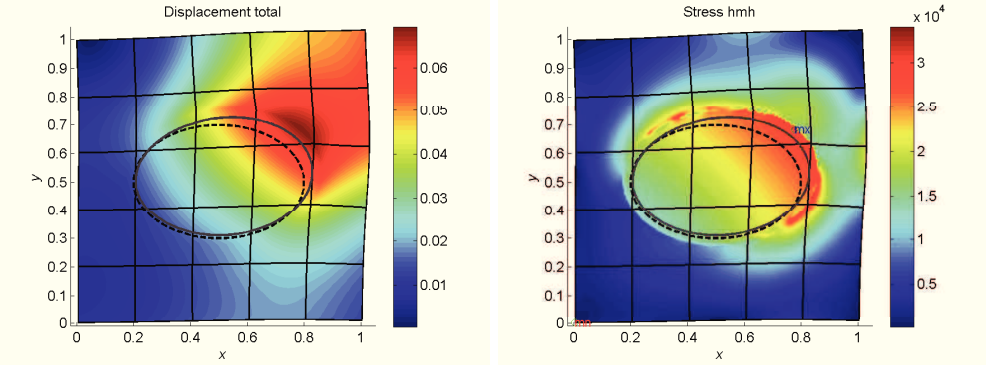

Figure 7.16: Ex.3. Total displacement and von Mises stress

Table 9: Ex.3. Computational results

s	64	144	196	256
h	1/256	1/384	1/448	1/512
Primal var.	139,393	313,632	426,888	557,568
Control var.	7,394	17,322	23,846	31,410
Matrix mult.	121	158	198	186
Time[s]	25	77	106	151
$E_{rel,(L_2(\omega))^2}$	1.2997e-04	6.1487e-05	6.0260e-05	5.0740e-05
$E_{rel,(H^1(\omega))^2}$	3.9284e-01	2.6998e-01	2.7220e-01	2.5035e-01
$E_{rel,(L_2(\gamma_u))^2}$	4.7326e-04	2.6885e-04	2.7752e-04	2.4780e-04

The domain ω is defined as the interior of the elipse

$$\omega = \left\{ (x,y) \in \mathbb{R}^2 | \frac{(x-0.5)^2}{0.3} + \frac{(y-0.5)^2}{0.2} < 1 \right\},$$

which is embedded into the fictitious domain $\Omega = (0,1) \times (0,1)$, see Fig. 7.17. The right-hand sides of (7.8) are $\mathbf{f} = -div\,\boldsymbol{\sigma}(\hat{\mathbf{u}})$, $\mathbf{c} = \hat{\mathbf{u}}|_{\gamma_u}$, and $\mathbf{p} = \boldsymbol{\sigma}(\hat{\mathbf{u}})\boldsymbol{\nu}$, where $\hat{\mathbf{u}}(x,y) = (0.1xy, 0.1xy)$, $(x,y) \in \mathbb{R}^2$. The auxiliary boundary Γ is constructed by shifting γ by the step δ in the direction of outward normal vector $\boldsymbol{\nu}$.

Fig. 7.18 shows the original and deformed geometry. In Fig. 7.19 we can see the total displacement and stress. Table 10 shows the computational results for the distance $\delta = 7h$ of the original and the auxiliary boundary.

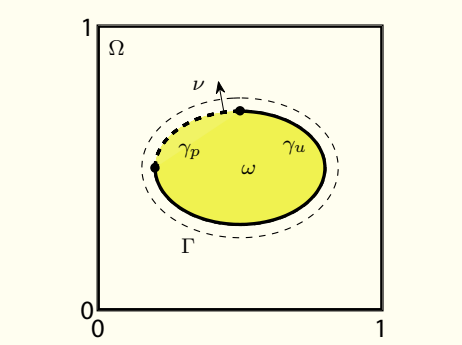

Figure 7.17: Ex.4. Geometry

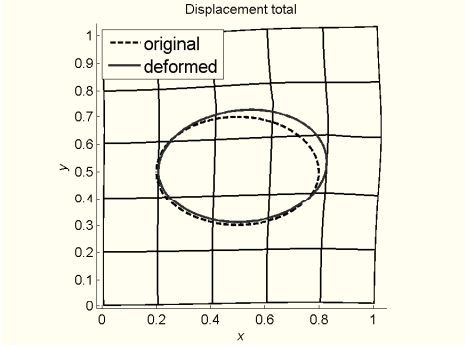

Figure 7.18: Ex.4. Original and deformed geometry

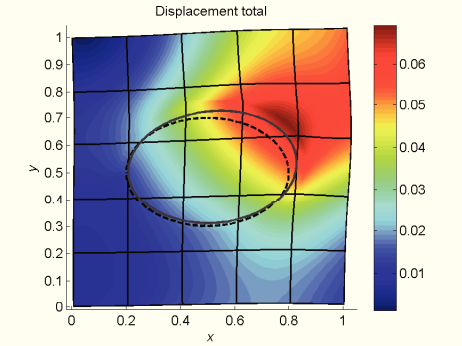

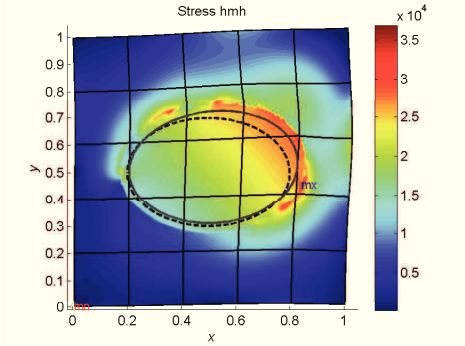

Figure 7.19: Ex.4. Total displacement and von Mises stress

Table 10: Ex.4. Computational results

s	64	144	196	256
h	1/256	1/384	1/448	1/512
Primal var.	139,393	313,632	426,888	557,568
Control var.	7,394	17,324	23,846	31,410
Matrix mult.	244	320	335	351
Time[s]	57.7	172	271	418
$E_{rel,(L_2(\omega))^2}$	1.2557e-02	4.2193e-03	5.4419e-03	3.6710e-03
$E_{rel,(H^1(\omega))^2}$	3.9361e+00	2.1909e+00	2.5014e+00	2.0973e+00
$E_{rel,(L_2(\gamma))^2}$	1.4491e-02	5.4557e-03	6.6058e-03	4.4691e-03

7.4.5 Example 5

In the last example, we introduce the solving procedure on the part of steel support which can be seen in Fig. 7.20. We consider the domain $\omega \subset \mathbb{R}^2$ which is represented by a part

of steel support and we formulate the equilibrium equation together with the Dirichlet boundary condition as:

$$\left.\begin{array}{rcl} -\mathrm{div}\,\boldsymbol{\sigma}(\mathbf{u}) &=& \mathbf{f} \quad \text{in} \quad \omega, \\ \mathbf{u} &=& \mathbf{c} \quad \text{on} \quad \gamma_u. \end{array}\right\} \tag{7.9}$$

The domain ω is embedded into the fictitious domain Ω. The right-hand sides of (7.9) are $\mathbf{f} = -div\,\boldsymbol{\sigma}(\hat{\mathbf{u}})$ and $\mathbf{c} = \hat{\mathbf{u}}|_{\gamma_u}$, where $\hat{\mathbf{u}}(x,y) = (0.1xy, 0.1xy)$, $(x,y) \in \mathbb{R}^2$. The auxiliary boundary Γ is constructed by shifting γ_u by the distance $\delta = 5h$ in the direction of outward normal vector $\boldsymbol{\nu}$.

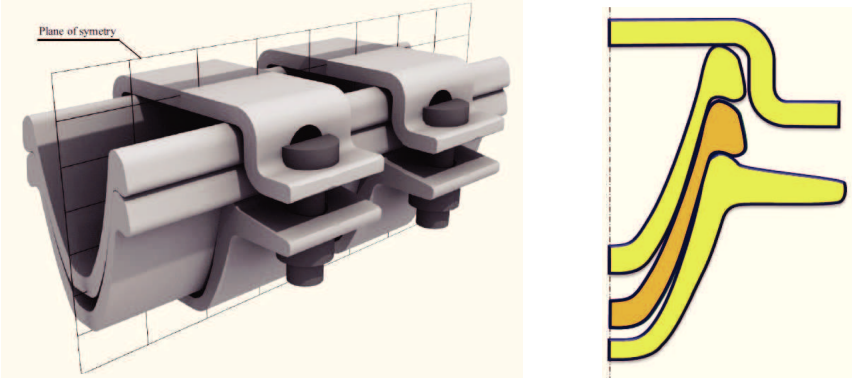

Figure 7.20: Ex.5. Steel support

The following figures and tables show the computational results for the modification of the fictitious domain Ω. For a comparison, let us have a fictitious domain Ω fixed by zero Dirichlet boundary conditions on its boundary $\partial\Omega$ in the first case and floating in the second case.

In Fig. 7.21, we can see the original and deformed geometry for different modification.

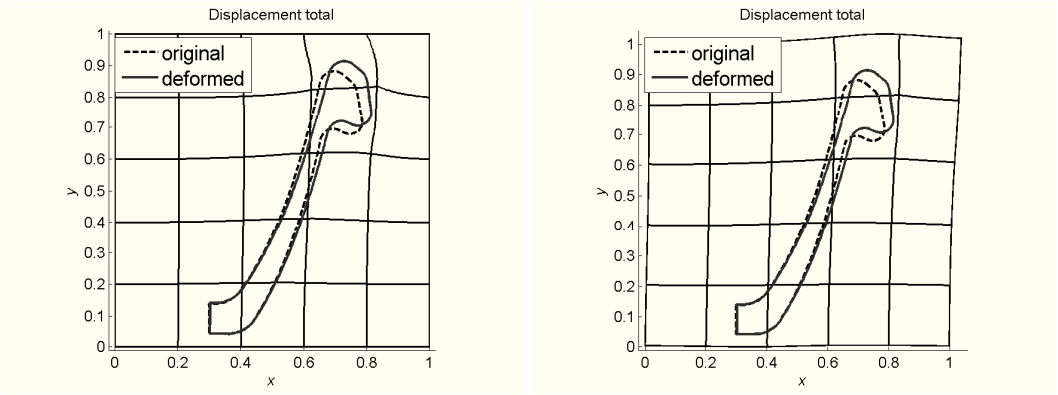

Figure 7.21: Ex.5. Original and deformed geometry

In Figs 7.22 and 7.23, we can see the total displacement, and stress in the fictitious domain Ω, respectively. Also Tables 11 and 12 show the computational results for different modification.

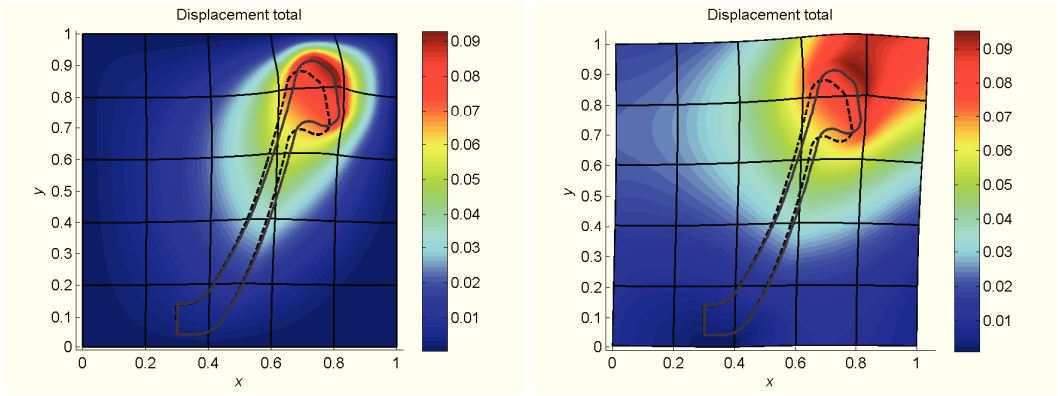

Figure 7.22: Ex.5. Total displacement

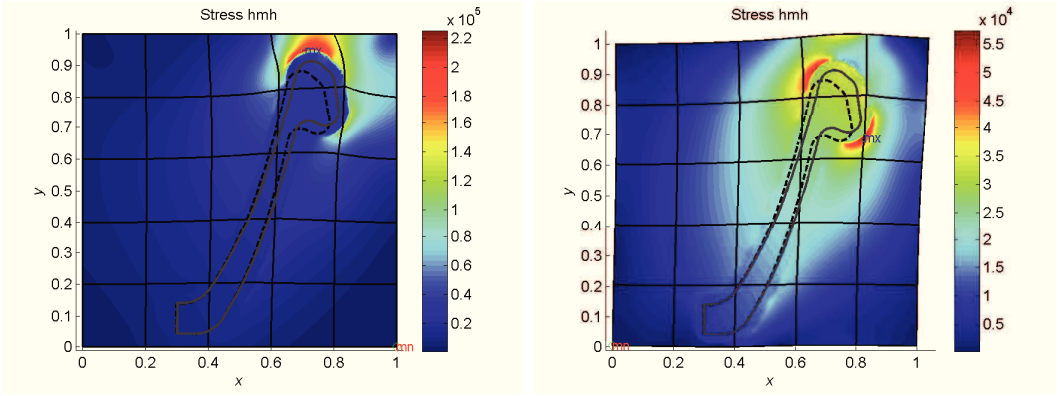

Figure 7.23: Ex.5. Distribution of von Mises stress

Table 11: Computational results Ex.5.: fixed domain Ω

s	64	144	196	256
h	1/256	1/384	1/448	1/512
Primal var.	139,393	313,632	426,888	557,568
Control var.	9,478	20,446	27,486	35,570
Matrix mult.	138	167	174	194
Time[s]	37	91	103	173
$E_{rel,(L_2(\omega))^2}$	4.5369e-04	2.2638e-04	1.3119e-04	1.1629e-04
$E_{rel,(H^1(\omega))^2}$	1.0572e+00	7.4775e-01	5.6466e-01	5.3617e-01
$E_{rel,(L_2(\gamma))^2}$	1.0884e-03	6.6122e-04	3.8387e-04	3.5628e-04

Table 12: Computational results Ex.5.: floating domain Ω

s	64	144	196	256
h	1/256	1/384	1/448	1/512
Primal var.	139,393	313,632	426,888	557,568
Control var.	7,430	17,372	23,902	31,472
Matrix mult.	135	210	206	221
Time[s]	33	111	113	188
$E_{rel,(L_2(\omega))^2}$	2.0050e-04	1.3057e-04	8.9508e-05	8.4492e-05
$E_{rel,(H^1(\omega))^2}$	7.0526e-01	5.6976e-01	4.5923e-01	4.5820e-01
$E_{rel,(L_2(\gamma))^2}$	4.5591e-04	3.8381e-04	2.5696e-04	2.6107e-04

7.5 Conclusions to examples

In previous section we introduced different examples of solving the linear elasticity problems based on the domain decomposition. We solved problems for a different real domains ω in combination with the pure Dirichlet or mixed boundary conditions. In figures we can see original and deformed geometry of the real domain ω, together with the total displacement and stress. The tables show the numerical results for $\delta = 5h$ and different discretization steps due to the decomposition into subdomains. With the increasing discretization step the number of iterations and matrix multiplication increase, but the relative errors decrease.

In Fig. (7.24) and (7.25) we can see the sensitivity of solution for Example 1 and Example 2, on the choice of distance δ, between real and auxiliary boundary. We compare the number of iterations and relative error $E_{rel,(L_2(\omega))^2}$. We can see increasing of number of iterations with increasing distance between real and auxiliary boundary. On the opposite side, there is a decreasing trend of the relative error $E_{rel,(L_2(\omega))^2}$. Thus we choose distance the δ optimally according to the number of iterations and the expected relative error.

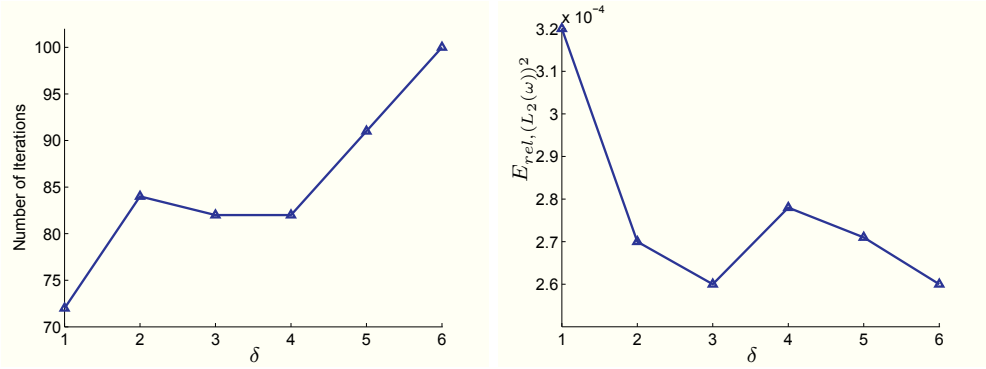

Figure 7.24: Ex.1. Sensitivity of the solution on δ

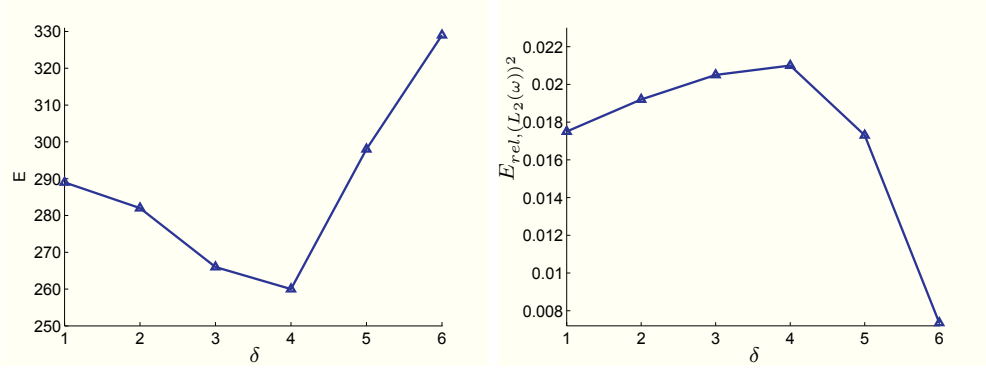

Figure 7.25: Ex.2. Sensitivity of the solution on δ

8 Conclusions

In this thesis, we dealt with solving elliptic boundary value problems for linear elasticity using the fictitious domain method and the effective solvers based on the discrete Fourier transform or the FETI domain decomposition. Its key idea is reformulating of a boundary value problem defined in the original domain ω to a new one defined in a domain Ω called a fictitious domain which contains ω in its interior. An advantage of this approach is in using special finite element partitions of the fictitious domain Ω resulting in a special structure of stiffness matrix which enables us to use fast solvers for evaluating the system of linear algebraic equations by fast methods.

We began with the introduction of the linear elasticity problem, we defined the most important elements in the theory of elasticity and then we introduced ideas how to formulate a new problem using the fictitious domain method. Firstly, we presented the classical approach based on the use of Lagrange multipliers to enforce the Dirichlet boundary conditions on boundary γ of the domain ω. A disadvantage of this approach is the singularity on the boundary γ. To avoid this problem, we described a new smooth approach introduced in [21]. We defined a new auxiliary boundary Γ surrounding γ and new controls to fulfill prescribed boundary conditions on γ. Furthermore, we presented two fast solvers for computing a pair $(\mathbf{u}, \boldsymbol{\lambda}) \in \mathbb{R}^{2n} \times \mathbb{R}^{2m}$ as a solution of a generalized saddle-point system resulted from a finite element discretization of the fictitious domain formulation of a given problem.

The first solver introduced in this thesis to improve efficiency of the solving procedure was based on the use of the Fourier transform. The discrete Fourier transform was applied for the spectral decomposition of the stiffness matrix $\mathbf{A}$ and then, we introduced the fast Fourier transform for evaluation of the generalized inverse matrix-vector multiplication arising in the solving procedure. Solving a given problem without storing the stiffness matrix $\mathbf{A}$ represents an advantage of the solver. This is a benefit compared to other competitive solvers, because the stiffness matrix has usually a big dimension for large problems, also the spectral decomposition of matrices are known a-priori. Disadvantage of this solver is that we can use it just for special separabile operators, which can be separated by application of the Kronecker product.

The second solver was based on the Total-FETI domain decomposition. The main idea of this method was the decomposition of the fictitious domain into non-overlapping subdomains and from that reason we could solve a given problem divided into smaller problems in parallel. According to the decomposition of the domain, we work with the smaller stiffness matrices, and it is not necessary to store all stiffness matrices due to the regular mesh of the fictitious domain. Also the advantage is that we can use this method for every kind of operators, unlike a solver based on the Fourier transform. This is caused by the choice of the space of testing functions which is defined on the fictitious domain Ω.

The solution of a generalized saddle-point system of a given problem was found by the method based on the Schur complement reduction in combination with the projected Krylov subspace method for non-symmetric operators using orthogonal projectors (proj BiCGSTAB). Also, numerical experiments of model examples and benchmarks, for

both proposed solvers were presented.

Summary of advantages and disadvantages of the fictitious domain method and its applicability to the academic and engineering tasks

Disadvantages

- Singularity on the boundary of the real domain ω as a result of the definition of the Lagrange multipliers to fulfil boundary conditions in symmetric case
- Implementation of the boundary conditions
  - Finding the intersection of the real boundary with the mesh of the fictitious domain
  - Dirichlet boundary conditions - smooth boundary is replaced by its piecewise linear approximation, divided for the use of the Lagrange multipliers
  - Neumann boundary conditions - assembling of the auxiliary derivatives ($\frac{\partial u_1}{\partial x_1}$, $\frac{\partial u_1}{\partial x_2}$, $\frac{\partial u_2}{\partial x_1}$, $\frac{\partial u_2}{\partial x_2}$)
- More primal and dual variables, due to embedding of the real domain into the fictitious domain
- Combination of the fictitious domain method with the solver based on the discrete Fourier transform leads to some limitations:
  - Requirement to use the regular mesh, due to the structure of the stiffness matrix. From that reason, there is also problem with the local refinement
  - Operator must be separabile, i.e., the stiffnes matrix is formed by application of the Kronecker product - product of the one dimensional matrices
- Three-dimensional cases: problems with the construction of the space of the control variables and with the construction of the auxiliary boundary
- Application to engineering problems that require only limited accuracy of the solution

Advantages

- The order of error approximation is improved due to the use of the modified fictitious domain approach
- Solver based on the Total-FETI remove restrictions to separabile operators, possibility of the local refinement of the mesh
- Finding of solution is very fast with the use of the both solvers

- Domain decomposition is easy to use, due to the simple shaped fictitious domain
- Solving procedure is well paralelized

The goals of this thesis were as follows. The extension of the modified smooth fictitious domain approach for solving elliptic boundary value problems to linear elasticity problems, the comparison of the two above mentioned solvers based on the discrete Fourier transform and the FETI domain decomposition technique, respectively and the extension of the FETI based implementation to problems with general geometry of the real domain, decomposition into more subdomains, and using the modified fictitious domain approach.

We also extended the MatSol library [28] by a solver based on the use of the fictitious domain method for solving the linear elasticity problems. The thesis is also a basis of the contributions presented during domestic and international conferences.

9 References

[1] Benzi M., Golub, G.H.; Liesen J.: *Numerical solution of saddle point problems*, Acta Numerica, 2005.

[2] Bjørstad Petter E., Widlund, Olof B.;: *To overlap or not to overlap: A note on a domain decomposition method for elliptic problems*, SIAM Journal on Scientific Computing, Vol. 10(5):1053-1061, 1989.

[3] Brezzi F., Fortin M.: *Mixed and hybrid finite element methods*, Springer-Verlag, New York, 1991.

[4] Brzobohatý, T., Dostál, Z., Kovář, P., Kozubek, T. and Markopoulos, A.: *Cholesky decomposition with fixing nodes to stable evaluation of a generalized inverse of the stiffness matrix of a floating structure*, International Journal for Numerical Methods in Engineering 88 (5), 493-509, 2011.

[5] Davis P.J.: *Circulant Matrices*, American Mathematical Society: New York, 1994.

[6] Dostál Z.: *Optimal quadratic programming algorithms: with applications to variational inequalities*, Springer, New York, 2009.

[7] Dostál, Z.; Horák, D.; Kučera, R.; *Total FETI - an easier implementable variant of the FETI method for numerical solution of elliptic PDE*, Communications in Numerical Methods in Engineering, 22(12), 2006, 1155-1162.

[8] Farhat, C., Lesoinne, M., LeTallec, P., Pierson, K., Rixen, D.; *FETI-DP: a dual-primal unified FETI method. I: A faster alternative to the two-level FETI method*, International Journal for Numerical Methods in Engineering, 2001, 50, 7: 15231544.

[9] Farhat, C., Mandel, J.; *The two-level FETI method for static and dynamic plate problems Part I: An optimal iterative solver for biharmonic systems*, Computer Methods in Applied Mechanics and Engineering, Vol. 155, No. 1-2.(1998), pp. 129-151

[10] Farhat, C, Mandel, J., Roux, FX; *Optimal convergence properties of the FETI domain decomposition method*, Computer Methods in Applied Mechanics and Engineering, Vol. 115, No. 3-4.(1994), pp. 365-385

[11] Farhat, C., Pierson, K., Lesoinne, M.; *The Second Generation of FETI Methods and their Application to the Parallel Solution of Large-Scale Linear and Geometrically Nonliner Structural Analysis Problems.*, Technical Report CU-CAS-99-01, College of Engineering, University of Colorado, 1999.

[12] Farhat, C; Roux, FX; *A method of finite element tearing and interconnecting and its parallel solution algorithm*, International Journal for Numerical Methods in Engineering 1991; 32:12051227.

[13] Farhat, C; Roux, FX; *Implicit parallel processing in structural mechanics*, Computational Mechanics Advances 1994; 2(1):1-124.

[14] Fragakis, Y.; Papadrakakis, M.; *The mosaic of high performance Domain Decomposition Methods for Structural Mechanics: Formulation, interrelation and numerical efficiency of primal and dual methods*, Computer Methods in Applied Mechanics and Engineering, Volume 192, Issues 3536,2003, pp. 37993830.

[15] Girault, V.; Glowinski, R.; *Error analysis of a fictitious domain method applied to a Dirichlet problem*, Japan Journal of Industrial and Applied Mathematics Volume 12, Number 3, 1995, pp. 487-514.

[16] Glowinski, R.; Pan, Tsorn-Whay; Periaux, J.; *A fictitious domain method for Dirichlet problem and applications*, Computer Methods in Applied Mechanics and Engineering, Volume 111, Issues 34, 1994, pp. 283303.

[17] Golub, G.H.; Van Loan, C.F.: *Matrix computation*, 3rd ed. The Johns Hopkins University Press, Baltimore 1996.

[18] Gray, R.M.; *Toeplitz and circulant matrices: a review*, Now Publishers Inc, 2006

[19] Haslinger, J.; Kozubek, T.; Kučera, R.; *Fictitious domain formulations of unilateral problems: analysis and algorithms*, Computing, Volume 84, Numbers 1-2, pp. 69-96,

[20] Haslinger, J.; Kozubek, T.; Kučera, R.; *Fictitous domain method for linear elasticity*, Seminar on Numerical Analysis & Winter School , Proceedings of the conference SNA'09, 2009.

[21] Haslinger, J.; Kozubek, T.; Kučera, R.; Peichl, G.; *Projected the Schur complement method for solving non-symmetric systems arising from a smooth fictitious domain approach.*, Numerical Linear Algebra with Applications, Volume 14, Issue 9, 2007, pages 713739.

[22] Haslinger, J.; Kozubek, T.; Peichl, G.; *A smooth embedding domain method based on the penalty approach*, Numerical Functional Analysis and Optimization, Volume 32, Issue 12, 2011, pp. 1252-1270.

[23] Chen, M.; *On The Solution of Ciruclant Linear Systems*, Research report YALEU/DCS/RR-401, 1985

[24] Kamath, C;*The FETI Level 1 Method: Theory and Implementation*, Lawrence Livermore National Laboratory, 2000.

[25] Klawonn, A; Widlund OB; *A domain decomposition method with Lagrange multipliers for liner elasticity*, John Wiley & Sons, 1999.

[26] Klawonn, A; Widlund OB; Dryja, M.; *Dual-primal FETI methods for three-dimensional elliptic problems with heterogeneous coefficients*, SIAM Journal on Numerical Analysis, 2002; 40:159-179.

[27] Kozubek, T.; *Metody fiktivních oblastí v úlohách tvarové optimalizace*, Ph.D. thesis, Ostrava, 2002.

[28] Kozubek, T,; Markopoulos, A,; Brzobohatý, T.; Kučera, R.; Vondrák, V.; Dostál, Z.; MatSol - MATLAB effcient solvers for problems in engineering. http://matsol.vsb.cz.

[29] Kozubek, T.; Mocek, L.; *The use of the Fourier transform for solving linear elasticity problems*, AMMCS-2011 Conference, AIP Conference Proceedings 1368, pp. 21-24 (2011).

[30] Kozubek, T.; Vondrák, V.; Menšík, M.; Horák, D.; Dostál, Z.; Hapla, V.; Kabelíková, P.; Čermák, M.; *Total FETI domain decomposition method and its massively parallel implementation*, Computers and Structures, submitted

[31] Kučera, R., Complexity of an algorithm for solving saddle-point systems with singular blocks arising in wavelet-galerkin discretizations, Application of Mathematics, 3, pp. 291-308, 2005.

[32] Kučera, R.; Kozubek, T.; Markopoulos, A.; Machalová, J.; *On the Moore-Penrose inverse in solving saddle-point systems with singular diagonal blocks*, Numerical Linear Algebra with Applications 2010; 00:1-20.

[33] Laub, Alan J.; *Matrix analysis for scientists and engineers*, SIAM, 2005

[34] Mandel, J.; *Balancing domain decomposition*, Communications in Numerical Methods in Engineering, Volume 9, Issue 3, 1993, pages 233241.

[35] Markopoulos, A; Mocek, L.; *Efficient solver for linear elasticity problems based on the use of fictitious domain method and TFETI domain decomposition*, Seminar on Numerical Analysis & Winter School , Proceedings of the conference SNA'12, 2012.

[36] Mocek, L.; *Linear elasticity problems solved by Fictitious domain based solver*, WOFEX 2010 - PhD Workshop, Proceedings of papers, VSB-TU Ostrava 2010, 283-288.

[37] Mocek, L.; *Fast solver based on Fourier transform for linear elasticity problem*, Seminar on Numerical Analysis & Winter School , Proceedings of the conference SNA'11, 2011, pp. 83-87.

[38] Mocek, L.; *Efficient solvers for linear elasticity problems based on the fictitious domain approach*, WOFEX 2011 - PhD Workshop, Proceedings of papers, VSB-TU Ostrava 2011, pp. 555-560.

[39] Mocek, L.; Kozubek, T.; *Efficient solvers for linear elasticity problems based on the discrete Fourier transform and TFETI decomposition*, ICNNAM-2011 Conference, AIP Conference Proceedings, Volume 1389, pp. 1813-1816 (2011).

[40] Mocek, L.; Markopoulos, A.; *Linear elasticity problems solved by using the fictitious domain method and Total - FETI domain decomposition*, ICCMS-2012 Conference, April 2012, paper accepted.

[41] Nečas,J.; Hlaváček, I.: *Mathematical theory of elastic and elasto-plastic bodies: an introduction*, Elsevier, Oxford, 1981.

[42] Rixen, D.J.; Farhat, C.; Tezaur,R.; Mandel,J.: *Theoretical comparison of the FETI and Algebraically Partitioned FETI Methods and Performence Comparisons with a Direct Sparse Solver*, Journal for Numerical Methods, 1999.

[43] Saad,Y; Martin, H.: *Elasticity: Theory, Applications and Numerics*, Elsevier, Oxford, 2005.

[44] Saad,Y.; *Iterative Methods for Sparse Linear Systems*, Society for Industrial and Applied Mathematics, Philadelphia,PA, second ed., 2003.

[45] Smith, B.; *domain decomposition algorithms for the partial differential equations of linear elasticity*, Technical report 517, Courant institute of Mathematical Sience, 1990.

[46] Smith, B., Bjørstad, P., Gropp, W.: *Domain Decomposition: Parallel Multilevel Methods For Elliptic Partial Differential Equations*, Cambridge University Press, New York, 1996.

[47] TERI - http://spc.vsb.cz

[48] Van der Vorst HA; *BiCGSTAB: a fast and smoothly converging variant of BiCG for solution of nonsymmetric linear systems*, SIAM Journal on Scientific Computing, 2003, 13:631-644.

Author's bibliography

Proceedings international

1. Kozubek, T.; Mocek, L.; *The use of the Fourier transform for solving linear elasticity problems*, AMMCS-2011 Conference, AIP Conference Proceedings 1368, pp. 21-24 (2011),*Scopus, WoS*.

2. Mocek, L.; Kozubek, T.; *Efficient solvers for linear elasticity problems based on the discrete Fourier transform and TFETI decomposition*, ICNNAM-2011 Conference, AIP Conference Proceedings, Volume 1389, pp. 1813-1816 (2011),*Scopus, WoS*.

3. Mocek, L.; Markopoulos, A.; *Linear elasticity problems solved by using the fictitious domain method and Total - FETI domain decomposition*, ICCMS-2012 Conference, April 2012, paper accepted, *will appear in WoS*.

4. Mocek, L.; Kozubek, T.; Kučera,R.; Markopoulos, A.; *Solving Unsymmetric Systems Arising in Numerical Solution of Partial Differential Equations Using a Fictitious Domain Method*, ICCAM-2012 Conference, July 2012, abstract accepted, *paper will be published in Journal of Computational and Applied Mathematics, journal with the impact factor*.

Proceedings domestic

1. Markopoulos, A; Mocek, L.; *Efficient solver for linear elasticity problems based on the use of fictitious domain method and TFETI domain decomposition*, Seminar on Numerical Analysis & Winter School , Proceedings of the conference SNA'12, 2012.

2. Mocek, L.; *Solving linear elasticity problems by fictitious domain method and efficient solvers*, Proceedings of papers, ČVUT Praha 2011.

3. Mocek, L.; *Efficient solvers for linear elasticity problems based on the fictitious domain approach*, WOFEX 2011 - PhD Workshop, Proceedings of papers, VSB-TU Ostrava 2011, pp. 555-560.

4. Mocek, L.; *Fast solver based on Fourier transform for linear elasticity problem*, Seminar on Numerical Analysis & Winter School , Proceedings of the conference SNA'11, 2011, pp. 83-87.

5. Mocek, L.; *Linear elasticity problems solved by Fictitious domain based solver*, WOFEX 2010 - PhD Workshop, Proceedings of papers, VSB-TU Ostrava 2010, 283-288.